

EVALUATION OF AROMATIC IODODEMETALLATION REACTIONS AS METHODS FOR LABELING RADIOPHARMACEUTICALS WITH IODINE-122

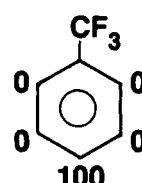
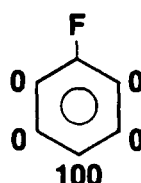
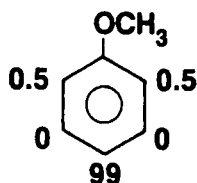
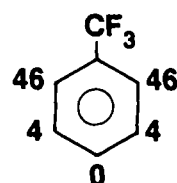
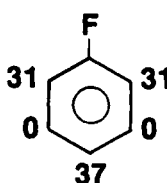
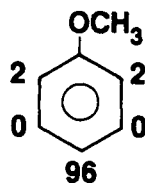
S.M. Moerlein, C.A. Mathis, and Y. Yano

Lawrence Berkeley Laboratory, University of California, Berkeley, CA 94720

Successful application of the generator-produced positron-emitter ^{122}I (77% β^+ , $T_{1/2} = 3.6$ m) (1,2) requires labeling techniques which give high radiochemical yields within the short half-life of this radiohalogen. Useful radioiodination yields with ^{123}I , ^{125}I and ^{131}I have been reported using reactions which involve displacement of aromatic tin (3), silicon (4), boron (5), germanium (6), and mercury (7) moieties. The reaction times which were employed in these studies exceed the practical limits for labeling with ^{122}I , prompting us to examine the use of these precursors at short reaction times to determine their suitability for this radionuclide.

TABLE. Radiochemical Yields for the No-Carrier-Added Iododemetalation Reactions

$\text{C}_6\text{H}_5\text{-M}$	$\xrightarrow[\text{dichloramine-T/EtOH}]{^{122}\text{I}}$	$\text{C}_6\text{H}_5\text{-}^{122}\text{I}$
<u>M</u>		<u>%$\text{C}_6\text{H}_5\text{-}^{122}\text{I}$</u>
$\text{Sn}(\text{CH}_3)_3$		87.1 ± 1.9
HgCl		80.8 ± 1.1
$\text{Ge}(\text{CH}_3)_3$		32.0 ± 0.6
$\text{B}(\text{OH})_2$		< 1
$\text{Si}(\text{CH}_3)_3$		< 1

FIGURE. No-Carrier-Added ^{131}I -Iododemetalation of Stannylated and Mercurated ArenesIododestannylation:Relative
Isomeric YieldTotal Aromatic
Substitution Yield
($t = 30$ s, DCT/EtOH) 93.8 ± 2.1 74.3 ± 2.0 65.6 ± 2.0 Iododemercuration:Relative
Isomeric YieldTotal Aromatic
Substitution Yield
($t = 30$ s, DCT/EtOH) 87.4 ± 1.1 67.2 ± 2.4 77.0 ± 0.3

Metallated arenes ($X-C_6H_4-M$; $X = CF_3, H, F, OCH_3$ and $M = Sn(CH_3)_3, Ge(CH_3)_3, Si(CH_3)_3, HgCl$, and $B(OH)_2$) were synthesized in 65-95% yield (8) and characterized spectroscopically and by elemental analysis. Radiohalogenation reactions were carried out at 25 C in sealed reaction vessels containing radioiodide, organometallic substrate, oxidant, and solvent. Reactions were quenched after times ranging from 5 sec to 5 min by addition of sodium bisulfite, and the radiochemical yields were determined using radio-HPLC with on-line radioactivity detection. For convenience, preliminary studies were performed using ^{131}I preceding application to ^{122}I labeling.

As shown in the Table, using non-activated substrates C_6H_5-M and dichloramine-T in ethanol, radioiodination yields with ^{122}I were highest for $M = Sn(CH_3)_3$ and $HgCl$, with moderate yields achieved for $M = Ge(CH_3)_3$. Radioiodination yields for $M = Ge(CH_3)_3, B(OH)_2$, and $Si(CH_3)_3$ were enhanced by the use of acetic acid as a reaction solvent, whereas the yields for $M = Sn(CH_3)_3$ or $HgCl$ were unaffected. Aromatic iododestannylation and iododemercuration resulted in the greatest labeling yields, independent of reaction solvent. Radioiodination yields via destannylation and demercuration reactions were also impervious to the effects of ring activation, with high yields achieved from substrates activated (OCH_3), non-activated (F), and deactivated (CF_3) toward electrophilic attack (see Figure). Whereas the use of stannylated precursors allowed regiospecific control over the site of iodination, the radioiodination products obtained from mercurated arenes were determined by the isomeric pattern of the mercuration reaction used in precursor synthesis.

The regiospecificity, high radiochemical yields, and lack of solvent or substituent effects make electrophilic iododestannylation the method of choice for labeling aromatic sites with ^{122}I . However, for compounds where regiospecificity of labeling is not essential, or for cases where stannylation is synthetically difficult, the use of mercurated or germylated arenes (especially in acidic reaction media) may be useful alternatives for the production of ^{122}I -labeled radiopharmaceuticals.

This research was supported by the U.S. Department of Energy (DE-AC03-76SF00098).

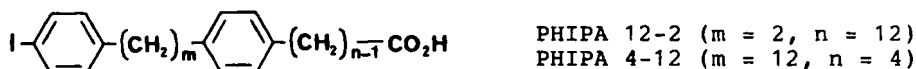
1. Richards, P., and Ku, T.H., *Int. J. Appl. Radiat. Isot.*, **30**, 250 (1979).
2. Mathis, C.A., Sargent III, T., and Shulgin, A.T., *J. Nucl. Med.*, **26**, 1295 (1985).
3. Seitz, D.E., Tonnesen, G.L., Hellman, S., Hansen, R.N., and Adelstein, S.J., *J. Organometal. Chem.*, **186**, C33 (1980).
4. Wilbur, D.S., Anderson, K.W., Stone, W.E., and O'Brien, H.A., *J. Lab. Compd. Radiopharm.*, **19**, 1171 (1982).
5. Kabalka, G.W., Sastry, K.A.R., and Muralidhar, K., *J. Labelled Compd. Radiopharm.*, **19**, 795 (1982).
6. Moerlein, S.M., *J. Chem. Soc., Perkin Trans. 1*, 1687 (1985).
7. Charleston, F.P., Flanagan, R.J., Synnes, E.I., and Wiebe, L.I., *J. Labelled Compd. Radiopharm.*, **21**, 1074 (1985).
8. *Methoden der organischen Chemie (Houben-Weyl)*, Vol. 13. G. Thieme Verlag, Stuttgart, 1972.

SYNTHESIS, LABELING, AND PHARMACOKINETICS OF ^{131}I LABELED PHENYLENE-IODOPHENYL-FATTY ACIDS (PHIPA)J. Liefhold, M. Eisenhut

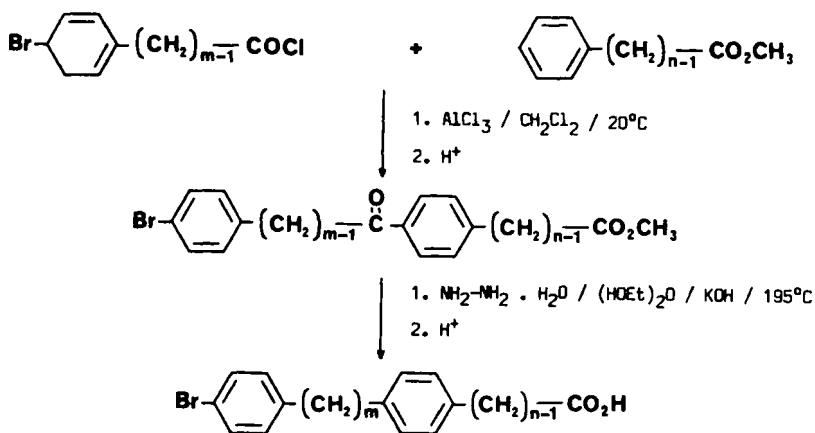
Klinikum der Universität Heidelberg, Forschungsgruppe Strahlenklinik, Im Neuenheimer Feld 328, 6900 Heidelberg, F.R.G.

The application of fatty acid analogues which are trapped during β -oxidation in the mitochondria of heart muscle cells seems to be a useful approach for an improvement of myocardial scintigraphy. Moreover metabolic trapping may clarify those components of the heart clearance which are not due to β -oxidation. FA's with a methyl substituent in the β -position were proposed as inhibitors of β -oxidation. They show high myocardial uptake and are retained in the heart muscle for at least one hour (1,2). There are, however, biological pathways that get over the methyl branching e.g. via α -oxidation or isomerisation of the enoyl-CoA-intermediate which is then further degraded by β -oxidation.

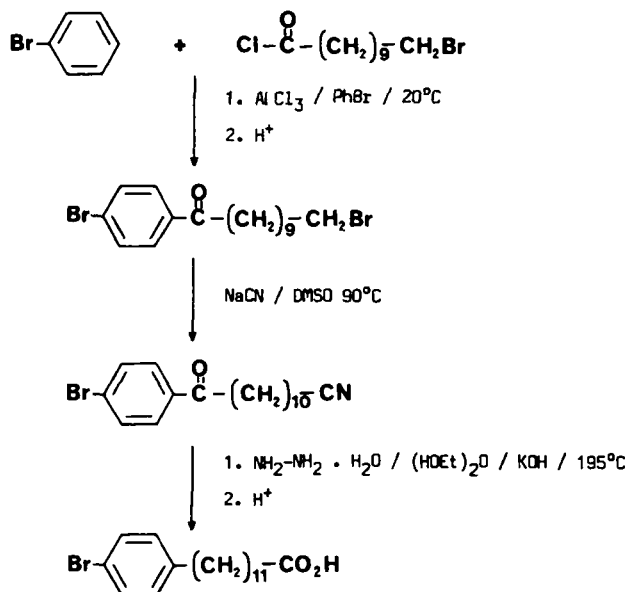
In order to inhibit chain degradation at distinct positions we synthesized a new class of structurally modified ω -phenylalkyl-fatty acids, in which the modifying element is a p-phenylene group in the alkyl chain leading to phenylene-iodophenyl-fatty acids (PHIPA):



PHIPA 12-2 and PHIPA 4-12 were synthesized via Friedel-Crafts acylation of the respective phenylalkanoic esters followed by Wolff-Kishner reduction and ester hydrolysis (Scheme I). 12-(p-Bromo-phenyl)dodecanoic acid was synthesized by the acylation of bromobenzene with 11-bromo-undecanoic acid, and reaction of the bromide function with cyanide which was then hydrolyzed to the acid during Wolff-Kishner reduction (Scheme II).



Scheme I. General route for the synthesis of phenylene-iodophenylfatty acids (PHIPA)



Scheme II. Synthetic route for 12-(p-bromo-phenyl)undecanoic acid

TABLE 1. Organ Distribution of ¹³¹I-PHIPA 12-2 in SD-Rats

Min	Heart	Blood	Lungs	Spleen	Liver	Kidney	Thyr.
5	3.99*	0.38	1.25	1.40	6.79	1.04	7.67
10	3.06	0.35	1.08	1.19	6.36	1.00	8.18
15	3.08	0.47	1.23	0.97	6.93	1.30	11.77
30	3.58	0.71	1.49	1.26	5.80	1.67	13.51
60	3.53	0.62	1.14	0.77	4.69	1.87	26.71

TABLE 2. Organ Distribution of ¹³¹I-PHIPA 4-12 in SD-Rats

Min	Heart	Blood	Lungs	Spleen	Liver	Kidney	Thyr.
5	2.63*	0.75	0.86	1.28	6.80	0.68	5.29
10	2.45	0.40	0.78	1.40	6.14	0.70	6.62
15	2.53	0.32	0.59	1.12	6.67	0.57	8.10
30	2.40	0.38	0.50	1.21	5.64	0.52	7.52
60	2.53	0.60	0.64	1.19	5.30	0.63	8.60
240	2.42	0.43	0.56	0.92	5.21	0.54	19.50

* % injected dose/g organ weight

Radioiodination at the terminal phenyl group was performed by bromine-radioiodine exchange at 200°C. The exchange yields were enhanced by the addition of small amounts of benzoic acid (3). Labeling yields ranged between 65% (PHIPA 4-12) and 90% (PHIPA 12-2). The desired ^{131}I labeled PHIPA derivatives were isolated non-carrier added by HPLC.

The biodistribution of the new substances was studied in female Sprague-Dawley rats. The animals received about 0.74 MBq ^{131}I labeled PHIPA derivative via the injection into a lateral tail vein. The results of the biodistribution of PHIPA 12-2 and PHIPA 4-12 are summarized in the Tables 1 and 2. The initial myocardial uptake did not decrease with time indicating the expected metabolic trapping by enzyme inhibition. The values for the other organs were comparable with 15-(p-iodo- ^{131}I -phenyl)pentadecanoic acid.

Acknowledgment. The Deutsche Forschungsgemeinschaft (DFG) is thanked for financial support and a grant to one of us (J.L.).

1. Elmaleh, D.R., Livni, E., Okada, R., Needham, F.-L., Schleuederberg, J., and Strauss, H.W., Nucl. Med. Comm., 6, 287 (1985)
2. Knapp, F.F., Goodman, M.M., Kirsch, G., and Callahan, A.P., J. Nucl. Med., 26, P123 (1985)
3. Eisenhut, M., Int. J. Appl. Radiat. Isot., 33, 499 (1982)

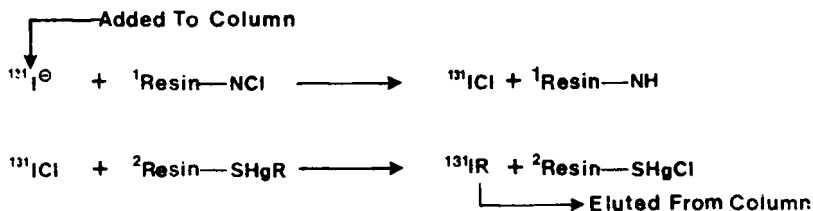
A HIGH SPEED, NO-CARRIER-ADDED RADIOCHEMICAL REACTOR FOR THE SYNTHESIS OF HALOGENATED RADIOPHARMACEUTICALS.

R.J.Flanagan, J.S.Wilson and L.I.Wiebe.

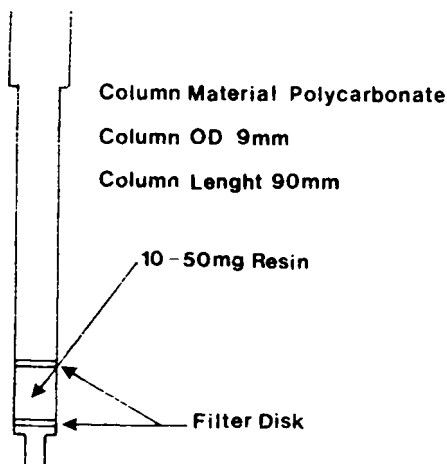
Merck-Frosst Canada Inc., Kirkland, Quebec H9H 3L1, Canada. and Faculty of Pharmacy and Pharmaceutical Sciences, University of Alberta, Edmonton, Alberta T6G 2N8, Canada.

As part of an ongoing program (1) to study the use of organomercury compounds for halogen radiolabelling a new type of radiochemical reactor has been developed. This reactor allows the facile synthesis of organic molecules labelled at predetermined positions with either radiobromine or radioiodine. The reactor is similar to a technetium generator in that it contains a preloaded column which is then eluted to provide the labelled material. The column is eluted with a solution of radiobromide or radioiodide. The halide is activated in the column to the zero-valent form which then reacts with the resin to produce the desired product. The formation of the product simultaneously cleaves the product from the resin which is then eluted at high specific activity.

The reactor consists of a two part resin bed. One part is an oxidizing resin containing an N-chloro-species which reacts with halide to form the corresponding iodine or bromine monochloride. The second resin contains a covalently bonded form of organomercury compound in which the substrate is preactivated by mercury towards electrophilic substitution. The organomercury substrate can be bonded to the resin in a number of different ways but the most general method is via a thiol linkage.



The halogen monochloride reacts at the carbon-mercury bond to selectively cleave that bond (2) and at the same time releasing the halogenated product. The mercury is retained in the column since it is covalently linked to the resin. There is no reaction between the N-chloro resin and organomercury resin, and the halogen monochloride reacts in a polarized fashion with the organomercury bond with no production of the corresponding chloro-substrate (3).



A number of different resins have been examined for suitability in this method. While each resin examined has some drawbacks the best examples we have found to date offer radiochemical yields of 90% or greater and radiochemical purities of greater than 95%. Typical elution times are of the order of 1 to 3 minutes.

Extensive studies on the co-valent loading of the resins will be described. A simple method will also be described for the measurement of the quantity of absorbed mercury on the resin. Stability studies over time periods indicate that such mercurated resins are stable at room temperatures.

Radiochemical reactors of this type using previously synthesized chloromercury compounds (4), (5), have been prepared for 6-halo-cholesterol, 6-halo-epiandrosterone, 6-halo-androstenediol, 6-halo-pregnenolone, 6-halo-pregnanediol, 7-halo-estradiol-6-ene and 4-iodo-N-isopropyl-amphetamine.

Financial support for this work was provided in part by an NSERC/Merck Frosst Fellowship (RJF), an Alberta Heritage Foundation for Medical Research, Research Allowance (RJF) and an Employment and Immigration Canada Constituency Funds Grant (JSW).

1. R.J.Flanagan, F.P.Charleson, E.I.Synnes and L.I.Wiebe, *In proceedings Fifth International Symposium on Radiopharmaceutical Chemistry*, Tokyo, Japan, July, 1984.
2. R.J.Flanagan, F.P.Charleson, E.I.Synnes, L.I.Wiebe, Y.X.Theriault and T.K.Nakashima. *Can.J.Chem.* **68**, 2853, (1985).
3. R.J.Flanagan, F.P.Charleson, E.I.Synnes and L.I.Wiebe, *J.Nuc.Med.* in press
4. R.J.Flanagan, V.V.Somayaji, J.Wilson, F.P.Charleson, E.I.Synnes and L.I.Wiebe *In proceedings International Symposium on the Radiohalogens* Banff, Alberta, Canada. September 1985.
5. R.J.Flanagan, V.V.Somayaji and Leonard I.Wiebe, *Int.J.App.Rad.Isot.* in press

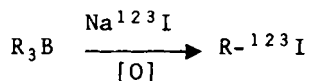
SYNTHESIS OF HIGH SPECIFIC ACTIVITY ^{123}I -LABELED N-ISOPROPYL
p-iodoamphetamine VIA ORGANOBORANE CHEMISTRY

G. W. Kabalka^{*†}, R. S. Varma^{*}, Y.-Z. Gai^{*}, R. M. Baldwin[§], N. E. Salazar[§], and C. L. Schimenti[§]

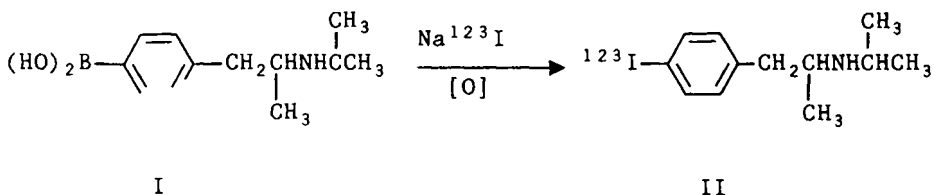
^{*}Department of Chemistry, University of Tennessee, Knoxville, TN 37996-1600. [†]Department of Radiology, University of Tennessee, Knoxville, TN 37920. [§]Medi+Physics, Emeryville, CA 94608

Radioiodinated amines such as ^{123}I -labeled N,N,N'-trimethyl-N'-[2-hydroxy-3-methyl-5-iodobenzyl]-1,3-propanediamine (HIPDM) and ^{123}I -labeled N-isopropyl p-iodoamphetamine (IMP) cross the blood-brain barrier and remain fixed for sufficient time to permit effective brain imaging via single photon emission tomography (1). To date, the preparation of ^{123}I -IMP by exchange has been found to be more difficult to accomplish than the synthesis of radioiodinated HIPDM (2) and high specific activity IMP has been obtained only with some difficulty (3).

Organoboranes have been successfully utilized to incorporate a number of isotopes into a variety of physiologically active compounds (4). The syntheses, including radioiodinations, are successful at the no-carrier-added level (5).



We wish to report that high specific activity [^{123}I]-IMP can be rapidly prepared in good yield (65-80%) via the reaction of the corresponding boronic acid with no-carrier-added iodine-123 labeled sodium iodide.



In a typical experiment, N-isopropyl amphetamineboronic acid, I, (1.0 mg) is dissolved in aqueous HCl (0.5 mL of 0.1 M HCl) at room temperature. Aqueous sodium iodide (NCA) in dilute base

(10 μ L of ~ 0.05 M NaOH) is added to the vessel, followed by aqueous chloramine-T (0.2 mL of a 0.1 M solution in water). After one min., basic sodium bisulfite (2 mL of 0.1 M NaHSO₃) is added and the mixture extracted with ether. The product is extracted out of ether with 0.1 M HCl and analyzed by TLC. [Ethyl acetate: methanol: water: NH₄OH (conc.) = 170:20:6:2 on silica gel].

This research was supported by the Division of Health and Environmental Research of the Department of Energy.

1. Holman, B.L., Hill, T.C., Polak, J.F., Lee, R.G.L., and Royal, H.D., In Holman, B.L., ed., *Radionuclide Imaging of the Brain*, Churchill Livingstone, 1985, pp 163-184.
2. Kung, H.F., Trampusch, K.M., and Blau, M., *J. Nucl. Med.*, 24, 66 (1983).
3. Srivastava, S.C., Yamamoto, K., Meinken, G.E., Yonekura, Y., Sacker, D.F., Richards, P., Brill, A.B., Coffey, J., Carlton, E., Hubner, K., *J. Nucl. Med.*, 24, P118 (1983).
4. Kabalka, G.W., *Acc. Chem. Res.*, 17, 215 (1984).
5. Kabalka, G.W., In *Developing Role of Short-Lived Radionuclides in Nuclear Medicine Practice*, DOE Symposium Series 56, Department of Energy, 1985, pp 377-383.

**SYNTHESIS OF HEAVY RADIOHALOGENIC DERIVATIVES OF METHYLENE BLUE:
POTENTIAL DIAGNOSTIC AND THERAPEUTIC PROBES FOR MALIGNANT MELANOMA**

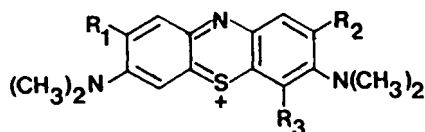
I. Brown, R.N. Carpenter, J.S. Mitchell, and E. Link

The Research Laboratories, The Radiotherapeutic Centre, Cambridge University School of Clinical Medicine, Addenbrooke's Hospital, Cambridge CB2 2QQ, ENGLAND

In view of the poor prognosis experienced by patients with disseminated malignant melanoma (1), the early detection and treatment of clinically occult metastatic disease is highly desirable. Consequently, an important objective in nuclear medicine is the design and development of melanoma-specific radio-pharmaceuticals for both diagnosis and therapy.

A number of compounds derived from the polycyclic phenazathiazines are, by virtue of their electron-deficient heterocyclic structure, known to readily form charge-transfer complexes with intra-cellular melanin (2). Additionally, several of these molecules also intercalate with DNA. One such compound, 3,7-(di-methylamino)-phenazathionium chloride (methylene blue (I), MTB) exhibits a high binding affinity for synthetic melanins. The β -emitting low-LET radio-analogue, [^{35}S]-methylene blue (3), has been shown to cause a significant retardation in the growth of transplanted pigmented melanomas in an animal model (4). However, from a radiobiological viewpoint, a radio-analogue which emits a high-LET quality radiation might prove more efficacious. Whilst several iodine radionuclides (i.e. ^{123}I , ^{124}I , ^{131}I , ^{132}I) possess attractive decay properties relevant to diagnostic scintigraphy, here, the only radiohalide which appears suitable for high-LET endoradiotherapy is [^{211}At]-astatine (5,6). The latter, of half-life 7.21 h, decays by the emission of potent 6.8 MeV mean energy α -particles. Such particles have a mean range of $\sim 65 \mu\text{m}$ in tissue, and a near optimal therapeutic LET of $\sim 100 \text{ keV}/\mu\text{m}$.

Several radio-iodinated and [^{211}At]-astatinated derivatives of methylene blue have been prepared with a view to their respective investigation as potential imaging and therapeutic agents for malignant melanoma.



	R ₁	R ₂	R ₃
I	H	H	H
II	H	H	^{131}I
III	H	H	^{211}At
IV	^{131}I	^{131}I	H
V	H	^{211}At	H
VI	I	^{211}At	H

Astatine-211 was produced by the $^{209}\text{Bi}(\alpha, 2n) ^{211}\text{At}$ nuclear reaction using the Nuffield 1.52m cyclotron at Birmingham University. The target, bismuth metal melted onto supporting copper foils, was irradiated with a 28 MeV α -particle external cyclotron beam. Astatine-211 was extracted from the target by dry distillation at 560°C, and flushed by a stream of helium into 100 mM NaOH solution containing 2 $\mu\text{mol Na}_2\text{SO}_3$. The radiochemical purity of ^{211}At was >99.9%.

The preparation of variously radiohalogenated methylene blue derivatives has been attempted by both electrophilic and nucleophilic substitution, and also by thermal isotopic halogen exchange in the presence of 18-crown-6 ether. Respective syntheses and yields are detailed in Table 1. All products (II-VI) were separated and isolated by radio-thin layer chromatography (silica gel UV₂₄₀; EtOH:NH₄OH:H₂O (2:1:2 v/v)); [^{211}At]-astatinated methylene blue derivatives were characterized by sequential analysis (7).

TABLE 1. Syntheses of Radiohalogenated Derivatives of Methylene Blue

Compound	Method	Experimental Details	Yield*
II	Diazonium salt ($^{125}\text{I}^-$)	Radio-iodination of the 4-diazonium salt of MTB, in aqueous solution at 5-10°C, in the presence of KI, for 30 min.	34-46%
	Homogeneous isotopic exchange	Thermal isotopic exchange ($^{125}\text{I}^-/\text{I}^-$) at 80°C for intervals 2-60 min, in the presence of 200 μL 18-crown-6 ether. Plateau yield at 5 min.	63-74%
III	Diazonium salt ($^{211}\text{At}^-$)	[^{211}At]-astatination, under carrier free conditions, of the 4-diazonium salt of MTB in aqueous solution at 5-10°C for 60 min. NO KI.	5-8%
	Heterogeneous isotopic exchange	Thermal isotopic exchange ($^{211}\text{At}^-/4\text{-iodo-MTB}$) at 100°C, over intervals of 2-90 min, in the presence of 200 μL 18-crown-6 ether. Plateau yield at 10 min.	68-79%
IV	Chloramine-T ($^{125}\text{I}^-$)	To 1 mL buffered solution (pH 4.5-6.5) chloramine-T and 10-20 μCi Na^{131}I or Na^{211}At was added 1 mg (I). This was stirred at room temperature for 30-60 min, after which a few drops of 0.1 M $\text{Na}_2\text{S}_2\text{O}_2$ added. For [^{131}I]-iodination, the highest yield was obtained at pH 5.5. The yield for [^{211}At]-astatination did not significantly vary with pH.	23-32%
	Chloramine-T ($^{211}\text{At}^-$)		2-7%
VI	Heterogeneous isotopic exchange	Thermal isotopic exchange ($^{211}\text{At}^-/2,8\text{-di-iodo-MTB}$) at 100°C, over intervals of 2-60 min, in the presence of 200 μL 18-crown-6 ether. Plateau yield at 5 min. The product was presumed to be a mixed mono-[^{211}At]-astatinated halogen derivative.**	60-71%

* corrected for radioactive decay

** Di-[^{211}At]-astatination statistically unlikely

Compounds (II), (III) and (VI) have been rapidly produced by thermal isotopic exchange ($^{131}\text{I}^- \rightarrow \text{I}$; $^{211}\text{At}^- \rightarrow \text{I}$) using the corresponding inert iodo-analogue dissolved in 18-crown-6 ether. Overall yields ranged from 52 - 67%; high specific activity and radiochemical purity were obtained. Other methods of radiohalogenation proved more time-consuming and far less efficient.

In particular, it has been established that 4-[^{211}At]-methylene blue (III) exhibits an affinity for melanin comparable with that of (I). In vitro studies have demonstrated a rapid and sustained accumulation of (III) in melanotic cells; parallel α -particle autoradiography has unambiguously confirmed its localization within melanosomes, both in the body and dendrites (8). At present, wide ranging biological studies with these compounds are in progress.

1. Halnan, K.E., ed., Treatment of Cancer. London, Chapman and Hall (1982).
2. Van Woert, M.H., and Palmer, S.H., Cancer Res., 29, 1952 (1969).
3. Panasiewicz, J., Rybakow, Z., Kaskiewicz, M., and Wiza, J., Radiochem. Radioanalyt. Lett., 33, 397 (1979).
4. Link, E., and Żukiewicz, S., Europ. J. Nucl. Med., 7, 469 (1982).
5. Brown, I., Appl. Radiat. Isotop. (Part A), In press (1986).
6. Brown, I., High Linear Energy Transfer Endoradiotherapeutic Drugs for Malignant Disease. M.D. Thesis, Cambridge University, U.K., pp465 (1986).
7. Meyer, G.-J., Rössler, K., and Stöcklin, G., J. Lab. Comp. Radiopharm., 12, 449 (1975).
8. Link, E., Brown, I., Carpenter, R.N., and Mitchell, J.S., In Proceedings Sixth European Workshop on Melanin Pigmentation, Murcia, Spain, p 33 (1985).

RADIOIODINATED FATTY ACID CARNITINE ESTER: SYNTHESIS AND BIODISTRIBUTION OF 15-(p-iodo(^{131}I)-phenyl)pentadecanoyl-D,L-carnitine chloride

M. Eisenhut, J. Liefhold

Klinikum der Universität Heidelberg, Forschungsgruppe Strahlenklinik, D-6900 Heidelberg, FRG

After the uptake into heart muscle cells long chain fatty acids enter predominantly into the triglyceride and phospholipid pool before they are degraded in the mitochondria by β -oxidation. Therefore the formation of fatty acid esters with glycerine obscures the functional ability of the heart namely to katabolize free fatty acids. The sum of the two reaction pathways are visualized by sequential heart scintigraphy with e.g. ^{131}I labeled 15-(p-iodo-phenyl)-pentadecanoic acid (IPPA).

Before the fatty acids can be degraded by β -oxidation they are bound to carnitine for mitochondrial membrane transport. Thus IPPA would not participate in lipid formation, if it is offered as 15-(p-iodo(^{131}I)-phenyl)-pentadecanoyl-D,L-carnitine chloride (IPPA-CE) to the heart muscle cells. Additionally carnitine esters of fatty acids are known to be better substrates for β -oxidation than free fatty acids (1). We were therefore interested in the biochemical fate of radioiodinated IPPA-CE after intravenous injection into laboratory animals.

The synthesis of radioiodinated IPPA-CE was started with 4-phenyl-1-bromobutane and 11-bromoundecanoic acid which were coupled by a Li_2CuCl_4 catalyzed Grignard reaction (2). The reaction scheme illustrates the formation of 15-Phenylpentadecanoic acid (PPA) (63.6 %). Esterification of PPA with D,L-carnitine was achieved with the acid chloride in trifluoroacetic acid (TFA) (31.8 %). Because of decomposition above 90°C the labeling of PPA-CE with radioiodine could not be performed by isotopic-iodine exchange using IPPA-CE and $^{131}\text{I}^-$. A convenient route to introduce radioiodine under mild conditions into the p-position of the phenyl group of PPA-CE exhibited the reaction of the organothallium intermediate with radioiodide. The formation of the organothallium intermediate was achieved with PPA-CE dissolved in trifluoroacetic acid (TFA), $\text{Tl}(\text{TFA})_3$ and a reaction temperature of 50°C . This reaction mixture served then as a stock solution for the labelings. About $0.5\ \mu\text{mol}$ dissolved in $10\ \mu\text{l}$ TFA was mixed at room temperature with $185\ \text{MBq Na}^{131}\text{I}$ containing $0.25\ \mu\text{mol NaI}$. The unreacted organothallium intermediate was destroyed by the subsequent addition of a mixture of the residual $0.25\ \text{mol NaI}$ dissolved in $1\ \text{N NaOH}$ and Na_2HPO_4 , resulting a product mixture of pH 8 which was then separated by HPLC. The radiochemical yield was about 90 % (isolated).

About $740\ \text{KBq }^{131}\text{I}$ labeled IPPA-CE was injected into a lateral tail vein of female Sprague-Dawley rats ($212 \pm 21\ \text{g}$). The animals were killed and dissected at the indicated time intervals. The table summarizes the % dose/g values of the individual organs. The uptake into the heart was rather small by comparison with the other organs. Even the blood values were at all time intervals greater and the disappearance of the activity from the blood pool was slow. This was probably due to strong binding of IPPA-CE to serum proteins. High values in the other organs may be the result of intramembrane trapping of the highly amphiphilic molecule. In conclusion ^{131}I labeled IPPA-CE did not show the expected rapid

turnover in heart muscle cells as it was found with hexadecanoyl carnitine and isolated rat liver mitochondria (1). The biochemical factors leading to this behaviour are currently under investigation.

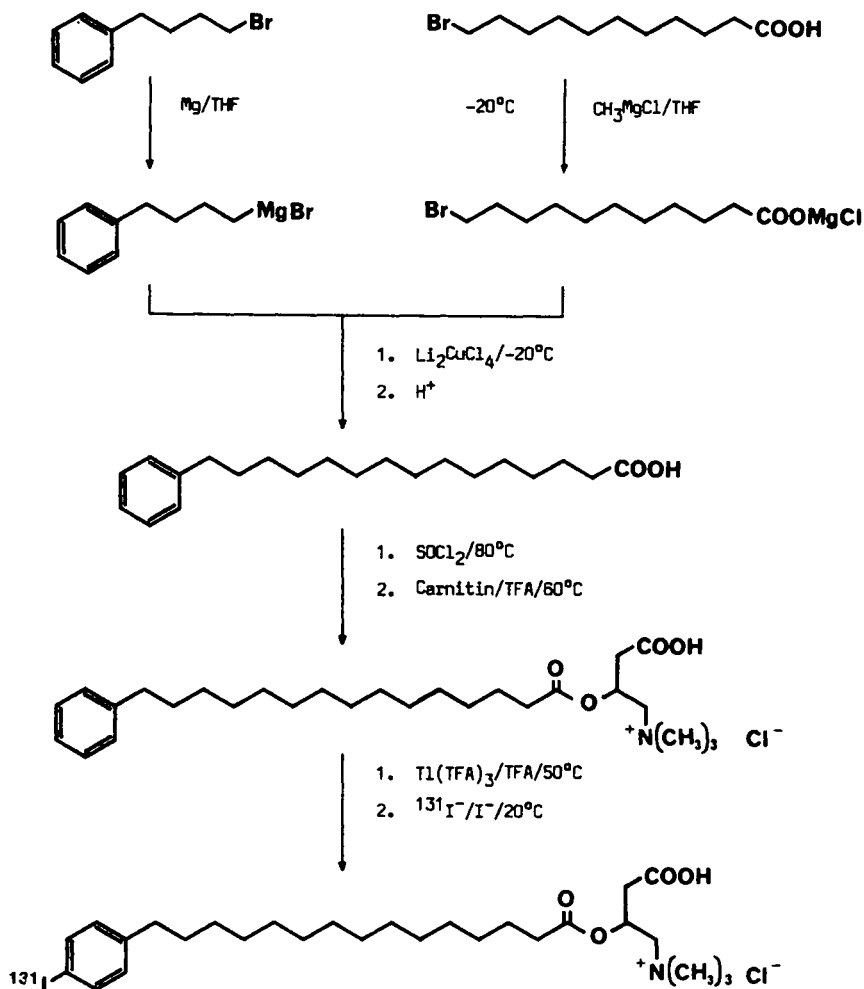


TABLE Organ Distribution of ^{131}I IPPA-CE in SD Rats

Organ	2 Min	5 Min	10 Min	30 Min	60 Min
Heart	1.60* 1.46-1.65	1.34 0.94-1.36	1.26 0.97-1.87	0.68 0.53-0.76	0.66 0.31-0.74
Blood	2.30 1.66-2.30	1.70 1.08-1.77	1.42 1.11-1.55	1.15 0.91-1.40	1.24 0.56-1.52
Lungs	2.77 2.46-3.17	2.95 1.97-3.31	2.65 2.51-2.78	1.81 1.32-1.95	1.56 0.75-1.75
Spleen	1.62 1.47-2.04	1.73 1.46-2.42	1.77 1.70-1.95	1.21 0.97-1.31	1.10 0.60-1.12
Liver	3.37 3.18-3.99	3.54 2.10-3.70	3.06 2.71-3.42	2.82 2.55-3.94	2.11 1.01-2.90
Kidneys	2.07 1.86-2.11	2.16 1.43-2.28	2.10 1.75-2.37	1.94 1.38-2.24	1.92 0.77-2.14
Muscle	0.16 0.11-0.19	0.21 0.12-0.27	0.24 0.17-0.27	0.24 0.18-0.28	0.23 0.08-0.25

*Median with range of % inj. dose/g tissue weight (three animals for each time period)

Acknowledgment. The Deutsche Forschungsgemeinschaft (DFG) is thanked for financial support and a grant to one of us (J.L.).

1. Al-Arif, A., and Blecher, M., *Biochim. Biophys. Acta* **248**, 406 (1971)
2. Baer, T.A., and Carney, R.L., *Tetrahedron Letters*, **1976**, 4697

SYNTHESIS AND BIOLOGICAL EVALUATION OF (E)-19-IODO-3,3-DIMETHYL-18-NONADECENOIC ACID, A NEW DIMETHYL-BRANCHED LONG-CHAIN FATTY ACID TO EVALUATE REGIONAL MYOCARDIAL FATTY ACID UPTAKE M. M. Goodman, K. R. Ambrose, K. H. Neff, and F. F. Knapp, Jr., Nuclear Medicine Group, Oak Ridge National Laboratory, Oak Ridge, TN 37831, USA.

Iodine-123-labeled structurally-modified long chain fatty acids that exhibit myocardial extraction and uptake similar to naturally occurring fatty acids, but which show prolonged retention are excellent candidates to evaluate aberrations in fatty acid metabolism that occur when the coronary arteries are normal and perfusion is not impaired. Recent quantitative autoradiographic studies in laboratory animals employing methyl-branched fatty acids have shown that hypertensive heart disease (1) and cardiomyopathies (2) are two heart disorders where there can be a dissociation between regional differences in fatty acid uptake and regional perfusion. Because of the clinical potential of using SPECT to evaluate cardiomyopathies and hypertensive disease, we have developed a variety of radioiodinated methyl-branched fatty acids (3,4). Although increased myocardial retention was achieved, these agents, however, did not demonstrate complete retention indicating catabolism was being impaired but not prevented. The goal of this study was to develop a dimethyl-branched fatty acid (5) with the radiolabel stabilized as a vinyl iodide with the objective of achieving high myocardial uptake with irreversible retention.

The synthetic method chosen for the preparation of (E)-19-iodo-3,3-dimethyl-18-nonadecenoic acid (19) involved introduction of substituents into the 2- and 5-positions of a thiophene ring followed by sulfur extrusion of a 2,5-dialkyl thiophene derivative to provide a key 3,3-dimethyl-branched fatty acid intermediate, 17-iodo-3,3-dimethylheptadecanoic acid (14) (Scheme I). Compound 14 was prepared by Friedel Crafts condensation of $\text{CH}_3\text{O}(\text{CH}_2)_7\text{COCl}$ with dimethyl-branched thiophene (7) followed by Wolff-Kishner reduction, sulfur extrusion with Raney nickel and treatment of the terminal methoxy methyl-branched intermediate (13) with $(\text{CH}_3)_3\text{SiI}$. The (E)-vinyl iodide was introduced into the terminal position of the dimethyl-branched acid by iododestannylation (Scheme II). The pivotal step in the synthesis of the (E)-iodovinyl acid involved hydrostannylation of 3,3-dimethyl-18-nonadecynoic acid (15) with $(n\text{-Bu})_3\text{SnH}$. Iododestannylation of the stannyl intermediate 17 with I^+ followed by basic hydrolysis gave 19. Tissue distribution studies of ^{125}I -labeled 19 (Table 1) and 14 (Table 2) were performed in fasted rats. Iodine-125 19 showed 90% retention of the initial myocardial uptake (4.56% dose/g, at 2 min) after 60 min. In contrast to the prolonged myocardial retention observed with 19, iodine-125 14 showed rapid myocardial washout and significant *in vivo* deiodination. The significant difference in myocardial extraction and retention of the iodovinyl agent compared with the iodoalkyl derivative dramatically illustrate the enhanced stability of iodide attached to an iodovinyl moiety.

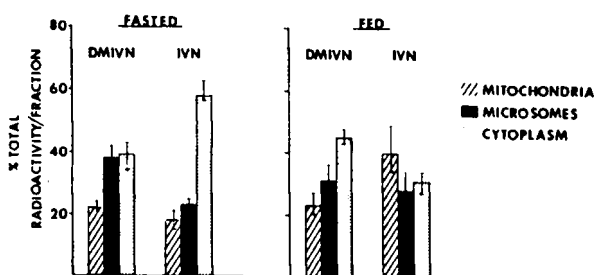
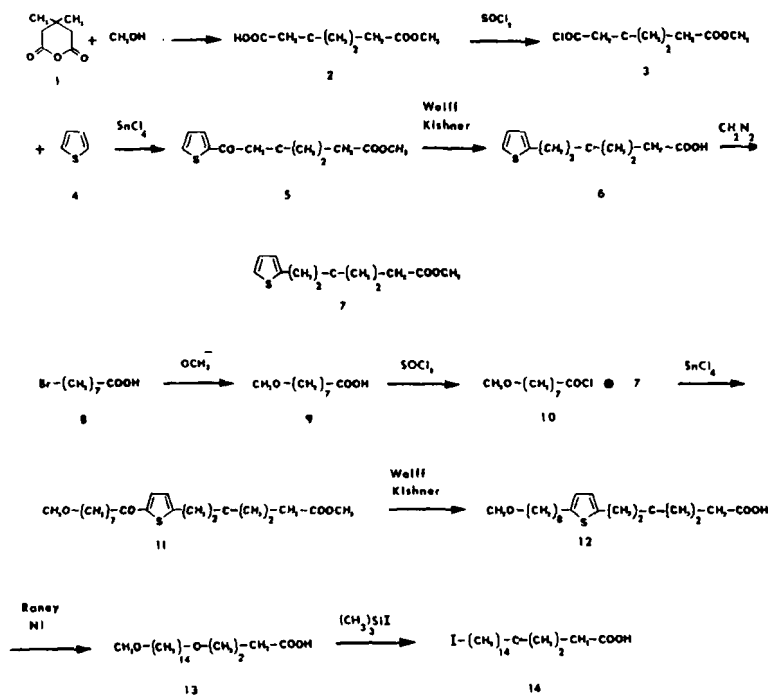


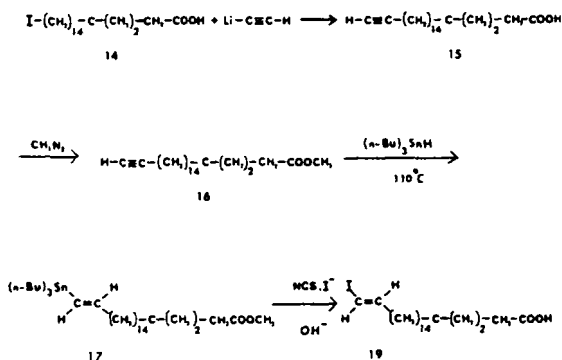
Fig. 1. Distribution (with ranges) of radioactivity in subcellular fractions from rat hearts 30 min after injection of ^{125}I -labeled DMIVN or IVN.

Myocardial subcellular distribution studies of the ^{125}I -labeled **19** (DMIVN) in fasted rats showed a higher association of radioactivity with the microsomes when compared to the results obtained with the 19-carbon straight chain analogue (**4**) (IVN) which appeared to exist primarily in the cytoplasm (Fig. 1). When the rats were nonfasted (fed) the distribution profiles of the two analogues showed differences that seemed to correlate with the differences in myocardial retention that fasting and feeding can induce.

The significant myocardial uptake, retention and high heart: blood ratios of agents of this type *now* may enable the diagnosis and management of patients with hypertensive disease and cardiomyopathies by SPECT.



Scheme I



Scheme II

Table 1. Distribution of Radioactivity (% Injected Dose/Gram of Tissue) in Fasted Rats at Various Times after Intravenous Administration of 19- 125 I]Iodo-3,3-dimethyl-18-nonaheptanoic Acid.^a

Tissue	Time after injection; percent injected dose/gram (range)				
	2 min	5 min	30 min	1 h	2 h
Heart	4.56 (4.30-5.05)	4.66 (4.29-4.83)	4.60 (4.14-5.26)	4.10 (3.62-4.56)	3.66 (3.12-4.28)
Blood	2.44 (2.09-2.84)	3.62 (1.41-3.84)	0.74 (0.66-0.80)	0.71 (0.65-0.74)	0.70 (0.67-0.72)
Lungs	2.17 (1.96-2.35)	2.09 (1.90-2.26)	1.42 (1.27-1.57)	1.22 (1.14-1.33)	1.05 (1.01-1.08)
Liver	7.27 (6.92-8.04)	7.27 (7.18-7.46)	5.88 (4.69-6.72)	4.93 (4.67-5.39)	3.89 (3.71-4.17)
Kidneys	1.38 (1.17-1.53)	1.46 (1.31-1.61)	1.49 (1.37-1.63)	1.46 (1.35-1.56)	1.29 (1.23-1.37)
Thyroid	24.21 (21.42-26.72)	23.53 (20.60-26.37)	40.62 (33.82-44.14)	83.10 (62.11-117.75)	157.04 (122.63-209.34)
Mean Heart:Blood	1.9:1	2.9:1	6.2:1	5.8:1	5.3:1

^aMean and range value for five female Fischer rats.

Table 2. Distribution of Radioactivity (% Injected Dose/Gram of Tissue) in Nonfasted Rats at Various Times after Intravenous Administration of 17- 125 I]Iodo-3,3-dimethyl-heptadecanoic Acid.^a

Tissue	Time after injection; percent injected dose/gram (range)				
	2 min	5 min	15 min	30 min	1 h
Heart	2.84 (2.50-3.27)	2.06 (1.91-2.31)	1.22 (1.12-1.42)	0.84 (0.73-0.90)	0.68 (0.54-0.84)
Blood	2.59 (2.14-2.98)	1.87 (1.75-2.01)	1.36 (1.29-1.43)	1.04 (1.00-1.09)	0.83 (0.74-0.96)
Lungs	2.19 (1.98-2.38)	1.96 (1.83-2.13)	1.40 (1.34-1.44)	0.98 (0.96-1.02)	0.64 (0.07-0.82)
Liver	5.26 (4.81-5.55)	3.99 (3.66-4.35)	2.34 (2.09-2.61)	1.44 (1.41-1.50)	1.07 (0.88-1.27)
Kidneys	1.38 (1.31-1.50)	1.48 (1.45-1.54)	1.33 (1.24-1.43)	0.97 (0.93-1.03)	0.74 (0.63-0.86)
Thyroid	15.93 (13.49-22.02)	16.83 (13.55-19.04)	42.89 (29.88-57.48)	78.40 (66.29-92.69)	148.83 (130.32-188.72)
Mean Heart:Blood	1.1:1	1.1:1	0.9:1	0.8:1	0.8:1

^aMean and range value for five female Fischer rats.

Research supported by the Office of Health and Environmental Research, U.S. Department of Energy, under contract DE-AC05-84OR21400 with Martin Marietta Energy Systems, Inc. and grant HL 35500-01 with National Institutes of Health.

1. Yonekura, Y., Brill, A., et al., *Science*, **227**, 1494 (1985).
2. Kubota, K., Som, P., et al., *J. Nucl. Med.* (in press).
3. Goodman, M., Knapp, Jr., F., et al., *J. Med. Chem.*, **27**, 390 (1984).
4. Goodman, M., Knapp, Jr., F., et al., *J. Med. Chem.*, **28**, 807 (1985).
5. Knapp, Jr., F., Goodman, M., et al., *J. Nucl. Med.*, in press.

FAST HIGH YIELD Cu(I) ASSISTED PREPARATION OF 123I-15 (4-I-PHENYL)-9 METHYLPENTADECANOIC ACID

J. Mertens¹, J. Eersels¹, W. Vanryckeghem¹ and M.S. Robbins²¹VUB-Cyclotron, VUB, B-1090 Brussel, ²Mallinckrodt Inc. St Louis, MO, USA.

The use of Cu(I) in reducing conditions, applied for kit labelling with ¹²³I- of different pharmaceuticals (1, 2, 3), has been successfully applied for the ¹²³I-radioiodination of 15 (4-I-phenyl)-9 methylpentadecanoic acid (9 MPDA) in mixed solvent conditions. It allows to obtain the pure radiopharmaceutical, ready for injection, within 90 minutes with an overall radiochemical yield of 84 %. ¹²³I-9MPDA, of which the biodistribution in animals has been described by Robbins et al (4) is tried for clinical evaluation as a diagnostic myocardial imaging agent.

Labelling conditions : 3 mg ascorbic acid, 1.5 mg 2,5 dihydroxybenzoic acid, 0.75 mg 9MPDA are dissolved in 400 µl of a 7/3 EtOH/H₂O solution. After addition of 25 µl of a 13 mM CuSO₄ solution and the ¹²³I⁻ solution (1–20 mCi (37–740 MBq), concentration ~0.5 mCi/µl, no carrier added), the reaction vial is septum closed. The reaction mixture is flushed, ice cooled during 10 minutes with N₂ and than heated during 60 minutes at 100°C.

Preparative HPLC : Waters HPLC set-up (U6K injector with 2 ml loop, M 6000 A pump, RI detector), Ortec NaI(Tl) detector and electronics, Shimadzu Intersmat integrators. Hibar RP-18, 7 µ, 250 x 10 mm column. Eluent : EtOH/H₂O//HoAc-85/15//0.5 at a flow rate of 6 ml/min. After recovery of the peak of interest, the eluent is evaporated by passing a stream of preheated (100°C) nitrogen. Then 250µl of ethanol are injected while rinsing the walls and a 4 % HSA solution is added with vigorous vortexing. The final solution is sterilized by means of a 0.22 µ millipore filter.

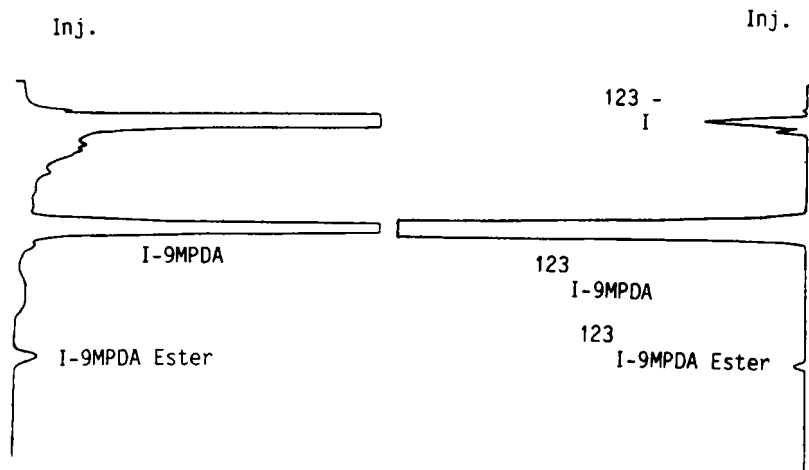


Figure 1. Preparative HPLC separation of the final reaction mixture. Left trace: UV signal. Right trace: radioactive signal.

Results and Discussion : When applying the described labelling conditions a mean radiochemical yield (determined by the area of the HPLC peaks) of 95 % is obtained (n = 12, min. = 92 %, max 99 %). As shown in Fig. 1 the final reaction mixture contains three

products : for the major part ($\sim 95\%$) ^{123}I -9MPDA ($t_r = 10.0$ min.), free $^{123}\text{I}^-$ and $^{123}\text{IO}_3^-$ which is eluted together with the reduction agents ($t_r = 2.5$ min) and a small amount ($\sim 0.5\%$) of the ethyl ester of ^{123}I -9MPDA ($t_r = 19.0$ min.) It was found that the EtOH/H₂O ratio of 7/3 used in the proposed procedure still dissolves the fatty acid while the smallest amount of ^{123}I -9MPDA ester is formed. Sn (II), which is a strong enough reductor to reduce iodate to iodide, has to be omitted in the reaction mixture as at the pseudo pH of 3.4 of the mixed solvent, a Sn(OH)₂ precipitate is generated. Acidifying the reaction mixture to improve the labelling yield (optimal pH for aqueous kit labellings < 2.5 (1,2)) as well as the solubility of Sn(II) results in high yields of the ethyl ester of ^{123}I -9MPDA (up to 30%). This means that reaching high labelling yields depends on the radiochemical purity of the ^{123}I - solution. The ethanolic solution obtained after evaporation of the eluent was controlled by means of a HPLC system different from the preparative one (Merck-Lichrosorb RP 18,5 μ , 150 x 3,2 mm column ACN/HoAC-99/1 as eluent). This fraction only contained pure ^{123}I -9MPDA (specific activity 1.3-26 mCi/mg depending on the initial activity).

The yields obtained when labelling smaller amounts (down to 0.2 mg) of I-9MPDA with ^{131}I in view of obtaining higher specific activities are reported in table 1.

Table 1 Radiochemical yield (%) with $^{131}\text{I}^-$ as a function of the amount of 15(4-I-phenyl)-9 methylpentadecanoic acid (9MPDA)

Amount of 9M-IPPA		n %		
mg	(μ mol)	^{131}I -9MPDA	$^{131}\text{I}^-$	^{131}I -ester
0.4	(0.88)	96.0	3.3	0.7
0.3	(0.66)	94.3	5.7	—
0.2	(0.44)	88.0	12.0	—

In these experiments 15 μ l of CuSO₄ solution were used instead of 25 μ l as indicated in the proposed procedure to keep the molar ratio of Cu(I) to the iodo-aryl containing substrate smaller than 0.5. Although labelling yields obtained with ^{131}I are generally more favorable than those obtained with ^{123}I , high yield preparations of ^{123}I -9MPDA, with a 4-8 fold higher specific activity, may be expected. The preparation of "carrier free" ^{123}I -9MPDA starting from 15(4-bromophenyl)-9 methylpentadecanoic acid, is studied.

The authors¹ thank Mallinckrodt Inc. (St Louis, USA) and Diagnostica (Petten, The Netherlands) for supplying the 15 (4-I-phenyl)-9 methyl-pentadecanoic acid and for financial support.

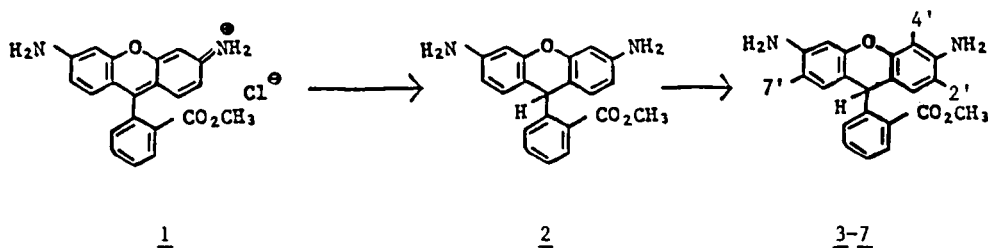
1. Mertens, J., Vanryckeghem, W., In Abstracts European Nuclear Medicine Congress, London 1985, p. 206
2. Mertens, J., Vanryckeghem, W., In Proceedings Second European Symposium on Radiopharmaceuticals and Labelled Compounds, Cambridge 1985, in press
3. Mertens, J.J.R., Vanryckeghem, W., Carlsen, L., In Proceedings 32nd Ann. Meeting society of Nuclear Medicine, Houston, 1985, p. 123
4. Robbins, M.S., Adams, M.D., Anderson, H.A., Dean, R.T., White, D.H., In Proceedings 32nd Ann. Meeting Society of Nuclear Medicine, Houston, 1985, p. 124.

SYNTHESIS OF IODINATED DERIVATIVES OF RHODAMINE

B.M. Kinsey, A.I. Kassis, F. Fayad, W.W. Layne, and S.J. Adelstein
Department of Radiology, Harvard Medical School, Boston, MA 02115

Rhodamine 123 (1) is a permeant cationic dye that has been used as a fluorescent stain for mitochondria (1). It is retained for a longer period by certain types of cancer cells (2–5 days) than by normal cells (1–16 hours)(2). Radioiodinated 1 might serve therefore as a tumor imaging or radiotherapeutic agent, as it would be washed out from normal cells at a faster rate than from cancerous cells.

Our attempts to iodinate 1 using a variety of iodinating agents such as chloramine T, Iodogen, and peracetic acid have yielded only starting material as determined by NMR. However, iodination of dihydrorhodamine (2) using N-chlorosuccinimide in CCl₄ yields mainly 2'-iododihydrorhodamine (3), and changing the iodination conditions allows isolation of other derivatives (4–7). Characterization of these compounds has been accomplished by NMR. Radioiodination of 2 using Na¹²⁵I produces the whole range of derivatives which are readily separated by flash chromatography and identified by TLC autoradiography.



COMPOUND	POSITION			% DISTRIBUTION OF RADIO- IODINATED PRODUCTS
	4'	2'	7'	
<u>3</u>	H	I	H	50
<u>4</u>	I	H	H	18
<u>5</u>	H	I	I	24
<u>6</u>	I	H	I	7
<u>7</u>	I	I	I	1

The compounds synthesized are fluorescent only in the oxidized form. It has been demonstrated that the reduction of ethidium bromide gives a product that is taken up by live mammalian cells and intracellularly oxidized back to ethidium (3). Similarly, when Chinese hamster V79 lung fibroblasts are incubated with a 10 μ M solution of dihydrorhodamine 123 (2) for 2 hours, the cell cytoplasm becomes fluorescent, indicating that this nonfluorescent dye is being oxidized to the highly fluorescent 1. After 24 hours, the fluorescence is localized in the mitochondria, and the staining pattern of 2 is exactly the same as that of 1. The same behavior is observed for the iodinated compounds 3–7 indicating that the presence of one or more iodine atoms on the molecule has not affected its ability to localize in the cell cytoplasm. No staining of the nucleus is observed for any of the derivatives, even though tetrabromorhodamine 123 has been reported to intercalate with DNA (4). In fact, we have observed no changes in the visible and fluorescence spectra of 1 when it is incubated with calf thymus DNA, which indicates that 1 does not interact/intercalate with DNA.

The uptake of the ^{125}I labeled compounds by V79 cells, as determined by the microfuge method (5), is shown in Table 1. The results indicate that all 5 iodinated derivatives are avidly concentrated by cells thereby confirming the results obtained by fluorescence microscopy. Furthermore, uptake was time dependent; at 20 hours there is a 2 to 5 fold increase over the 2-hour values. When the intracellular contents in pCi/cell are converted to $\mu\text{Ci/ml}$ (V79 cells have a volume of 570×10^{-12} ml/cell), under these conditions these drugs are almost 100 to 300 times as concentrated inside the cell as in the extracellular environment. The *in vitro* and *in vivo* uptake and retention of these compounds in normal and tumor cells will be reported.

TABLE 1. Uptake of ^{125}I -Dihydrorhodamine Derivatives by Chinese Hamster V79 Lung Fibroblasts*

Compound	Location of ^{125}I	Cellular Uptake (pCi/cell \pm s.e.m.)	
		2 hours	20 hours
<u>3</u>	2'	0.21 \pm 0.007	1.04 \pm 0.033
<u>4</u>	4'	0.33 \pm 0.011	0.90 \pm 0.012
<u>5</u>	2', 7'	0.72 \pm 0.11	1.44 \pm 0.13
<u>6</u>	4', 7'	0.56 \pm 0.003	1.22 \pm 0.065
<u>7</u>	2', 4', 7'	0.70 \pm 0.028	1.65 \pm 0.27

*Cells were incubated at 37°C in 3.39 ± 0.06 $\mu\text{Ci/ml}$

1. Johnson, L.V., Walsh, M.L., and Chen, L.B., Proc. Natl. Acad. Sci. USA, 77, 990 (1980).
2. Lampidis, T.J., Bernal, S.D., Summerhayes, I.C., and Chen, L.B., Ann. N.Y. Acad. Sci., 397, 299 (1982).
3. Gallop, P.M., Paz, M.A., Henson, E., and Latt, S.A., Biotechniques, 2, 32, (1984).
4. Wong, J., Hogan, M., and Austin, R.H., Proc. Natl. Acad. Sci. USA, 79, 5896, (1982).
5. Kassis, A.I., and Adelstein, S.J., J. Nucl. Med., 21, 88 (1980).

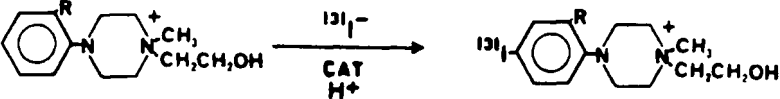
RAPID LABELING OF RADIOPHARMACEUTICALS WITH IODINE-122

C.A. Mathis, S.M. Moerlein, Y. Yano, A.T. Shulgin, R.N. Hanson*, H.F. Kung**
 Donner Laboratory, Lawrence Berkeley Laboratory, University of California,
 Berkeley, CA 94720, *Section of Medicinal Chemistry, Northeastern University,
 Boston, MA and **VA Medical Center, Buffalo, NY

The short half-life of the positron emitter ^{122}I ($t_{1/2}$ 3.6 min) collected from its ^{122}Xe parent ($t_{1/2}$ 20.1 h) requires rapid labeling methods for the incorporation of ^{122}I into radiopharmaceuticals for PET studies (1,2). We have investigated three types of iodination reactions with several useful radiopharmaceuticals which illustrate the versatility of ^{122}I labeling chemistry. The reaction types include: (I) iododeprotonation of highly activated aryl systems such as the *meta*-substituted dimethoxyamphetamines for brain imaging studies (1) and several quaternary phenylpiperazinium compounds for use as heart imaging agents (3,4); (II) rapid ^{122}I -for- ^{127}I exchange to produce ^{122}I -labeled N,N,N' -trimethyl- N' -[2-hydroxy-3-methyl-5-iodobenzyl]-1,3-propanediamine (^{122}I -HIPDM) for cerebral blood flow studies (5); and (III) iododemetalations of three precursors of N,N -dimethyl-4- ^{122}I -phenylisopropylamine, which is a model representing a class of slightly activated mono-substituted amphetamine analogs.

The syntheses of ^{122}I -labeled *meta*-dimethoxy- N,N -dimethylphenylisopropylamines have been reported and labeling yields of 50-85% achieved in 60 s (2). From a generator containing 100 mCi of ^{122}Xe , 20-30 mCi of the purified product were available at the end of synthesis for injection. Preliminary labeling studies of two phenylpiperazinium salts were conducted with ^{131}I for convenience to evaluate reaction conditions resulting in high labeling yields in a short time (Table 1). Radioiodinations were carried out at 25°C and 70°C in sealed vials containing 400 μg of the precursor, 100 μg chloramine-T, and 500 μl solvent. The reactions were quenched at the indicated times by the addition of 500 μg sodium metabisulfite and the radiochemical yields determined utilizing radio-HPLC. For animal studies, the unreacted radioiodine was removed by passage of the crude reaction products through an anion exchange column resulting in a solution >95% radiochemically pure. These labeling methods can be extended to the tertiary aryl phenylpiperazine brain agents as well (6).

Table 1. Radiochemical Yields of ^{131}I -Iodination of Phenylpiperaziniums.



R	T(°C)	Radiochemical Yields (%)		
		0.5 min	1 min	5 min
CH ₃	70	41±9	55±4	52±5
H	25	82±8	93±3	93±4

Labeling conditions suitable for the rapid exchange of ^{122}I -for- ^{127}I utilizing 1 mg of HIPDM were investigated and included an acidic reaction medium (0.1M phosphoric acid), elevated temperature (100°C), and a trace of oxidant (50 μg KIO_3). Labeling yields of 80% in 3 min were achieved resulting in 15 mCi of ^{122}I -HIPDM for injection from a 100 mCi ^{122}Xe generator. Anion exchange chromatography removed inorganic ^{122}I , resulting in product radiochemical purities >98%.

Three metallated aryl derivatives of *N,N*-dimethylphenylisopropylamine were synthesized in 20-30% overall yields (Figure). Radiohalogenation reactions utilizing both ^{131}I and ^{122}I were conducted to evaluate the speed of radioiodination (Tables 2,3). Reaction conditions were optimized; variables included solvents, pH, temperature and reaction time (30 s to 5 min). Radioiodination yields from the $\text{Sn}(\text{CH}_3)_3$ derivative (**1**) were high within 30 s at 25°C and increased slightly at 70°C. Radioiodination yields from the $\text{Ge}(\text{CH}_3)_3$ (**2**) and $\text{B}(\text{OH})_2$ (**3**) substrates were substantially less than those achieved for **1** at 25°C and increased to modest levels at 70°C.

Highly activated compounds such as the phenylpiperazinium salts and the *meta*-substituted dimethoxyamphetamines can be radioiodinated directly with good radiochemical yields in short reaction times. HIPDM can undergo rapid exchange reactions with ^{122}I resulting in high yields. The use of a stannylated aryl precursor for the rapid, regiospecific iodination of non-activated aromatic systems appears promising; germylated and boronic precursors may also be useful for rapid iodinations of aromatic systems that contain a greater degree of activation towards electrophiles. This research was supported by the U.S. Department of Energy (DE-AC03-76SF00098).

Figure. Synthesis of Metallated Precursors.

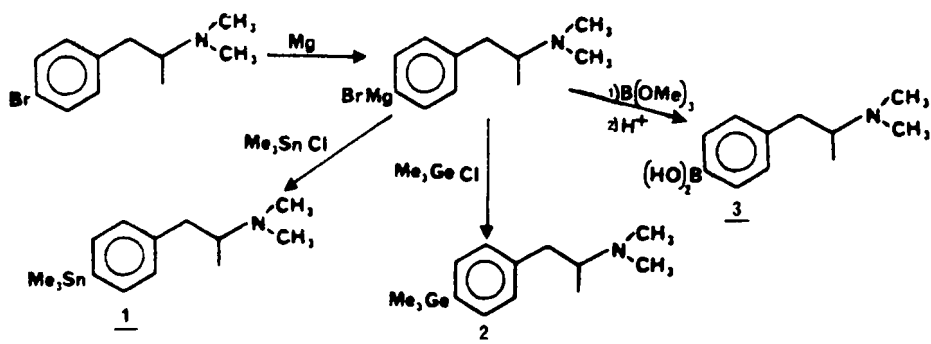
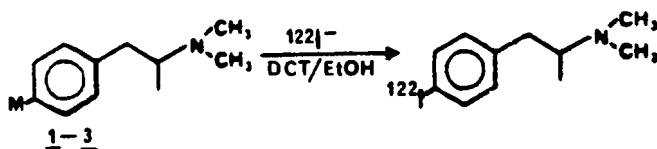


Table 2. Radiochemical Yields for ^{131}I -Iodination of Metallated Precursors.

Precursor	pH	T(°C)	Radiochemical Yield (%)		
			0.5 min	1 min	5 min
<u>1</u>	1.5	25	72±7	74±5	80±3
<u>1</u>	4.3	25	46±9	67±6	71±4
<u>1</u>	7.4	25	02	03	05±3
<u>2</u>	1.5	70	41±7	48±3	65±4
<u>2</u>	4.3	70	03	05±3	08±3
<u>2</u>	7.4	70	<1	<1	<1
<u>3</u>	1.5	70	05	07	12±3
<u>3</u>	4.3	70	09±6	17±3	26±4
<u>3</u>	7.4	70	07	09	18±4

Table 3. Radiochemical Yields for ^{122}I -Iodination of Metallated Precursors[†].

Precursor	Radiochemical Yield (%)			EOS Yields (mCi) [‡]		
	1 min	3 min	5 min	1 min	3 min	5 min
<u>1</u>	66±5	70±9	72±12	33	24	16
<u>2</u>	07	--	17	03	--	04
<u>3</u>	<1	--	<1	<1	--	<1

[†]Reaction solvent 100% EtOH (2 ml) with dichloramine-T oxidant (500 μg) and 2 mg precursor (1-3) at 25°C.

[‡]End of synthesis yields based upon a 100 mCi $^{122}\text{Xe}/^{122}\text{I}$ generator.

1. Mathis, C.A., Sargent III, T., and Shulgin, A.T., *J. Nucl. Med.*, 26, 1295 (1985).
2. Mathis, C.A., Shulgin, A.T., and Sargent III, T., *J. Labelled Compd. Radiopharm.*, in press.
3. Hanson, R.N., *Int. J. Nucl. Med. Biol.*, 10, 219 (1983).
4. Hassan, M.A. and Hanson, R.N., *J. Med. Chem.*, submitted.
5. Kung, H.F., Tramposch, K.M., and Blau, M., *J. Nucl. Med.*, 24, 66 (1983).
6. Hanson, R.N., *Int. J. Nucl. Med. Biol.*, 12, 315 (1985).

SYNTHESIS AND IDENTIFICATION OF CHLOROGLYCOLURIL FOR RADIOIODINATION

Yue, Jia Yu and Li, Yong Jian

Shanghai Institute of Nuclear Research, Academia Sinica, P.O. Box 8204, Shanghai, The People's Republic of China

The well-documented methods including iodine monochloride, chloramine, electrolysis, peroxidase and conjugation have been proved frequently unsatisfactory for labelling bioactive proteins with respect of labelling rate, bioactivity, simplicity or feasibility. The newly emerged solid phase oxidants such as 1,3,4,6-tetrachloro-3 α ,6 α -diphenylglycoluril (chloroglycoluril) (1) has shown some promising features to solve these troubles. Although chloroglycoluril product is commercially available (under the trade name Iodogen) but the results of its applications in protein labelling sometimes diverged considerably. This paper describes the preparation, analysis, and identification of pure chloroglycoluril for evaluation of its merits in radiiodination of protein (in a separate paper).

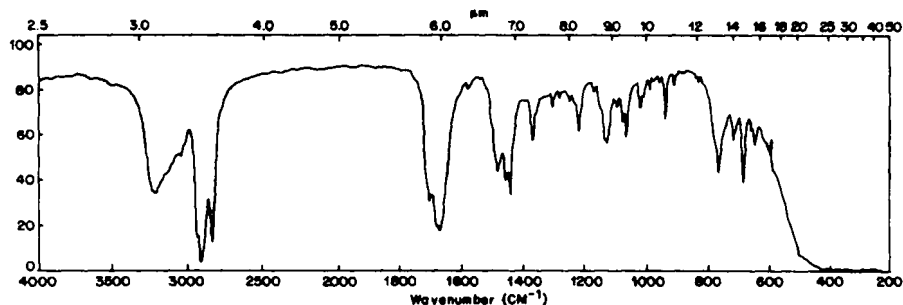
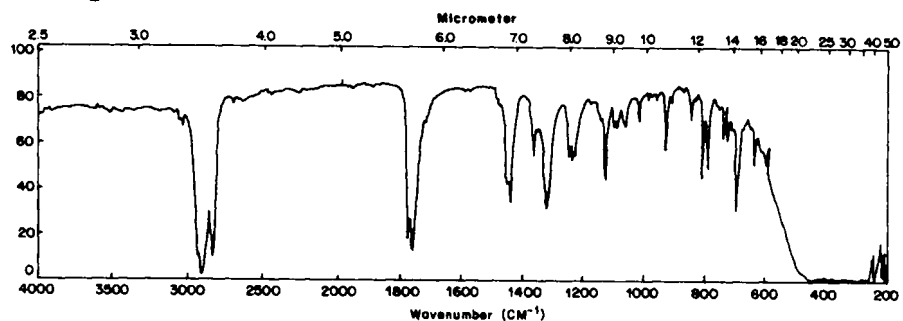
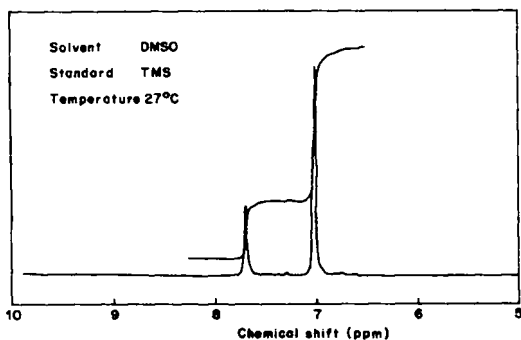
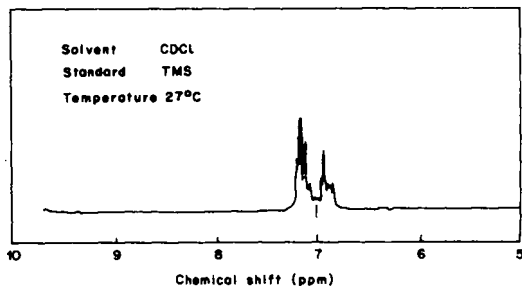
The synthesis of chloroglycoluril was started from condensation of benzil and urea in hydrogen chloride/ethanol system to produce intermediate 3 α ,6 α -diphenylglycoluril (glycoluril) which was pure white crystal after washing with water and dried, 97.8% in yield. Glycoluril was further chlorinated in weak alkaline solution with the presence of aerosol OT to form chloroglycoluril with a yield of 89.64%. The crude product washed with water, dried at 100°C for 3 hours was recrystallized from chloroform/petrol ether solution giving a recovery over 83.6%.

The refined product had a m.p. of 246.5-247.0°C, and elemental composition as follows:

ELEMENTS	C	H	N	Cl
Experimental Wt%	44.44	2.21	12.95	32.83
Theoretical Wt%	44.48	2.33	12.97	32.83

Its ultraviolet spectrum has only one absorption at λ_{max} 288nm ($\log \epsilon = 317$) attributing to benzene ring.

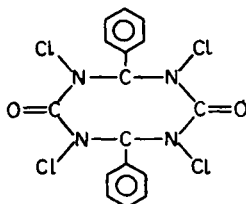
The infra red spectrum (IP) of 3 α ,6 α -diphenylglycouril (Fig.1) in nujol mull was identical to standard spectrum (2). While the IR spectrum of chloroglycoluril (Fig.2) lost the ν_{NH} absorption at

Fig.1 IR spectrum of 3 α ,6 α -diphenylglycolurilFig.2 IR spectrum of 1,3,4,6-tetrachloro-3 α ,6 α -diphenylglycolurilFig.3 $^1\text{H-NMR}$ of
3 α ,6 α -diphenylglycolurilFig.4 $^1\text{H-NMR}$ of
1,3,4,6-tetrachloro-3 α ,
6 α -diphenylglycoluril

3300-3000 cm^{-1} and retained ν_{CH} and δ_{CH} absorption of benzene. In $^1\text{H-NMR}$ of glycoluril (Fig.3) the singlet peak of chemical shifts $\delta 7.7(\tau 2.7)$, $\delta 7.02(\tau 2.98)$ and the integrate curve showed 4 protons of amine group and 10 protons on benzene nuclei, while NMR

of chloroglycoluril gave no peak at $\delta 7.7$ ($\tau 2.3$) (Fig. 4). This was consistent with the IR.

By the information thus obtained the chemical structure of chloroglycoluril could properly be assigned as follows:



This was also supported by its mass spectrum (MS). The major peaks of cracking fragments found in MS are listed as follows:

m/e*	430	395	361	372	318	269	234	215	206	181	138
n*	4	3	2	1	2	1	0	2	0	1	1

* m/e = ratio of mass to charge; n = no. of chlorine atom

The chloroglycoluril was unstable in solution under the light, turning to bright yellow in a few hours. Its chloroform solution decomposed vigorously when it was heated to 60°C. It was soluble in aqueous alkaline solution (pH \geq 10) but insoluble in acidic. By storing in refrigerator within a dark vacuum desiccator the structure of chloroglycoluril was kept unchanged for more than a year.

- (1) Fraker, Pamela J. and Speck, John C., Jr, *Biochem. Biophys. Res. Commun.* **80**, 849 (1978)
- (2) Pouchert, C. J., *The Aldrich Library of Infrared Spectra*, Aldrich Chemical Co. Inc. 901 (1970)

THE APPLICATION OF CHLOROGLYCOLURIL IN RADIOIODINATION OF PROTEINXue, Jia Yu and Li, Yong Jian

Shanghai Institute of Nuclear Research, Academia Sinica, P.O. Box 8204, Shanghai, The People's Republic of China

The novel method of using 1,3,4,6-tetrachloro-3 α ,6 α -diphenylglycoluril (chloroglycoluril) for radioiodination that first introduced by Fraker and Speck (1) has been found to be a reproducible, gentle, efficient and technically simple approach in labelling biomolecules (2)(3)(4). In this paper the human fibrinogen (hFbg) was labelled as a model protein to investigate the applicability of chloroglycoluril towards radioiodination of bioactive material. This was compared with conventional chloramine-T. The chloroglycoluril (synthesized by the method referred separately) was used either in form of thin film on the wall of polyethylene container or as fine suspension in reaction solution. In iodination 1.7 mg (5×10^{-9} mol) of hFbg in 150 μ l of sodium phosphate buffer (PBS 0.05 M, pH 7.4), 20 μ l Na¹²⁵I and 30 μ l of KI (8.3 μ g) were brought in contact with chloroglycoluril (1.16×10^{-7} mol) at 0°C for a certain time and the reaction was stopped by withdrawing from the solid. Alternatively, with other conditions remaining unchanged, 50 μ l PBS solution of chloramine-T (1.16×10^{-7} mol) was used instead of chloroglycoluril where the reaction was ceased by adding 100 μ l of sodium metabisulfite in PBS. The labelled product was purified by passing through a 1x10 cm column of Sephadex G-25 that previously saturated with 1% BSA. The labelling rate (1) were calculated from the radioactivities of precipitate R_1 (precipitated with 50 μ l 1% BSA carrier by trichloroacetic acid, TCA) and supernatant R_0 .

$$\frac{R_1 \cdot f_{II}}{R_0 + R_1} \times 100 \% \quad (1)$$

f_{II} is the correction factor (determined by experiments)

The clottability (2) was obtained by a method similar to Pegoeczi (5).

$$\frac{R_I \times f_I}{R_I \cdot f_I - R_{II} \cdot f_{II}} \times 100 \% \quad (2)$$

R_I, R_{II} are the radioactivities of clot formed by thrombin and precipitate formed by TCA; f_I, f_{II} are correction factors for clotting and precipitation (determined by experiments)

It can be seen from Fig.1 and fig.2 that increasing of either chloroglycoluril or reaction time enhanced labelling rate and

reached a constant rapidly, but caused no influence upon clottability.

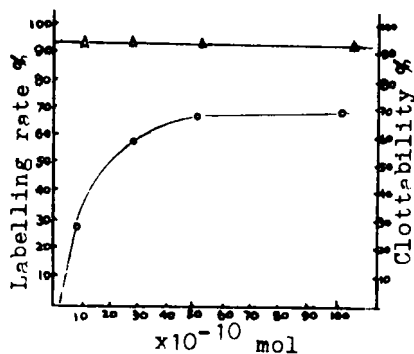


Fig. 1 The dependences on chloroglycoluril
 ○ - labelling rate
 △ - reaction times

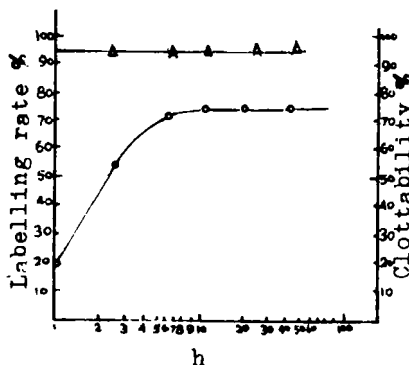


Fig. 2 The dependences on reaction times

Generally, for 1.7 mg hFbg and 1.16×10^{-7} mol of chloroglycoluril 10 min. of reaction time is enough to give a optimal labelling rate with clottability over 90%. The mod of using chloroglycoluril film was better than suspension in labelling rate, but no difference in clottability. This iodination system withstood dil- of reaction volume to 50 folds without any change on labelling rate or clottability.

The comparison of chloroglycoluril and chloramine-T is shown as follows:

Oxidant	Consumption (mol)	Clottability (%)	Labelling rate (%)
Chloroglycoluril	1.16×10^{-7}	91.32 ± 1.34	73.28 ± 0.92
Chloramine-T	1.16×10^{-7}	79.01 ± 1.40	62.51 ± 1.26
	4.63×10^{-7}	11.19 ± 1.33	35.52 ± 3.04

Thus the chloroglycoluril radiodination was proved to be a mild, efficient, simple, rapid and less restrictive method especially suitable for labelling bioactive materials.

- (1) Fraker, Pamela J. and Speck, John C., Jr, Biochem. Biophys. Res. Commun. 80, 849 (1978)
- (2) Markwell, Marry Ann K. and Fox, C. Fred, Biochem. 17, 4807 (1978)

- (3) Wood, William Graham, Wachter, Christine, and Scriba, P. C.
Fresenius' Z. Anal. Chem, 301, 119 (1980)
- (4) Wood, William Graham, Wachter, Christine, and Scriba, P. C.
J. Clin. Chem. Clin. Biochem. 19, 1051 (1981)
- (5) Regoeczi, E. Brit. J. Haematol. 20, 649 (1971)

DIAZONIUM SALTS FOR NO CARRIER ADDED IODINATION: AN

IODOTAMOXIFEN, D.H. Hunter, L.A. Strickland, Y.Z. Ponce, Department of Chemistry, The University of Western Ontario, London, Ont. N6A 5B7, Canada; G. Morrissey, B. Reid, A.A. Driedger, Department of Nuclear Medicine, Victoria Hospital, London, Ont. N6A 4G5, Canada; E.R. Tustanoff, Department of Clinical Biochemistry, Victoria Hospital, London, Ont. N6G 2A7, Canada.

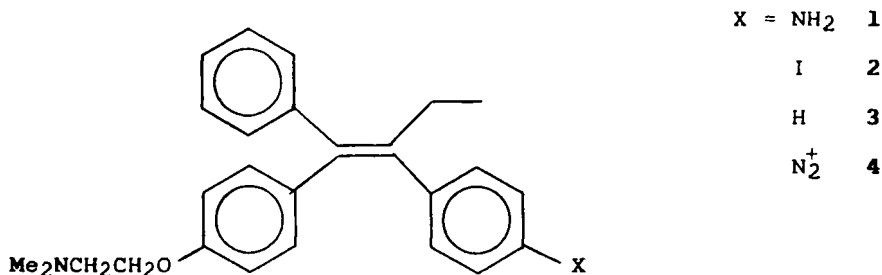
A synthetic route has been developed that has provided gram quantities of each of the E and Z geometrical isomers of an aminotamoxifen 1 which are being used as precursors to the corresponding iodotamoxifens 2.

Tamoxifen diazonium salts 4 were successful intermediates in the preparation of the iodotamoxifens 2 from 1 using cold iodide. Thus 2 can be prepared in reasonable yields from 4 using a large excess of iodide ion and activated copper bronze as a catalyst. However, reactions with no carrier iodide added resulted in radiochemical yields of about 5% and specific activities of only about 40 Ci/mmol.

A number of experiments have been run using isolated salts of 4, equimolar iodide ion, and a variety of catalysts in an attempt to find "good catalysts". None of the "catalysts" used resulted in improved yields of 2.

A series of experiments were also run using isolated salts of 4, 100-200 μ Ci of Na 131 I and a range of non-aqueous solvents. This approach proved much more successful and it has been possible to produce no carrier added 131 I-4 in about 40% radiochemical yield and -100% radiochemical purity.

These tamoxifens (1, 2, 3) have been investigated for their estrogenic binding affinities. The no carrier added 131 I-tamoxifens have been employed in biodistribution studies with immature female rats and in studies using mice with implanted tumors. These preliminary results are promising.



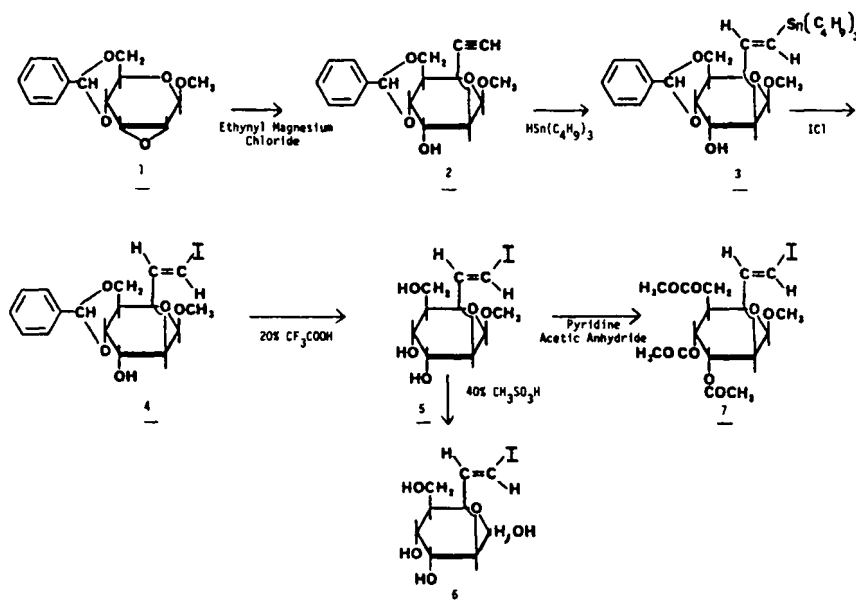
DESIGN, SYNTHESIS AND EVALUATION OF 2-DEOXY-2-IODOVINYL-BRANCHED CARBOHYDRATES AS POTENTIAL BRAIN IMAGING AGENTS M. M. Goodman, A. P. Callahan, and F. F. Knapp, Jr., Nuclear Medicine Group, Oak Ridge National Laboratory, Oak Ridge, Tennessee 37831, USA

Glucose is the primary energy source of the brain and is also an important metabolic substrate for the normoxic heart. A number of glucose analogues labeled with the positron emitting radionuclides, carbon-11 and fluorine-18, have been utilized noninvasively to determine regional cerebral glucose metabolism in humans. Clinical studies using the glucose analogue, 2-[^{18}F]-fluoro-2-deoxy-D-glucose (2-FDG) have shown that the metabolic rate for glucose utilization in the brain varies in patients with pathological disorders (1,2,3). In patients with Alzheimers' disease (4,5), Parkinsons' disease (6), and dementia (5,7), 2-FDG shows a characteristic distribution of reduced glucose metabolism in the parietal region of the brain. However, because carbon-11 ($t_{1/2} = 20$ min) and fluorine-18 ($t_{1/2} = 110$ min) are short-lived radioisotopes and because only a few regions have clinical institutions with in-house cyclotrons and positron tomographic devices, only a small patient population can utilize these revolutionary diagnostic techniques available from these agents. Radioiodinated glucose analogues are better candidates for widespread clinical use because of the attractive radionuclidic properties of iodine-123, a single photon emitter (159 keV) with a 13.3 h half-life.

Radioiodinated carbohydrates such as 2-deoxy-2-iodo-D-glucose (8) and 3-deoxy-3-iodo-D-glucose (9) undergo facile chemical or in vivo deiodination which precludes their use as radiotracers of glucose metabolism in tissues. To overcome the problems resulting from in vivo deiodination, we explored the concept of stabilizing radioiodide on a model carbohydrate, (E)-C-3-iodovinyl-D-allose (10) as an iodovinyl moiety. This agent did not exhibit brain specificity but showed low in vivo deiodination which demonstrated for the first time that radioiodide can be stabilized on a carbohydrate. The goal of this study was to develop a deoxy-branched carbohydrate with radioiodide stabilized as a vinyl iodide with the objective of achieving high brain uptake.

The synthetic approach for the preparation of the deoxy iodovinyl-branched carbohydrate involved the scission of a 2,3 anhydro sugar with a Grignard

Scheme 1. Synthesis of 2-Deoxy-2-Iodovinyl Altriose Derivatives



reagent. Methyl 2,3-anhydro-4,6-O-benzylidene- β -D-allopyranoside (1) was treated with ethynyl magnesium chloride to afford methyl 4,6-O-benzylidene-2-deoxy-2-ethynyl- β -D-allopyranoside (2) (Scheme 1). Hydrostannylation of 2 with tri-*n*-butyltin hydride (n -Bu)₃SnH gave the key intermediate, methyl 4,6-O-benzylidene 2-deoxy-2-(E)-(tributyltin)ethylene- β -D-allopyranoside (3). Iodide was introduced into the geminal position of the ethylene moiety by iododestannylation of the tin intermediate 3. Treatment of 3 with sodium iodide and *N*-chlorosuccinimide gave methyl 4,6-O-benzylidene 2-deoxy-2-(E)-iodovinyl- β -D-allopyranoside (4). Hydrolysis of 4 with 40% CH₃SO₃H gave 2-deoxy-2-(E)-iodovinyl-D-altróse (6), whereas hydrolysis with 20% CF₃COOH followed by treatment with pyridine-acetic anhydride gave methyl 2-deoxy-2-E-iodovinyl-2,4,6-O-triacetyl- β -D-allopyranoside (7). Tissue distribution studies of ¹²⁵I-labeled 7 (Table 1) and 6 were performed in rats. Iodine-125 7 showed good brain uptake, 1.65% dose/gm at 5 min, and 55% retention of radioactivity in the brain, 0.89% dose/gm at 30 min. In addition, the agent showed low *in vivo* deiodination which resulted in low thyroid uptake, 33% dose/gm at 60 min.

The high brain uptake of methyl 2-deoxy-2-E-iodovinyl-2,4,6-O-triacetyl β -D-allopyranoside (7) is most likely due to passive diffusion since 7 is not a substrate for the carrier system required for active sugar transport across the blood/brain barrier. Nevertheless, the delivery to the brain of a radioiodinated sugar with radioiodide stabilized as an iodovinyl moiety has been successfully demonstrated with the synthesis of this model agent. A series of iodovinyl deoxy sugars with active D-gluco and D-manno configurations are presently being prepared for biological evaluation.

Table 1. Distribution of Radioactivity in Tissues of Fischer 344 Rats Following Intravenous Administration of Methyl-2-deoxy-2-(E)-iodovinyl-2,4,6-O-triacetyl- β -D-allopyranoside (7)

Tissue	Mean % injected dose/g (range) at the following times after injection			
	5 min	15 min	30 min	60 min
Brain	1.65 (1.56-1.73)	1.19 (1.10-1.32)	0.89 (0.75-1.05)	0.72 (0.71-0.75)
Blood	1.05 (1.00-1.10)	0.93 (0.89-0.96)	0.80 (0.74-0.89)	0.65 (0.64-0.68)
Heart	1.14 (1.09-1.16)	1.07 (1.01-1.17)	0.87 (0.81-0.94)	0.68 (0.64-0.73)
Kidneys	1.55 (1.50-1.59)	1.57 (1.49-1.63)	1.68 (1.52-1.84)	1.57 (1.41-1.74)
Lungs	1.19 (1.09-1.33)	1.03 (0.97-1.11)	0.83 (0.74-0.92)	0.66 (0.66-0.67)
Liver	1.39 (1.34-1.42)	1.37 (1.33-1.39)	1.23 (1.12-1.42)	1.05 (0.97-1.10)
Thyroid	20.64 (20.06-21.27)	18.91 (17.53-20.53)	25.70 (22.95-30.15)	33.49 (27.79-43.47)

Research supported by the Office of Health and Environmental Research, U.S. Department of Energy, under contract DE-AC05-84OR21400 with Martin Marietta Energy Systems, Inc.

1. Phelps, M.E., Huang, S.C., Hoffman, E.J., et al., *Ann. Nuerol.*, **6**, 371 (1979).
2. Reivich, M., Kuhl, D., Wolf, A.P., et al., *Circ. Res.*, **44**, 127 (1979).
3. Reivich, M., Alvi, A., Wolf, A.P., et al., *J. Cereb. Blood Flow Metab.*, **2**, 307 (1982).
4. Hoffman, E.J., Phelps, M.E., Huang, S.C., *J. Nucl. Med.*, **26**, P 28 (1985).
5. Kuhl, D.E., Metter, E.J., Benson, D.F., et al., *J. Nucl. Med.*, **26**, P 69 (1985).
6. Metter, E.J., Riege, W.H., Kuhl, D.E., et al., *J. Nucl. Med.*, **25**, P 109 (1984).
7. Alavi, A., Chawluk, J., Hurtig, R., et al., *J. Nucl. Med.*, **26**, P 69 (1985).
8. Fowler, J.S., Lade, R.E., MacGregor, R.R., et al., *J. Lab. Cmpd. Radiopharm.*, **16**, 7 (1979).
9. Kloster, G., Laufer, R., Stocklin, G., *J. Lab. Cmpd. Radiopharm.*, **20**, 391 (1983).
10. Goodman, M.M., Knapp, Jr., F.F., *J. Nucl. Med.*, **26**, P 121 (1985).

SYNTHESIS OF ¹³¹I-LABELLED (E)-5(2-iodovinyl)-2'-FLUORO-2'-DEOXYURIDINE FOR DIAGNOSIS OF HSV-ENCEPHALITIS

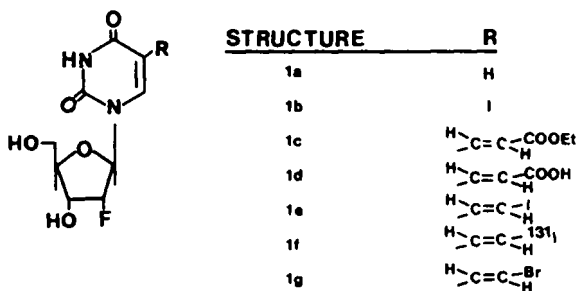
T. Iwashina, E.E. Knaus and L.I. Wiebe

Faculty of Pharmacy and Pharmaceutical Sciences, University of Alberta, EDMONTON, Canada, T6G 2N8

Several 5-substituted pyrimidine nucleosides have been developed for treatment of viral infections. Two such compounds, (E)-5(2-bromovinyl)-2'-deoxyuridine (BVdU) and (E)-5(2'-iodo-vinyl)-2'-deoxyuridine (IVdU) are potent, highly specific agents with anti-HSV activity. IVdU and BVdU owe their high antiviral potency and low mammalian cell toxicity to selective phosphorylation in cells containing virus-encoded thymidine kinase (1). This selective "metabolic trapping" has formed the rationale for using the radiolabelled analogues as radiopharmaceuticals for the clinical diagnosis of HSV encephalitis (2). Unfortunately, both IVdU and BVdU are rapidly inactivated through phosphorolytic cleavage in vivo; the (radiolabelled) uracil base (IVU or BVU) has a long plasma half-life which effectively masks selective uptake of the nucleoside by infected cells (3,4) (E)-5(2-Iodovinyl)-2'-fluoro-2'-deoxyuridine (**1e**), a structural analogue of IVdU which is expected to be less susceptible to phosphorolysis, has now been synthesized and radioiodinated. The synthetic route employed allows for rapid electrophilic radiohalogenation at low or no-carrier added specific activities, with incorporation of the label in the final synthetic step.

Commercially available 2,2'-anhydrouridine was converted to 2'-fluoro-2'-deoxyuridine (**1a**) upon reaction with anhydrous HF/dioxane(5). Iodination with electrophilic iodine(6) gave 5-Iodo-2'-fluoro-2'-deoxyuridine (**1b**) which was reacted with ethyl acrylate in the presence of bis(triphenylphosphine)palladium(II) chloride and triethylamine in dry acetonitrile (24h at 77°) to afford (E)-5(2-carbomethoxyvinyl)-2'-fluoro-2'-deoxyuridine (**1c**) in 55% isolated yield. The carbomethoxy ester (**1c**) was hydrolysed using aqueous 0.5N KOH at room temperature (2h). After neutralization with Dowex 50X8-200 [H⁺] resin, the filtrate was evaporated in vacuo and the residue was recrystallized from acetonitrile-methanol to provide (E)-5(2-carboxyvinyl)-2'-fluoro-2'-deoxyuridine (**1d**) in 52% yield (Scheme).

(E)-5(2-Carboxyvinyl)-2'-fluoro-2'-deoxyuridine(**1d**) was iodinated by adding a solution of chloramine T in dry DMF to a solution of (**1d**), sodium acetate and iodide in dry DMF. The reaction mixture was stirred for 1 h at 25 °C, then evaporated to dryness under nitrogen. The product, (E)-5(iodovinyl)-2'-fluoro-2'-deoxyuridine(**1e**) was obtained by purification on preparative layer chromatography (Whatman PLK5F; 10% methanol in chloroform) in 28% yield.



[¹³¹I]-Iodine was introduced at NCA and CA specific activities by iodinating (**1d**)(500μg) in DMF(100μL), as described for (**1e**)(above). Radiochemical yields of (**1f**) after HPLC purification (reverse phase ODSII column; 40% methanol in water, eluant) were typically 47% at 104 MBq μmole⁻¹ and 30% for the NCA synthesis.

The brominated analogue, (E)-5(2-bromovinyl)-2'-fluoro-2'-deoxyuridine (**1g**) was prepared in a similar manner from (**1d**) using NaBr or NH₄¹³¹Br. Yields ranged from 25-30%.

1. J. Descamps and E. DeClercq. J. Biol. Chem. 256, 5973 (1981).
2. M.J. Gill, J. Samuel, L.I. Wiebe, E.E. Knaus and D.L. Tyrrell. Antimicrob. Agents Chemother. 25 476 (1984).
3. C. Desgranges, G. Razaka, M. Rabuad, H. Baricaud, J. Balzarini and E. DeClercq. Biochem. Pharmacol. 32, 3583 (1983).
4. J. Samuel, M.J. Gill, T. Iwashina, D.R. Tovell, D.L. Tyrrell, E.E. Knaus and L.I. Wiebe. Antimicrob. Agents Chemother. 29, (1986).
5. D.N. Abrams, J.R. Mercer, E.E. Knaus and L.I. Wiebe. Int. J. Appl. Rad. Isotopes. 36, 233 (1985).
6. J.R. Mercer. Ph.D. Thesis, U. Alberta, Edmonton (1985).

This work was supported by the Medical Research Council of Canada, grant no. MT-5965.

NEW HIGH YIELD Cu(I) ASSISTED NUCLEOPHILIC RADIOBROMINATION

J. Mertens¹, M. Gysemans¹, W. Vanryckeghem¹, M. Guillaume², C. Brihaye²¹VUB-Cyclotron, VUB, B-1090 Brussels, ²Centre Recherches du Cyclotron, ULg, B-4000 Liège.

Radiobromination with the short-lived ⁷⁵Br of arylcompounds has become an important labelling reaction for the development of receptor antagonists or agonists for radioneurological diagnosis (1). The aim of this paper is to show that a high specific activity molecular regiospecific radiobromination of non activated phenylcompounds can be performed within a short time using a Cu(I) assisted nucleophilic non isotopic exchange in an acidic reducing medium until now applied for isotopic radioiodide exchange (2, 3, 4). The results shown are obtained for the ⁷⁷Br for I exchange on p-I-phenylalanine, which was chosen as a model molecule.

Production of ⁷⁵Br and ⁷⁷Br : a mixture of ⁷⁵Br and ⁷⁷Br was produced by a p, 2n reaction on natural Se (Na₂Se O₃ target) at the Liège 520 CGR-MeV compact cyclotron. ⁷⁷Br, with a specific activity of 1 mCi (37 MBq)/μM was mostly used for the labelling studies.

Labelling reaction : 5 mg of p-I-phenylalanine (DL), 5 mg of 2,5 dihydroxybenzoic acid, 0.5 mg of SnSO₄, 100 μl of glacial acetic acid, 340 μl of bidistilled H₂O, 60 μl of a 325 mg CuSO₄·5H₂O/100 ml H₂O solution and 100 μl of a radiobromide solution (0.1 mCi) are mixed in a 700 μl septum closed reaction vial. The reaction mixture is flushed with N₂ during 10 minutes and heated during 30 minutes at 140°C.

Radiochemical control and recovery : a Waters HPLC set-up was used with a waters Nova-Pak C 18, 5 μ, 150 x 3,9 mm column and with a MeOH/H₂O//HOAc/TMA : 35/65//0.9/0.35 mixture as eluent at a flow rate of 0.5 ml/min. The signals of a UV detector and a NaI (Tl) scintillation detector were traced simultaneously.

The radiochemical yield n was determined as the ratio of the activity of the collected peak to the total injected activity as well as the ratio of the area of the p-⁷⁷Br-phenylalanine (p-⁷⁷Br-φ-Al) peak (t_r : 6.1 min) to the sum of the area's of the ⁷⁷Br (t_r : 1.9 min) and p-Br-phenylalanine peaks.

Results and discussion : As shown in table 1, the amount of acetic acid is critical for the course of the labelling reaction.

TABLE 1 : Radiochemical yield (n %) as a function of the amount of HoAc (tot. react. vol. 600 μl)

Trial	Fraction HoAc	% ⁷⁷ Br-φ-Al	% ⁷⁷ Br ⁻	% ⁷⁷ Br-X
1	0.167	97.8	2.2	-
2	0.333	96.5	3.2	0.3
3	0.500	82.1	1.5	16.4
4	0.667	66.7	0.7	33.0

In the trials 3 and 4, the formation of a radioactive side product ⁷⁷Br-X (t_r : 18.0 min), more lipophilic than p-I-phenylalanine (p-I-φ-Al)(t_r : 8.6 min), has been observed. At least 100μl of acetic acid corresponding to a fraction of 0.167, is needed in the reaction mixture to reach a pH which is low enough to satisfy the requirements for an optimal reaction as the radiobromide solution used in our experiments is alkaline due to the production procedure. When applying the described labelling

conditions neither labelled nor cold side products have been observed.

As shown in table 2 the radiochemical yield η strongly depends on the amounts of substrate involved in the reaction.

TABLE 2 : Radiochemical yield ($\eta\%$) as function of the amount of p-I-phenylalanine (mg (μmol))

(reaction $^{\circ}\text{T}$:140 $^{\circ}\text{C}$, reaction time: 60 min)

Amount mg	p-I- ϕ -Al (μmol)	% ^{77}Br - ϕ -Al	% $^{77}\text{Br}^-$
1	(3.90)	60.9	39.1
3	(11.67)	87.4	12.6
5	(19.45)	96.8	3.2

Fig. 1 shows the labelling yield as a function of time for respectively the ^{77}Br - for I exchange on p-I- ϕ -Al and the isotopic ^{77}Br - for $^{\text{nat}}\text{Br}$ exchange on p-Br- ϕ -Al at two reaction temperatures, 140 $^{\circ}\text{C}$ and 120 $^{\circ}\text{C}$.

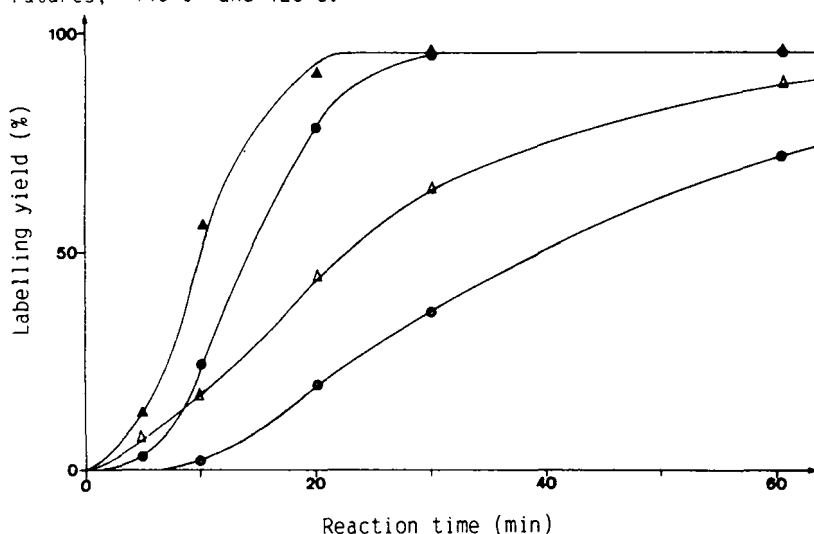


Figure 1. Yield of p- ^{77}Br - ϕ -Al as a function of time for:

- ^{77}Br for Br exchange at 140 $^{\circ}\text{C}$ (▲)
- ^{77}Br for Br exchange at 120 $^{\circ}\text{C}$ (△)
- ^{77}Br for I exchange at 140 $^{\circ}\text{C}$ (●)
- ^{77}Br for I exchange at 120 $^{\circ}\text{C}$ (○)

The difference of labelling rate between the two types of reaction is the more expressed at the lower reaction temperature. Assuming that $\Delta\eta/\Delta t$, between 10 and 30 minutes, is proportional to the reaction rate, the Cu(I) assisted isotopic bromo exchange at 120 $^{\circ}\text{C}$ is roughly 1.5 times as great as the non isotopic Br for I exchange. These results are in contradiction with the displacement theory of Bacon and Hill (5) but in agreement with the statement of Liedholm (6) that the iodo compounds react at a lower rate than the bromo ones due to the less favourable geometry of the intermediate Cu(I) complex and to the large size of the iodine atom. It appears unlikely that the rate determining step involves the breaking of respectively the C-I and C-Br bonds. This supports our Cu(I) complex model sited in earlier papers (7). As, when applying the described Cu(I) procedure for the ^{131}I

for Br exchange on p-Br- ϕ -Al and Brominated Spiperone, labelling yields of respectively 99.9 % and 90 % (only using 0.5 mg of Brominated Spiperone at 150°C) are obtained, a high yield for the non isotopic nucleophilic radiobromination of Spiperone or other arylgroup containing neuroleptic drugs is expected.

The authors thank the IKW (Interuniversity Institute for Nuclear Research) for financial support ; Dr Laduron and Dr Leysen of Janssen Pharmaceutica (Belgium) for supplying Brominated Spiperone ; G. Tihange², D. Terriere¹ for technical assistance ; R. Cantineau² for helpful discussion.

- 1 Kloster G., Stocklin G., In Cox P.H., Limouris G., Woldring, M.G., eds, Progress in Radiopharmacology, 1985, pp89-121.
2. Mertens J., Vanryckeghem W., In Proceedings Second European Symposium on Radiopharmacy, Cambridge, 1985, in press.
3. Mertens J., Vanryckeghem W., Eur. J. Nucl. Med, 11, A39 (1985)
4. Mertens J., Vanryckeghem W., J. Nucl. Med. 26, P123 (1985)
5. Bacon, R.G.R., Hill H.A.O., J. Chem. Soc. T097 (1964).
6. Liedholm, B, Acta Chem. Scand. 25, 113 (1971)
7. Mertens, J.J.R., Vanryckeghem, W., Bossuyt, A, In Proceedings International Conference on Radiopharmaceuticals and Labelled Compounds, International Atomic Energy Agency, Tokyo 1984, p. 303.

SYNTHESIS OF [¹³¹I]-IODOALIPHATIC AMINES AS POTENTIAL RADIOPHARMACEUTICALS FOR THE STUDY OF LUNG FUNCTION

G. Gopalakrishnan, Y.W. Lee, A.A. Noujaim and S.F.P. Man†

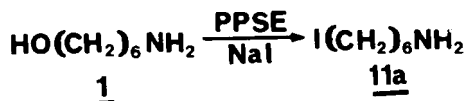
Faculty of Pharmacy, University of Alberta, Edmonton, Alta., Canada

†Faculty of Medicine, University of Alberta, Edmonton, Alta., Canada

The ventilatory function of the lungs is normally evaluated by gaseous exchange studies which are informative only in cases of advanced lesions. We are proposing a series of new radiopharmaceuticals with the potential of diagnosis of early lung injury. Circulating endogenous and exogenous amines have been demonstrated to be substrates of the monoamine oxidase (MAO) enzyme system of pulmonary endothelial cells(1). We have reported the uptake and metabolism of aliphatic amines by the lungs(2). Physical injury and/or pathophysiological lesions of the lungs would affect the uptake and subsequent metabolism of these amines.

We have synthesized a number of ω -[¹³¹I]-labelled straight chain and β -monosubstituted aliphatic amines. The α -position is open to permit MAO enzymatic reactions. The β -position is monosubstituted with various alkyl groups to alter the orientation and interaction between the substrates and the MAO enzyme system.

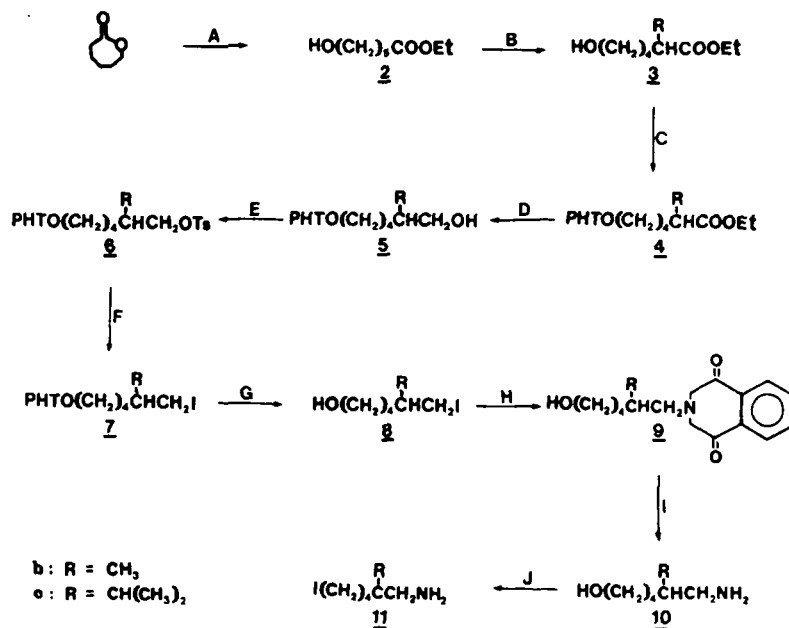
The synthesis of 1-amino-6-iodohexane **11a** (73%) was carried out by treatment of commercially available 1-amino-6-hydroxyhexane **1** with trimethylsilyl polyphosphate (PPSE) and NaI(3) (Scheme 1).



Scheme 1. Synthesis of 1-Amino-6-iodohexane

The synthesis of 1-amino-2-methyl- and 1-amino-2-isopropyl-6-iodohexane **11b** and **11c** was achieved according to Scheme 2. Ethyl-6-hydroxyhexanoate **2** (90%) was synthesized by the acid catalyzed ring opening of ω -caprolactone with dry ethanol. Alkylation of the hydroxyester **2** using lithium diisopropylamide (LDA) and the appropriate alkyl iodide yielded the α -alkylated esters **3b** and **3c** respectively (78% and 58%). The ω -hydroxyl group was protected as the tetrahydropyranyl ether **4b** and **4c** (91% and 90%) by treatment with dihydropyran and *p*-toluenesulfonic acid prior to reduction of the ester to the alcohol **5b** and **5c** (80% and 90%) by lithium aluminum hydride. The primary alcoholic groups of **5b** and **5c** were derivatized with *p*-toluenesulfonyl chloride in pyridine to afford **6b** and **6c** (99% and 81%). Treatment of the tosyl derivatives with NaI in acetone yielded **7b** and **7c** (both 88%). The ω -hydroxyl groups were then released by treatment with *p*-toluenesulfonic acid in methanol to give **8b** and **8c** (82% and 92%). The iodides **8b** and **8c** were converted to the phthalimido derivatives **9b** and **9c** (75% and 60%) by treatment with potassium phthalimide in DMF. Hydrazinolysis of **9b** and **9c** afforded the ω -hydroxyamines **10b** and **10c** (58% and 54%). These alcohols were converted to the iodoamines **11b** and **11c** (67%, 60%) using PPSE and NaI in methyl ethyl ketone. The spectral data of the compounds reported here are in accordance with their respective structures.

The synthesis of radioactive **11a-c** from the corresponding hydroxyamines was achieved similarly using PPSE and [¹³¹I]-NaI/NaI (Radiochemical yields 67%, 61%, 55%; specific activity 340 GBq mmol⁻¹).



A = dry EtOH/conc. H₂SO₄; B = LDA/THF/R₁; C = DHP/CH₂Cl₂/TsOH;
 D = LAH/Et₂O; E = TsCl/pyridine; F = NaI/acetone; G = TsOH/MeOH;
 H = potassium phthalimide/DMF; I = NH₂NH₂/MeOH; J = PPSE/NaI/MEK

Scheme 2. Synthesis of 1-Amino-2-alkyl-6-iodohexane

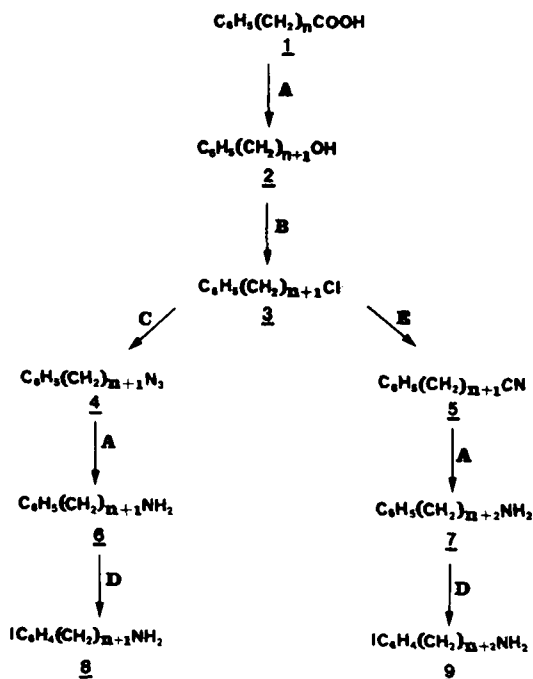
Acknowledgement. This work is supported by the Medical Research Council of Canada.

- Gilles, C.N. and Pitt, B.R., *Ann. Rev. Physiol.* **44**, 269 (1982).
- Abrams, D.N., Man, S.F.P., Noujaim, A.A. and Washburn, L.C., *In Third Int. Symp. Radiopharmacology*, Freiburg, West Germany, 1983.
- Imamoto, T., Matsumoto, T., Kusumoto, T. and Yokoyama, M., *Synthesis* 460 (1983).

SYNTHESIS OF ω -(4-[¹³¹I]-IODOPHENYL)ALKYLAMINES AS POTENTIAL LUNG IMAGING RADIOPHARMACEUTICALS

G. Gopalakrishnan, Y.W. Lee, A.A. Noujaim and S.F.P. Man†
 Faculty of Pharmacy, University of Alberta, Edmonton, Alta., Canada
 †Faculty of Medicine, University of Alberta, Edmonton, Alta., Canada

Present pulmonary function tests do not allow early diagnosis of pulmonary physiological impairments. As a continuing program in the design of new lung imaging agents to provide information on early lung injury we have developed a series of radioiodinated aliphatic amines which are metabolised by the monoamine oxidase system of the lungs(1). Preliminary physical and biological data suggest that some of the compounds have a labile C-I bond. We now report the synthesis of a series of ω -(4-[¹³¹I]-iodophenyl)alkylamines **8** and **9**. In addition to an expected greater C-I bond strength any cleaved iodophenyl function would be readily removed from circulation as iodohippurate. The synthesis of the iodinated amines **8** and **9** was accomplished according to Scheme 1.



A = $BH_3 \cdot THF/THF$; B = $SOCl_2$; C = $NaN_3/H_2O/Adogen\ 464^{TM}$;
 D = $TTFA/NaI/CH_3CN$; E = $NaCN/H_2O/Adogen\ 464^{TM}$; n=3, 5

Scheme 1. Synthesis of ω -(4-[¹³¹I]-iodophenyl)alkylamines

γ -Phenylbutyric acid (**1**, n=3) was available commercially. 5-Phenylhexanoic acid (**1**, n=5) was prepared according to literature procedure(2). The reduction of the acids **1** (n=3, 5) was carried out using borane-tetrahydrofuran by a method similar to that reported by Brown *et al*(3) to yield quantitatively the corresponding alcohols **2**. The alkyl chlorides **3** were prepared from the corresponding alcohols by refluxing with excess thionyl chloride. The excess thionyl chloride was removed under reduced pressure. The chlorides were used without further purification in the synthesis of the corresponding azides **4** using sodium azide and the phase-transfer catalyst (PTC) Adogen 464TM in 75% yield(4). Reduction of the azides **4** with borane-tetrahydrofuran yielded the corresponding amines **6** in 73% and 64% yield respectively.

Treatment of the alkyl chlorides **3** with sodium cyanide under essentially the same PTC conditions as above yielded the nitriles **5** in 72% yield which were reduced to the amines **7** by treatment with borane-tetrahydrofuran in 65% yield.

Iodination of the amines **6** and **7** with thallium trifluoroacetate (TTFA) and sodium iodide in acetonitrile yielded the amines **8** and **9** in 50-60% yield. The *para* position of the iodo substituent was confirmed by 300 MHz NMR spectra.

The synthesis of [¹³¹I]-labelled amines was carried out similarly with [¹³¹I]-NaI/NaI via thallation in 15 to 20% radiochemical yield (specific activity 300 to 400 GBq mmol⁻¹). Biodistribution studies of the above compounds have been studied using gamma camera techniques.

Acknowledgement. The financial support of the Medical Research Council of Canada is gratefully acknowledged.

1. Gopalakrishnan, G., Lee, Y.W., Noujaim, A.A. and Man, S.F.P., In Sixth Intern. Symp. Radiopharm. Chemistry, Boston, 1986.
2. Papa, D., Schwenk, E. and Hankin, H., *J. Am. Chem. Soc.* **69**, 3018 (1947).
3. Brown, H.C., Krishnamurthy, S. and Stocky, T.P., *J. Org. Chem.* **38**, 2786 (1973).
4. Reeves, W.P. and Bahr, M.L., *Synthesis* 823 (1976).

DESIGN OF A FULLY AUTOMATED, IN-BEAM, CONTINUOUS-FLOW I-123 PRODUCTION SYSTEM.

S. Mirzadeh, L.F. Mausner, and S.C. Srivastava

Medical Department, Brookhaven National Laboratory, Upton, New York 11973

Iodine-123 has been prepared at the Brookhaven Linac Isotope Producer (BLIP) (1) from the Xe-123 precursor produced by I-127(p,5n) reaction. The radiopurity is excellent and the chemical form suitable for labeling (2). However, the relatively time consuming, labor intensive, and inefficient batch mode is not readily scaled up to allow BLIP to become a meaningful contributor in a nationwide distribution effort. The in-beam, continuous-flow process will help solve this problem because it offers much higher I-123 yield and is amenable to automation. We describe here the target design and our system for fully automated production.

A target has been developed, a plastic mockup of which is shown in Figure 1. The target consists of two concentric disks (7.5 cm O.D., 1.5 cm thickness and 10.3 cm O.D., 2.1 cm thickness) which are housed in a square frame (10.5 x 10.5 x 2.8 cm). The inner disk holds the NaI target salt and contains a heating element, a thermocouple and a line for He to flow across the salt surface. The outer disk is primarily a secondary containment to prevent irradiated salt from getting out if the inner vessel leaks, and it also provides some thermal insulation between the hot inner vessel (~670°C) and BLIP cooling water. The outer can is also connected to an adapter tube (2 cm O.D., ~35 cm height) which houses the He and electrical lines. The square frame provides a means of attaching the target assembly to the BLIP target-drive-chain mechanism. The target assembly is made entirely from stainless steel and is connected to the BLIP operating floor by a 30 foot PVC hose and cable bundle. The two concentric disks and the adapter tube are made as a single unit and can be remotely separated from the rest of the target assembly and replaced.

The basic features of the experimental setup are shown in Figure 2. During irradiation, He flows past the target salt and sweeps out radio-Xe produced by $^{127}\text{I}(p,xn)$ reactions. The gas then flows through a trap at -40°C, to remove condensable NaI and I₂ vapor, a Ag-SiO₂ trap at ~-110°C to further scrub possible iodine vapor, and into up to three coil traps at -196°C which remove all the xenon. Then the He flows through a hold-up volume and is finally vented. After 3-4 hours of Xe collection, coil 1 is bypassed and radio-Xe is collected in coils 2 and 3. After allowing Xe to decay for 2-3 hours, the undecayed Xe is pumped out from coil 1 and subsequently .01 N NaOH is introduced to the coil to wash out the iodine-123. For anhydrous $^{123}\text{I}^-$ preparation instead, immediately after collection the ^{123}Xe is cryogenically transferred to ampoules 1-5 where it decays. These steps can be repeated for coil 2, or alternatively the entire coil removed for shipment of the ^{123}Xe itself.

The new gas collection process design consists of more than 50 solenoid valves, two mass flow controls, three mass flow meters, 10 thermocouples and liquid nitrogen level indicators, five vacuum gauges, and several radiation monitors and interlocks. The unit is located at the BLIP hot cell, which has a continuous flow of air (25,000 l/min) vented through a charcoal filter, a HEPA filter, and out a 10-meter stack.

The in-beam continuous-flow $^{123}\text{Xe}/^{123}\text{I}$ production system is expected to operate 6-8 h daily for 5 days per week. An automated control system is required to minimize manpower requirements and enhance reliability and safety.

The control system is based on a centralized configuration consisting of a Digital Equipment Corporation (DEC) PDP 11/73 computer with the DEC RSX-11M operating system. A CRISP multi-task software from Anaconda Advanced Technologies (ANATEC) is installed in the computer. In this configuration, the execution of the process control algorithm and the color graphic is done within

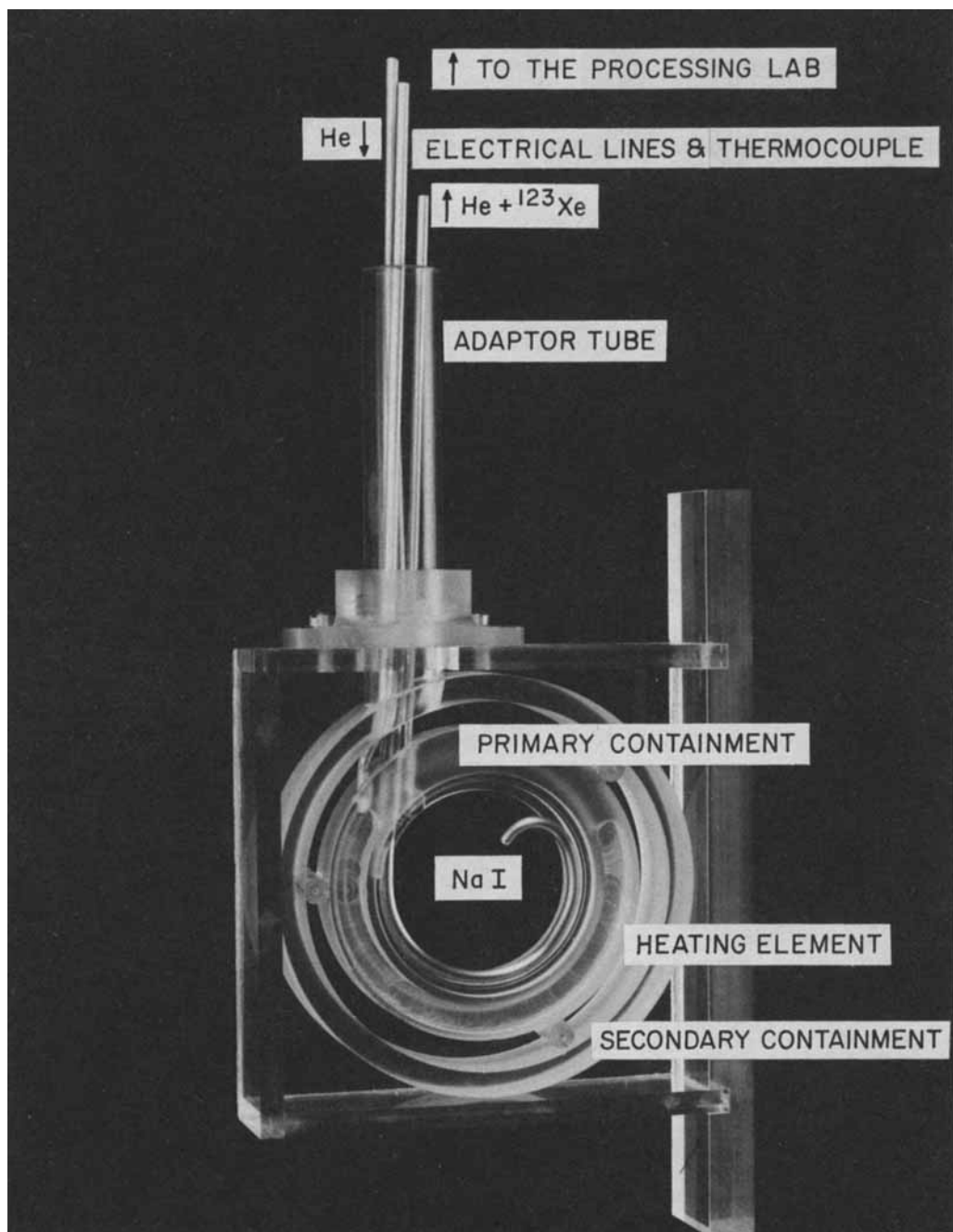


FIG. 1. A TARGET DESIGN FOR THE IN-BEAM CONTINUOUS-FLOW I-123 PRODUCTION.

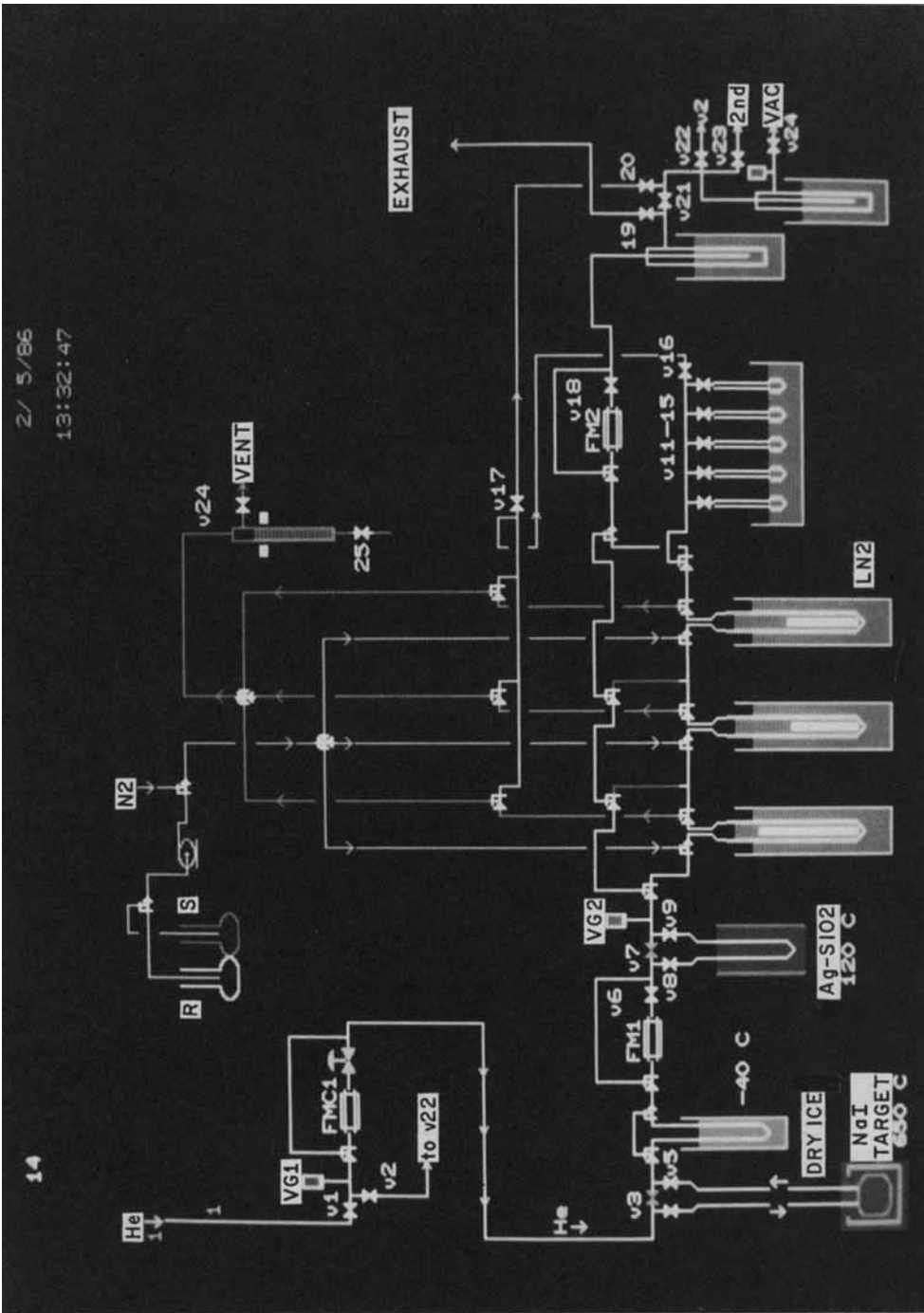


FIG. 2. A NEW GAS COLLECTION PROCESS DESIGN.

the central processing unit (cpu), along with servicing of the I/O subsystem and associated peripherals.

The hardware components consist of the field interface electronics (I/O subsystem). Inputs include pressures, flows, temperature, liquid levels, and signals from radiation monitors. The outputs include on/off positions for valves, pumps, power settings for heaters, and step-motors. The logic processing task is in the form of a continuous loop with a scan rate of 60 passes per minute. The variable inputs are scanned and converted where necessary to engineering units. High and low limits can be applied to the controller output to prevent runaway conditions. The range of these limits can be modified during processing without the necessity to recompile the program.

The operator interface is a 19" color CRT with a keyboard. Custom graphics is used to monitor and control the process. The custom graphics can show the entire process or subunits in as much detail as might be required for the safe, efficient operation of the $^{123}\text{Xe}/^{123}\text{I}$ process. The color graphic displays permit color changes as a process variable goes out of limits, with blinking values until acknowledged by the operator. Valves change color, e.g. from red (off) to green (on), as the process proceeds. The operator can request other color video frames for monitoring and control of the process by a push of a labeled button. These features significantly enhance the safety and simplicity of the system.

The most important safety feature of the $^{123}\text{Xe}/^{123}\text{I}$ control system is the capability for programmable alarms and interlocks. Visual communication through the color CRT is used for warning purposes. All alarms are logged on file by the computer and this file can be recalled on request. The safety interlock strategy for the system consists of various programmed shutdown sequences in the event of leaks, pump failures, blocked process lines, etc. All the failures are handled in a safe manner to protect personnel and equipment, and to allow fast restart of the process in order to complete the run in a timely manner.
(Research supported under U.S. Department of Energy Contract DE-AC02-76CH00016.)

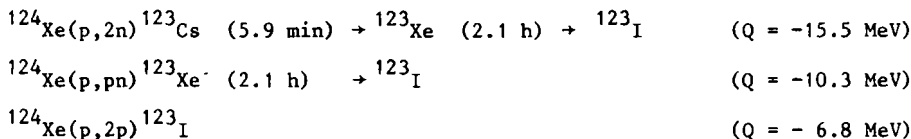
1. Mausner, L.F., and Richards, P., IEEE Trans. Nucl. Sci. NS-30, 1793 (1983).
2. Mausner, L.F., Srivastava, S.C., Mirzadeh, S., Meinken, G.E., and Prach, T., Int. J. Appl. Radiat. Isot., (1986), in press.

PRODUCTION OF IODINE-123 VIA PROTON IRRADIATION OF 99.8% ENRICHED XENON-124

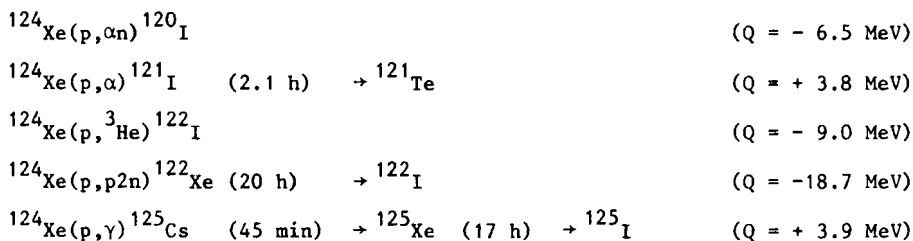
A.J. Witsenboer (1), J.J.M. de Goeij (1,2), and S. Reiffers (3)
 Department of Physics, Eindhoven University of Technology, Eindhoven, The Netherlands (1), Interuniversity Reactor Institute, Delft, The Netherlands (2) and Hospital De Weezenlanden, Zwolle, The Netherlands (3).

For commercial production of iodine-123, two routes are currently used, viz. the direct reaction $\text{Te-124}(p,2n)\text{I-123}$ and the indirect reaction $\text{I-127}(p,5n)\text{Xe-123} \rightarrow \text{I-123}$. The iodine-123 produced is contaminated with other radioisotopes of iodine, the main contaminant in the first route is I-124, formed by the $\text{Te-124}(p,n)\text{I-124}$ reaction, and in the second route I-125, formed by the $\text{I-127}(p,3n)\text{Xe-125} \rightarrow \text{I-125}$ reaction. Typical radionuclidic impurity levels are given in Table 1.

Production of sizeable quantities of iodine-123 of higher purity is possible via proton irradiation of highly enriched xenon-124 /1,2/. Reactions leading to iodine-123 are:



Reactions leading to other radioisotopes of iodine are:



The cross section for the interfering $\text{Xe-124}(p,\gamma)$ reaction is relatively low in the energy range of 27-20 MeV, so that only a minute I-125 impurity is to be expected. Since iodine-120, iodine-121 and iodine-122 have short half-lives (1.35 h, 2.1 h, and 3.5 min respectively), no substantial contamination with these radioisotopes will be present at calibration time.

Highly enriched xenon-124 is expensive (US \$ 150,000 per liter STP) due to its natural abundance of only 0.096%. This calls for an effective gas target and a reliable gas handling system. In the past years considerable experience has been obtained at the Eindhoven cyclotron laboratory in handling enriched krypton-82 gas for the production of rubidium-81 for krypton-81m generators. Since June 1984 this technology is being applied and further improved for the production of iodine-123 via proton bombardment of the enriched xenon-124. To our knowledge, two other laboratories are presently involved in the production of iodine-123 by this method, viz. in Vancouver, Canada /3/ and in Karlsruhe, FRG.

To optimise the use of the protons entering the target gas chamber, a computer model has been developed for the calculation of the proton scattering in the xenon gas and in the entrance foil. Based on the results of this model and the theoretical cross section data of Grabmayr en Nowotny /2/, the target gas chamber has been designed. The chamber has a conical shape, with a length of 250 mm and a volume of 50 ml.

The chamber is filled with 120 ml STP 99.8 percent enriched xenon-124. The initial pressure of 2.4 bar rises to 4 – 5 bar during irradiation. For the handling of the gas a computer-controlled system has been developed, including an emergency recovery system in case of foil disrapture during irradiation. The losses of xenon-124 averages to 0.2% per production run.

The xenon gas is irradiated with a 30 μ A beam of 27 MeV protons for 8 h. After bombardment, the xenon gas is pumped cryogenically to a temporary storage vessel and the I-123 absorbed on the wall of the gas chamber is recovered by rinsing with 20 ml of water containing 20 μ g of cesium iodide and 160 μ g NaOH. The xenon-123 is allowed to decay to iodine-123 for 6.6 h, after which the xenon-124 is recovered and the iodine-123 is collected, also by rinsing. Both rinsings are passed through an anion exchanger to remove tellurium-121 and to concentrate the iodine-123.

The total yield of iodine is about 6 mCi per μ Ah at point of maximum activity (EOB + 3 h). The radionuclidic impurities at calibration time are listed in Table 1. The specific activity amounts to 10 Ci/mg at calibration time. During the past year iodine-123 is being produced twice a week in batches of 1.2 Ci. The product is supplied to Dutch hospitals as NaI, hippuran, ω -heptadecanoic acid, meta-iodobenzylguanidine, and N-isopropyl-iodoamphetamine.

The advantages of the new production route for iodine-123 are: (i) reduction of the radiation dose to patients (up to 70%, which may be important for patients who receive large doses, e.g. of meta-iodobenzylguanidine), (ii) longer shelf-life and (iii) reduction of the amounts of radioactive waste in the hospital.

The new product broadens the range of radionuclidic qualities of iodine-123 products available from various sources. This underlines again the desirability to come to an internationally accepted classification for the radionuclidic quality of iodine-123 products /4/. For our product the indication pRI4, is being used, where RI stands for radionuclidic impurities, and p for the negative logarithm, corresponding to the definition of the pH.

TABLE 1. Main Radionuclidic Impurities in Iodine-123 Products at Calibration Time (= EOB + 32 h).

Radionuclidic impurity	Preparation route		
	I-127(p,5n)	Te-124(p,2n) ^{a)}	Xe-124(p,2n) ^{b)}
I-121	< 0.001% ^{c)}		< 0.001%
I-124		2 – 2.5% ^{d)}	
I-125	~ 1% ^{d)}		< 0.01% ^{d)}

a) Isotopic enrichment of 96–98% for the target; b) Isotopic enrichment of 99.8% for the target; c) Only when high-energetic protons are used; d) Depends on irradiation and/or processing conditions.

- /1/ Van den Bosch, R.L.P., Thesis, Eindhoven University of Technology, Eindhoven, The Netherlands, Preposition 8 (1979).
 /2/ Grabmayr, P., Nowotny, R., Int. J. Appl. Rad. Isot., 29, 261 (1978).
 /3/ Graham, D., Trevena, I.C., Webster, B., Williams, D., J. Nucl. Med., 26, 105 (1985).
 /4/ Van den Bosch, R.L.P., de Goeij, J.J.M., Tertoolen, J.F.W., Tielemans, M.W.M., Int. J. Appl. Rad. Isot., 29, 343 (1978).

A NEW ELECTROCHEMICAL METHOD FOR THE SEPARATION OF RADIOBROMINE
FROM A SELENIUM TARGET FOLLOWING PROTON IRRADIATION.

C. BRIHAYE, G. TIHANGE, J.C. HOET and M. GUILLAUME.
University of Liege, Cyclotron Research Center - B30
Sart Tilman, B - 4000 Liege (Belgique).

A new method for the separation of bromine from a selenium target after irradiation with protons has been developed using electrochemical oxidation of the bromide ions to bromine and the concomitant extraction of Br_2 in CCl_4 . This method has been investigated in order to separate ^{75}Br produced from a selenium-76 target using the (p,2n) reaction with protons of 23 MeV as described previously (1-2). An average of 75 % of the bromine activity produced is recovered by this procedure. For the development of the method natural selenium was used.

Sodium selenite dried by increasing the temperature from 60 to 250°C is irradiated with 23 MeV protons at a current of 15-20 μA without any target degradation producing ^{75}Br , ^{76}Br and ^{77}Br as bromide ions as shown by electrophoresis studies. After irradiation, the target is dissolved in 1N HNO_3 and 1 μg of Br carrier is added. The solution is transferred into an electrochemical cell provided with a large surface platinum electrode and an Ag/AgCl reference electrode. A second compartment of the cell containing a platinum cathode is filled with 1N KNO_3 solution and connected to the main compartment with a agar bridge. The potential of the platinum anode is held at 1.2 V (vs. Ag/AgCl) by means of a 3-electrode potentiostat connected to a current booster to allow passage of a large current intensity. Voltametric studies have shown that, under these conditions, bromide ions are oxidized to Br_2 from 0.8 to 1.6 V. Oxidation to HOBr or bromate ions does not occur and selenite ions are not electroactive at a platinum electrode. During the electrooxidation, the Br_2 formed is simultaneously extracted with CCl_4 . After 15 min of oxidation, the organic and aqueous phases are separated. If required, the Br_2 in CCl_4 can be reduced to Br^- by adding 1 ml of a saturated SO_2 solution in methanol. The solvent is evaporated on a water-bath. The aqueous solution containing the selenite ions is evaporated and can be re-used.

The advantages of this new method of separation are the following :

1. The method is simple and reproducible with a separation yield of 75 %.
2. The nature of the Br species produced is well defined as it is the result of an electrochemical process.
3. Depending on the subsequent requirements, Br can be obtained as either Br^- or Br_2 .
4. As no reagent is added, the target can be recycled for further use.

References.

- (1) PAANS A.M.J., WELLEWEERD J., VAALBURG W., REIFFERS S. and WOLDRING M.G.
Int. J. Appl. Radiat. Isotopes, 31, 267-273 (1980).
- (2) KOVACS Z., BLESSING G., QAIM S.M. and STOCKLIN G.
Int. J. Appl. Radiat. Isotopes, 36, 635-642 (1985).

EFFICIENT CONJUGATION OF DTPA TO MONOCLONAL ANTIBODIES IN BIOLOGICAL FLUIDS FOR USE IN RADIOLABELING

B.M. Kinsey, A.I. Kassis, W.W. Layne, and S.J. Adelstein

Department of Radiology, Harvard Medical School, Boston, MA 02115

Monoclonal antibodies (MoAb) conjugated to diethylenetriamine pentaacetic acid (DTPA) can be labeled with metallic radionuclides such as indium-111 (^{111}In), and bismuth-212 (^{212}Bi) for tumor imaging and radiotherapy. Several conditions must be met: 1) to preserve the immunoreactivity of the MoAb, it must be manipulated as little as possible; 2) for efficient conjugation and subsequent removal of free DTPA, there must be a high protein concentration (1); 3) trace metal contamination of the conjugated proteins must be avoided (2). We have developed a simple, quick, and efficient method using cyclic DTPA anhydride (cDTPA) that meets these three criteria.

Ascites fluid from mice bearing MoAb-producing hybridomas has a protein concentration of 20 to 25 mg/ml, of which 50 to 60% is albumin (MW \approx 70,000). On a molar basis, albumin represents 70 to 95% of the protein present, depending on the molecular weight of the MoAb (IgM \approx 900,000; IgG \approx 150,000). When the MoAb is an IgM, it can be separated from other immunoglobulins and albumin by HPLC using a TSK-300SW column (Waters Associates) with 2.5% triethylamine in 0.1 M Na_2SO_4 , pH 4.5, as eluting buffer. Since adding DTPA and then excess ^{111}In to the buffer before and after it had passed through the column revealed no difference in the capacity of the added DTPA to chelate ^{111}In , indicating that trace metal contamination from the column does not pose a problem, we investigated the conjugation of a MoAb in the presence of other proteins in the ascites fluid and the use of HPLC to purify the DTPA-conjugated MoAb and separate it from excess cDTPA.

cDTPA in dimethylsulfoxide (DMSO) was added to the ascites fluid such that the final DMSO concentration did not exceed 5%. The cDTPA to protein molar ratio was based on an approximate calculation of the number of moles of protein present in the ascites fluid. The MoAb peak was collected post HPLC and 0.1 M citrate buffer, pH 6.0, followed by ^{111}In , was added immediately. After 0.5 hour incubation at room temperature, the labeled protein(s) was purified by gel filtration. Low specific activity ^{111}In was used to assay the number of DTPAs per molecule. The HPLC eluate was reinjected in order to determine the protein concentration of the MoAb by comparison of the HPLC peak height with a standard protein concentration curve. The results obtained from two different cDTPA to protein ratios are summarized in Table 1.

TABLE 1. Labeling of MoAb in Ascites Fluid with cDTPA

MoAb	Class	$\mu\text{mol cDTPA} /$ $\mu\text{mol Protein}$	DTPA / Protein Molecule
Thy 1,2	IgM	10/1	0.24
		20/1	1.2

1. Paik, C.H., Ebbert, M.A., Murphy, P.R., Lasseran, C.R., Reba, R.C., Eckelman, W.C., Pak, K.Y., Powe, J., Steplewski, Z., and Koprowski, H., *J. Nucl. Med.*, 24, 1158 (1983).
2. Paik, C.H., Hong, J.J., Ebbert, M.A., Heald, S.C., Reba, R.C., and Eckelman, W.C., *J. Nucl. Med.*, 26, 482 (1985).

COMPARISON OF CARBOHYDRATE DIRECTED VERSUS AMINE DIRECTED ATTACHMENT OF DTPA TO MURINE MONOCLONAL ANTIBODIES.

B.A. Brown, C.B. Dearborn, W.P. Neacy, H. Sands, and B.M. Gallagher
Immunopharmaceutical R&D, E.I. duPont de Nemours, Co., Inc.
No. Billerica, MA 01862

The attachment of bifunctional chelators to murine monoclonal antibodies (Mab) requires chemical modifications that may result in alteration of their biological behavior. The biochemical, immunological, and biological characteristics of ¹¹¹In labeled B6.2 and B72.3 were compared to the appropriate radiolodinated MAB's following either reaction with the bis cyclic anhydride of DTPA (cDTPA) (1) or periodate oxidation of the carbohydrate moieties of the MAB's (2) and reaction with a dihexylamine DTPA analogue (dDTPA). Reaction of MAB's with cDTPA versus dDTPA gave differing forms of crosslinking and aggregation as measured on reducing and non-reducing SDS-PAGE (see Table 1) as well as size-exclusion HPLC as shown on Table 2 (at 1-3 mg/ml of Mab/ 10-fold molar excess of cDTPA and 10 mM periodate for 10 minutes).

TABLE 1. Structural Alterations Upon Modification as Determined by Reducing SDS-Page

Molecular Weights	% of A585 on Coomassie Stained Gel					
	B6.2		B72.3		B72.3	
	cDTPA		dDTPA		dDTPA	
28K (Light Chain)	40	38.2	37.8	35	29.3	34.9
57K (Heavy Chain)	60	59.9	59.4	65	40.3	47.9
83K	-- ^a	1.9	1.8	--	7.4	1.5
100K	--	--	--	--	2.8	1.1
130K	--	--	1.0	--	--	--
150K	--	--	--	--	19.1	14.6
180K	--	--	--	--	0.8	--

^aNo band observed

TABLE 2. Structural Alterations upon Modification as Determined by SEC-HPLC

Molecular Weights	B6.2		B72.3		B72.3	
	cDTPA		dDTPA		dDTPA	
150K	100	100	98.6	100	97.4	92
300K	0	0	1.4	0	2.6	8

Thus, dDTPA modification of B6.2 or B72.3 resulted in little change as measured on SEC-HPLC but showed significant intramolecular crosslinking on SDS-PAGE. cDTPA modification, in contrast, was relatively innocuous.

The chemistries of cDTPA modification of both B6.2 and B72.3 were optimized to retain full immunoreactivity when compared to the appropriate radioiodinated MAB's in direct solid phase immunoassays.

TABLE 3. Immunoreactivity Remaining After Cyclic Dianhydride DTPA Reaction

MOLAR RATIO cDTPA:MAB	ANTIBODY	
	B6.2	B72.3
^{125}I	80%	100%
1X	100%	--
10X	85%	92%
100X	71%	45%

In competitive radioimmunoassays with appropriate radioiodinated MAB's, the dDTPA modified MAB's retained full immunoreactivity.

The *in vivo* behavior of both antibodies with I-125 unmodified MAB's, ^{111}In -cDTPA, and ^{111}In -dDTPA-MAB's were studied in normal CD1 mice. At 1-6 hours both forms of labeled MAB's distributed to the various organs and cleared from the blood at similar rates (see Table 4). However, at 24 hours significant differences were seen in blood clearance (^{111}In -dDTPA-MAB > ^{111}In -cDTPA-MAB = I-125-MAB) and kidney (^{111}In -dDTPA-MAB > ^{111}In -cDTPA-MAB > I-125-MAB) (see Table 5).

TABLE 4. Biodistribution of ^{125}I - and ^{111}In -Labeled B6.2 in CD1 Mice One Hour Post Injection

	Average % Injected Dose/Gram		
	^{125}I	^{111}In -cDTPA	^{111}In -dDTPA
Blood	19.2 ^a	23.1	19.7
Liver	5.7	6.4	6.7
Kidney	4.7	6.5	7.7
Muscle	1.3	0.8	0.5

^an = 3-5 animals

TABLE 5. Biodistribution of ^{125}I - and ^{111}In -Labeled B6.2 and B72.3 in CD1 Mice Twenty-four Hours Post-Injection

	Average % Injected Dose/Gram					
	^{125}I		^{111}In -cDTPA		^{111}In -dDTPA	
	B6.2	B72.3	B6.2	B72.3	B6.2	B72.3
Blood	11.5 ^a	14.72	11.41	12.46	4.15	3.35
Liver	3.1	2.67	4.23	4.44	3.73	4.93
Kidney	2.7	3.08	8.40	8.10	13.28	16.05
Muscle	0.9	0.98	2.14	1.03	1.72	1.47

^an = 3-5 animals

In these normal animals, the liver does not accumulate ^{111}In regardless of the chemistry of conjugation. In contrast, there is significant accumulation of ^{111}In in the livers of athymic mice bearing antigen-specific tumors (3) possibly due to circulating antigen or metabolism of ^{111}In -MAB at the tumor. These results suggest that by different chemical methods of attachment of bifunctional chelators there may be a means of selection of the biological distribution to the non-target organs to suit the application. The faster blood clearance of the dDTPA-MAB could permit early imaging assuming that the MAB had a sufficiently high affinity for tumor localization.

1. Hnatowich, D.J., Layne, W.W., Childs, R.L., Lanteigne, D., Davis, M.A., Griffin, T.W., and Doherty, P.W., *Science*, 220, 613 (1983).
2. Murayama, A., Shimado, K., and Yamamoto, T., *Immunochem.*, 15, 523 (1978).
3. Brown, B.A., Comeau, R.D., Jones, P.L., Liberatore, F.A., Neacy, W.P., Sands, H., and Gallagher, B.M., *Soc. of Nuclear Medicine Proc.*, 26, P45, (1985).

SYNTHESIS AND IN VIVO COMPARISON OF ANTIBODY DTPA CONJUGATES WITH DIFFERENT CHEMICAL BONDS

S.M. Quadri, C.H. Paik, K. Yokoyama and R.C. Reba.

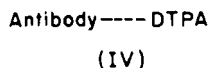
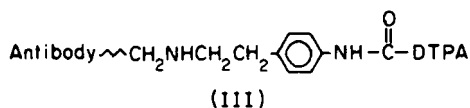
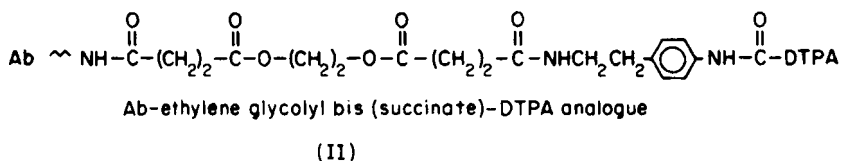
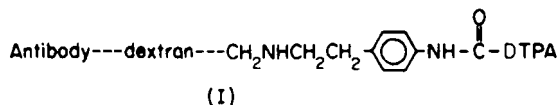
George Washington University Medical Center, Washington, DC and NIH, Bethesda, MD.

The quality of radioimmunoimaging depends on a relative term, a tumor to normal (or blood) ratio of radiolabeled antibody injectate. Radioimmunoimaging is often delayed mainly because of persistent background activity. For a tumor antibody with a given specificity and affinity constant, an early radioimmunoimaging could be achieved if the background activity cleared fast. To achieve this goal, three new analogues of antibody DTPA conjugates with chemical bonds more easily metabolized than a peptide (or acylamide) bond were synthesized.

A bifunctional chelator, DTPA-p-(aminoethyl)-anilide was first synthesized by reacting β -(4-aminophenyl)-ethylamine with cyclic DTPA dianhydride at pH 5. The first analogue (I) of antibody-DTPA conjugates contains dextran as a spacer between DTPA moieties and anti human serum albumin antibody (Ab). This was synthesized by the reaction of the amino group of DTPA-p-(aminoethyl)-anilide with some of aldehyde groups derived from the oxidation of hydroxy groups of dextran by periodate (1). The remaining aldehyde groups of dextran were then reacted with antibody. The unsaturated bonds were reduced by NaCNBH₃. The second (II) contains a spacer with two ester bonds. For the synthesis of this analogue the amino group of the bifunctional chelator was reacted with one carbonyl group of the succinimidyl succinate of ethylene glycolyl bis (succinimidyl succinate) (2). The amino group of Ab was then reacted with another carbonyl group of the succinimidyl succinate containing DTPA. The third (III) was obtained by conjugating the amino group of the bifunctional chelator to the aldehyde groups derived from the oxidation of carbohydrate moieties in Fc region of Ab with periodate (3). The imine bonds were reduced by NaCNBH₃. The products, I, II and III were separated from smaller molecules by the filtration with centricones (molecular cutoff of 30,000), radiolabeled with ¹¹¹In and affinity purified. Their in vivo distribution were compared with ¹¹¹In labeled Ab-DTPA prepared by a direct acylation reaction with cyclic DTPA dianhydride (4). This Ab-DTPA (IV) is linked by an acylamide bond.

A tumor model similar to that reported by Otsuka, et al (5) was used for a primary screening of the radiopharmaceuticals. Human serum albumin (HSA) was conjugated to CNBr activated Sepharose 4B (60-180 μ m diam). Sepharose 4B-HSA-DTPA-¹¹¹In was found to localize almost quantitatively in rat lungs immediately after iv injection similar to Otsuka et al. 96% of whole body activity was found in the lungs at 24 hr. For biodistribution studies Sepharose 4B-HSA in 0.2ml PBS containing 25% sucrose was injected into a tail vein of rats (250-300g) and 15 min later 0.2ml of the following radioimmunoimaging agents (35 μ g, 4 μ Ci) were injected into another tail vein. The number of DTPA molecules conjugated per Ab for the biodistribution studies was 6 for I and II, and 2 for III and IV. Comparing organ activities in % ID/g at 24hr, the target (lung) activities of I (2.98), II (3.75), III (4.26), and IV (3.67) were similar. However, the target to blood ratio showed a large variation (38 for II, 8.2 for I, 6.7 for III, 1.3 for IV). The target to liver ratio was the highest for III (4.4) followed by I (2.8), II (2.3) and IV (1.3). The order of the target to kidney ratio was II (3.8), I (2.8), III (2.3) and IV (1.0). The target to spleen activity was the highest for III (4.7) followed by II (1.8), IV (1.7) and I (1.3). Although these are preliminary data based on averages of duplicate to triplicate experiments, these studies support the hypothesis that a target to background ratio could be optimized by chemical modifications of the bond linking the chelator and antibody.

The structures of ANTIBODY-DTPA CONJUGATES.



- (1) Arnon, R., Sela, M.: *Immunol Rev* 62, 5 (1982).
- (2) Abdella, P.M., Smith, P.K., Royer, G.P.: *Biochem Biophys Res Comm* 87, 734 (1979).
- (3) Alvarez, V.L., Lee, C., Rodwell, J.D., McKearn, T.: *Intl Symposium on Monoclonal Antibodies*, Florence, Italy, 1984.
- (4) Paik, C.H., Hong, J.J., Ebbert, M.A., et al: *J Nucl Med* 264, 482 (1985).
- (5) Otsuka, F.L., Welch, M.J., McElvany, K.D., et al: *J Nucl Med* 25, 1343 (1984).

INVESTIGATIONS OF AVIDIN-BIOTIN IN RADIOPHARMACEUTICAL DESIGN

D.J. Hnatowich, M. Rusckowski, F. Virzi and P.W. Doherty

Department of Nuclear Medicine, University of Massachusetts Medical Center, Worcester, MA 01605

The extreme affinity of avidin for biotin (about one million times stronger than most antigen-antibody reactions) has been exploited in a variety of immunoassays and other *in vitro* techniques. To our knowledge, however, avidin and biotin have not previously been studied for *in vivo* use. This laboratory has lately considered the use of the avidin-biotin interaction in radiopharmaceutical design. For example, we are investigating the labeling of antibodies at high specific activities by attaching avidin containing many DTPA groups to the biotinylated proteins. In addition to improving the specific activity of the labeled protein, the biotin (and thus the avidin) may be directed to silent areas of the proteins such as the Fc region of antibodies, thereby minimizing the effect of the attachment on protein function. Furthermore, the addition of avidin may, under certain circumstances, improve the *in vivo* performance of proteins. For example, diffusion from the peritoneum may possibly be reduced through the attachment of one or more avidins (MW 66,000 daltons) to antibodies thereby helping to localize therapeutic radionuclides therein in the treatment of metastatic ovarian carcinoma.

Working thus far only with antibodies, we have followed published procedures for attaching biotin via the hydrazide (to carbohydrates) and the succinimide ester containing a five carbon spacer (to lysines), both commercially available. Avidin has been coupled with DTPA using the cyclic anhydride. Size exclusion HPLC has been used to demonstrate, via a shift in the radioactivity profile towards shorter retention times (i.e., higher molecular weight), that avidin attachment occurred (in the same manner we have shown that labeled avidin does not bind to biotin-free antibodies and that biotinylated antibodies do not bind ^{111}In nonspecifically as the acetate). The stability in 37°C of the avidin-biotin interaction was demonstrated similarly by observing an absence of a shift towards longer retention times following incubation in 37°C serum which would signify the release of avidin from the protein. The stability was further confirmed by incubation in serum of commercial biotin-conjugated plastic beads to which DTPA coupled avidin, labeled with ^{111}In , was attached. The bead assay was also used to show that avidin may be conjugated with at least 15 DTPA groups without decreasing its ability to bind biotin, presumably because avidin is multivalent.

Using avidin conjugated with 12 DTPA groups per molecule, we have achieved a specific activity of $300 \mu\text{Ci}/\mu\text{g}$ of ^{111}In on IgG antibody. Furthermore, following IP administration into normal mice, large differences in biodistributions were observed between DTPA conjugated avidin on IgG vs. DTPA coupled directly to IgG, both labeled with ^{111}In . Both the images and the biodistribution results obtained at 24 hours post-administration indicate that diffusion was reduced in the case of the avidin-conjugated protein. These preliminary results suggest that the avidin-biotin interaction may have application in the design of radiopharmaceuticals.

This work was supported in part by NIH grant CA33029 and DOE contract ACO2-83ER60175.

APPLICATION OF DIAMIDE DIMERCAPTIDE N_2S_2 BIFUNCTIONAL
CHELATING AGENTS FOR ^{99m}Tc LABELING OF PROTEINS.

S. Kasina, J.L. Vanderheyden, and A.R. Fritzberg
NeoRx Corporation, Seattle, WA 98119.

The formation of Tc- 99m diamide dimercaptide (N_2S_2) complexes of high purity and stability make them very attractive for bifunctional chelate applications (1,2). Studies with ^{99m}Tc -2,3-dimercaptoacetamidopropanoate (CO₂DADS) showed that additional functional groups attached to the chelate ring do not interact with the metal (3,4). We have extensively studied the application of these N_2S_2 ligands for Tc- 99m labeling of proteins, particularly monoclonal antibodies. The results of conjugation of these antibodies with Tc- 99m complexes containing activated esters as conjugating groups will be presented.

^{99m}Tc -4,5-Dimercaptoacetamidopentanoate was prepared in high yield and purity by either exchange or direct reduction of pertechnetate at basic pH. Active esters including phenyl, 2-chloro-4-nitro, 2,4,5-trichloro, 2,3,5,6-tetrafluoro (TFP) and 1-hydroxybenzotriazole were prepared using water soluble carbodiimide (5). The yields of active esters ranged from 40-80%. The active esters were purified from excess reactants by preparative reversed phase chromatography. Conjugation reactions were carried out by adding buffered solutions of either amino acids or proteins to dried residues of the ^{99m}Tc - N_2S_2 active esters.

Evidence for protein conjugation between the ^{99m}Tc - N_2S_2 active esters and lysine amino groups of proteins was further supported by model studies with the L-amino acid lysine. Lysine (Lys). Lys reacted with Tc- N_2S_2 -TFP ester almost quantitatively, whereas no reaction was observed with the phenyl ester. Addition of 1N sodium hydroxide to the TFP ester resulted in quantitative yield of the hydrolyzed carboxylate forms of the ^{99m}Tc - N_2S_2 complexes. Additional reactions of the TFP ester with glycine (Gly), aspartic acid (Asp), glutamic acid (Glu) and arginine (Arg) resulted in the corresponding conjugation adducts (Table 1). Maximum yields with several antibodies ranged from 50-70% at pH 8.5.

Table 1. Reactivity of ^{99m}Tc - N_2S_2 TFP esters with various amino acids.

Conditions: in 0.2M Phosphate buffer pH 9; room temperature
(Results expressed as % ^{99m}Tc - N_2S_2 TFP esters measured by ITLC-SG in CH₃CN solvent)

	Quant. (mg)	0 min	15 min	60 min
Control H ₂ O	—	93.5	91.4	88.6
0.2M Pi pH 9	—	89.9	85.1	65.2
GLY	25mg	6.0	2.8	—
GLY	10mg	20.4	3.0	—
GLY	1mg	45.6	15.3	—
LYS	25mg	6.6	2.6	—
LYS	10mg	7.3	2.7	—
LYS	1mg	32.7	5.9	—
GLU	3.75mg	89.8	80.5	34.8
GLU	1mg	89.0	—	28.5
ASP	1mg	96.7	—	49.5
ARG	15mg	4.0	—	3.7
ARG	1mg	41.1	—	17.4

HPLC analysis of the crude esterification reaction indicated that the major products are the chelate ring epimeric pair and a 5-10% of a pair of less lipophilic products (Fig. 1). These minor products were shown to be formed in the absence of alcohol in 40-60% yield (Fig. 2) and thus appeared to be carbodiimide adducts. These species did not react with lysine, indicating that they were, in fact, stable mixed uras from the carbodiimide used for esterification.

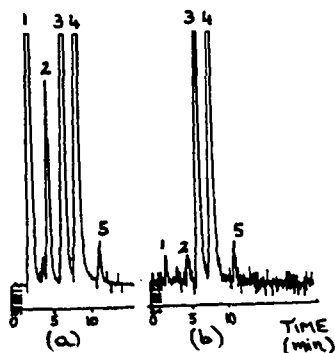


Fig. 1 HPLC chromatograms of (a) the crude esterification reaction, and (b) the esters after preparative reverse phase chromatography.

(1) $^{99m}\text{Tc}-\text{CO}_2\text{DADS}$; (2) ^{99m}Tc -mixed uras; (3,4) $^{99m}\text{Tc}-\text{N}_2\text{S}_2\text{-TFP}$ esters; (5) unknown impurity.

HPLC Conditions: Ultrasphere C_{18} 5 μm ; 34% $\text{CH}_3\text{CN}/0.01$ M Phosphate buffer pH 7; 1.0 $\mu\text{l}/\text{min}$; gamma detection.

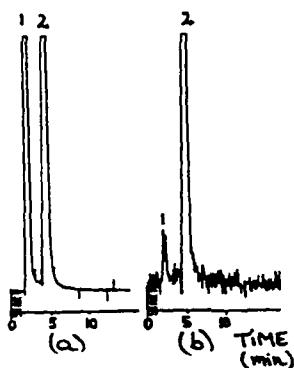


Fig. 2 HPLC chromatograms of (a) the crude esterification reaction in the absence of alcohol, and (b) crude material purified upon reaction with Lys.

(1) $^{99m}\text{Tc}-\text{CO}_2\text{DADS}$; (2) ^{99m}Tc -mixed uras.

HPLC Conditions: same as Fig. 1

^{99m}Tc Diamide dimercaptide complexes have been esterified and the resulting active esters conjugated to antibodies. Advantages include lack of nonspecific labeling of antibodies that is problematic when ^{99m}Tc is exchanged into chelating agents conjugated to protein. Antibodies labeled with the preformed chelation approach have demonstrated high retention of immunoreactivity with high stability of the ^{99m}Tc label. The ^{99m}Tc chemistry correlates with previously observed N_2S_2 chemistry at the carboxylate and ester stages and labeling of proteins occurs by well established protein derivatization chemistry.

The support of NIH Grant CA 40528-02 to Alan R. Fritzberg is gratefully acknowledged.

1. Fritzberg, A.R., Kuni, C.C., Klingensmith, W.C. III., Stevens, J., and Whitney, W.P., *J. Nucl. Med.*, 23, 592 (1982)
2. Kasina, S., Fritzberg, A.R., Johnson, D.L., and Eshima, D., *J. Med. Chem.*; accepted for publication (in press)
3. Fritzberg, A.R., Rao, T.N., Adhikesabulu, D., Camerman, A., and Vanderheyden, J.L., Abstract submitted to Sixth International Symposium on Radiopharmaceutical Chemistry, Boston, June 29-July 3, 1986.
4. Fritzberg, A.R., and Nunn, A.D., *Analytical and Chromatographic techniques in Radiopharmaceutical Research - Chapter 9*, 1986, pp. 183-212.
5. Gross, E., and Meienhofer, J., *The Peptides - Analysis, Synthesis, Biology*, Volume 1 Major Methods of Peptide Bond Formation. London, 1979.

^{89}Zr FOR ANTIBODY LABELING AND POSITRON EMISSION TOMOGRAPHY

J.M. Link, K.A. Krohn, J.F. Eary, R. Kishore, T.K. Lewellen, M.W. Johnson, C.C. Badger, K.Y. Richter, and W.B. Nelp
 Radiology Department, School of Medicine, University of Washington, Seattle, WA 98195; and Veterans Administration Medical Center, Albany, NY 12208

The use of gamma-emitting radiolabeled anti-tumor monoclonal antibodies (MAb) as potential diagnostic or therapeutic agents has yielded encouraging results. An important requirement, especially for therapy, is to measure quantitatively the time course for deposition of MAb in tissue or tumor to calculate internal radiation dosimetry. To do this with single photon emitters and conventional gamma cameras or SPECT requires elaborate calibrations using phantoms and necessitates assumptions that would not be required if a positron emitting label were available for following the pharmacokinetics of MAb.

We report here the production of ^{89}Zr , a positron emitter with half-life of 78.4 hours (1), and its first evaluation as a protein label. ^{89}Zr was produced from ^{89}Y (100% natural abundance) by the (p,n) reaction on a Y foil (286 mg cm^{-2}). This reaction cross section peaks at about 550 mb for 13.3 MeV protons and is about 200 mb at 9 MeV (2). The competing (p,2n) and (p,pn) reaction thresholds are 13 MeV and 12 MeV, respectively, but do not contribute substantially to product yield below about 17 MeV (2). In our target we have irradiated the Y foil at an incident energy of 13 MeV with a beam of 10 μA of protons for 40 minutes and achieved a yield of 7 mCi of ^{89}Zr . By increasing the efficiency of cooling of the Y foil, we anticipate production of about 40 mCi/hr with a 40 μA beam.

At a higher proton irradiation energy we can also make ^{88}Zr which has a half-life of 83.4 days (1). The (p,2n) reaction cross section peaks at about 26 MeV at almost 1200 mb and has a substantial cross-section extending from 20 to 35 MeV (2). The longer lived form of zirconium decays totally by electron capture with emission of a 394 KeV gamma (1) and may, in itself, be a useful tracer for antibodies. The (p,pn) reaction on the Y foil produces ^{88}Y . Although the reaction yield is low at incident proton energies below about 25 MeV, the ^{88}Y is a convenient by-product in that it provides a small amount of yttrium activation to aid in measurement of the purity of the ^{88}Zr and ^{89}Zr free of carrier yttrium from the target foil.

^{89}Zr decays via positron emission only 22% of the time (1). Virtually all decays go through a 909 KeV excited state to the daughter nucleus. This excited state has a $T_{1/2}$ of 16 sec so that events from the excited state will be uncorrelated with events from annihilation. We have tested the feasibility of imaging ^{89}Zr using both BaF_2 and BGO detectors. The detectors used were standard Scanditronix 3000 BaF_2 modules and Harshaw BGO detectors (25.4 mm dia, 25.4 mm deep). The detectors were placed 90 cm apart and the time spectra were collected for a ^{89}Zr point source in air and in a 30 cm water bath. The ratio of the true to accidental events (the peak area to background ratio) of the spectra, R, was determined for a variety of lower level energy discriminator settings. While both detectors produced acceptable values of R (R_{BaF_2} @ 150 KeV = 58, R_{BGO} @ 230 KeV = 15), the higher R for BaF_2 makes it more favorable for imaging ^{89}Zr , particularly when the signal-to-noise improvements with time-of-flight reconstruction are taken into account.

Zirconium is separated from yttrium by extraction followed by anion exchange chromatography (3,4). The Y foil (approx. 2 grams) is dissolved in 5 ml 12N HCl and then diluted to 100 mL of 4N HCl. The Zr(IV) is extracted with two 10 mL aliquots of 0.5M 4,4,4-trifluoro-1-(2-thienyl)-1,3-butanedione (TTA) in xylene (3). About one-half of the Zr(IV) is extracted into the organic phase, along with $\leq 1\%$ of the Y(III). The Zr(IV) is then back extracted from the TTA, using an equal volume of 0.5N HNO_3 + 0.5N HF, with nearly quantitative efficiency. The aqueous phase from back extraction is evaporated to dryness then dissolved in 12N HCl to form ZrCl_8^{-4} . This solution is then passed through a Dowex 1x8 anion exchanger (chloride form, 8 mL). Elution with 25 mL of 12N HCl washes through >99% of the remaining Y(III). The Zr(IV) is then eluted with 30 mL 1N HCl + 0.01M oxalate to recover >80% of the zirconium. This is evaporated to reduce volume and has been used in protein labeling studies. About 25% of the zirconium that is produced in the target has been recovered with <.001% of initial Y

remaining. These radiochemical procedures require further improvement in recovery of ^{89}Zr and purity from carrier Y but the $^{89}\text{Zr(IV)}$ oxalate made by these methods has already proved useful for some pilot biology experiments.

Zr(IV) as the chloride or oxalate transchelates nonspecifically to plasma proteins, resulting in a weakly bound label. When Zr-oxalate was injected into mice, it cleared with a half time consistent with that of a labeled plasma protein. In contrast Zr-DTPA injected into animals was rapidly cleared by the kidneys, similar to excretion of Tc-DTPA, indicating that the Zr-DTPA complex was stable in vivo. Zr-labeled protein has been synthesized by transchelation of Zr(IV) from citrate or oxalate to DTPA which was previously attached to MAb by the cyclic dianhydride method (5). When the initial zirconium product was prepared as the oxalate, the formation of weakly labeled serum proteins was inhibited. We are optimistic about the future potential of ^{89}Zr for radioimmunoscintigraphy.

This research was supported in part by PHS grants CA29639 and CA39675 awarded by the National Cancer Institute, DHHS.

1. Lederer C.M. and Shirley V.S., ed. Table of Isotopes, seventh edition. New York, John Wiley & Sons, 1978.
2. Hellwege K.H., ed. Landolt-Bornstein: Numerical data and functional relationships in science and technology. New Series, Group 1: Nuclear Particle Physics, Vol. 5. Q-values and excitation functions for charged particle induced nuclear reactions, Berlin, Springer-Verlag, 1973.
3. Moore, F.L., Anal. Chem., 28, 997 (1956).
4. Larsen, E.M., Adv. Inorg. Chem. Radiochem. 13, 1 (1970).
5. Hnatowich, D.J., Layne, W.W., Childs, R.C., Int. J. Appl. Radiat. Isot., 33, 327 (1982).

IODINATED MONOCLONAL ANTIBODY INTERNALIZATION BY TUMOR CELLSA.I. Kassis¹, C.N. Venkateshan¹, W.W. Layne¹, G. Eisenbarth², A. Kaldany², B.M. Kinsey¹, and S.J. Adelstein¹¹Department of Radiology, Harvard Medical School, Boston, MA 02115²Joslin Clinic, New England Deaconess Hospital, Boston, MA 02115

The hepatic dehalogenation of radiolabeled monoclonal antibodies (MoAb) has been observed and reported repeatedly. The reason for this phenomenon has not been examined even though it is believed that the mechanism is enzymatic in nature. Although it is conceivable that this reaction could occur at the cell surface, it is more likely that it takes place within the cell following internalization of the radiolabeled antibody. We have examined the latter possibility by testing three MoAb available to us: A₂B₅ (IgM), A₁D₂ (IgG), and 3G5 (IgM) (1). These MoAb have been raised against the cell surface antigens of a well established rat insulinoma cell line RINm5F (2). The methods used were direct radioimmunoassay and fluorescence microscopy.

Binding of MoAb: Suspended RINm5F cells were incubated for 1 hour at 37°C with Protein-A purified mouse MoAb, washed, and at 0, 1, 2, and 3 hours reincubated with fluoresceine isothiocyanate (FITC) labeled antimouse IgG antibody (30 minutes, 37°C). The cells were washed, transferred onto slide covers and scored (+1 to +4) under a fluorescence microscope (Zeiss). The results [Table 1, columns 1 & 2] show that following the 1-hour incubation of cells in the MoAb, the cell membranes exhibited bright fluorescence. However, when these cells were then incubated at 37°C, the intensity of membrane-bound fluorescence decreased with time, almost disappearing completely by 3 hours. This indicates that these antibodies either detached from the cells (by themselves or as antigen-antibody complexes) or were internalized by the cells.

TABLE 1. Monoclonal Antibody Binding and Retention by RINm5F Cells In Vitro

Time (hr)	Cell Membrane Fluorescence	Cell Associated CPM ± SD (% Retained)		
		A ₂ B ₅	A ₁ D ₂	3G5
0.0	+++	7276 ± 1127	866 ± 31	2109 ± 110
1.0	+++		466 ± 101(53.8)	971 ± 65(46.0)
2.0	++			
3.0	±	6949 ± 1068(96)	490 ± 23(56.6)	
5.0				590 ± 80(28.0)
24.0		5922 ± 1302(81)	595 ± 15(68.7)	200 ± 50(10)

Internalization of MoAb: The MoAb were radioiodinated by the Iodogen method and the free Na¹²⁵I removed by column chromatography on a Sephadex G-25 column. Suspended RINm5F cells were then incubated for 1 hour at 37°C with the ¹²⁵I-MoAb, washed, and the radioactivity associated with the cells determined in a gamma counter. The cells were resuspended in fresh medium and incubated at 37°C. During a 24 hour period, the radioactive content of the cells was determined.

Following a three hour incubation in medium, 96% of the radiolabeled A₂B₅ antibody remained associated with the RINm5F tumor cells [Table 1, columns 1 & 3] while disappearing almost completely from the surface [Table 1, columns 1 & 2].

In fact, more than 80% of the radioactivity was still associated with the cells even after an overnight incubation. These results clearly indicate that A₂B₅ was internalized by the tumor cells.

By the first hour, 53.8% of the bound $^{125}\text{I-A}_1\text{D}_2$ was still associated with the cells and this value did not change significantly by 3 hours (56.6%) or by 24 hours (68.7%) [Table 1, columns 1 & 4]. The slow increase in the % retained may be due to the slight uptake resulting from unwashed antibody released during the first hour of incubation. These results, together with the fluorescence microscopy data, show that about 50% of the antibody initially bound to the tumor cells was released from the cells within one hour post incubation. However, the remaining 50% stayed with the cells while disappearing from the surface, thus indicating that it was internalized by the tumor cells.

After 5 hours, 28% of the original cell-associated ^{35}S radioactivity was still with the cells [Table 1, columns 1 & 5], and by 24 hours this radioactivity had decreased to approximately 10%. Therefore, this MoAb is the only antibody among the three tested that was not internalized by the tumor cells following its attachment.

Taken together, the present findings indicate that some antibodies are internalized by tumor cells following attachment to the cell surface antigens. This would allow the intracellular enzyme to have access to these antibodies and dehalogenate them. Studies to compare the dehalogenation of these antibodies in vivo are under way.

1. Eisenbarth, G.S., Shimizu, K., Bowring, M.A., and Wells, S., Proc. Natl. Acad. Sci. USA, 79, 5066 (1982).
2. Gazdar, A.F., Chick, W.L., Oie, H.K., King, D.L., Weir, G.C., and Lauris, V., Proc. Natl. Acad. Sci. USA, 77, 3519 (1980).

RADIOIODINATION OF DF3 ANTIBODY: OPTIMIZATION USING IN VITRO BINDING ASSAYS

M.R. Zalutsky, D.F. Hayes, and D.W. Kufe
Harvard Medical School, Boston MA and Duke University Medical Center, Durham, NC

An important aspect of radiolabeled monoclonal antibody development is to obtain a meaningful assessment of the effects of radiolabeling on the immunoreactivity of the labeled antibody. Expression of immunoreactivity as the antibody affinity constant should be particularly useful because it could facilitate comparison with results obtained with different antibodies and labeling techniques in other laboratories. Herein we report the use of both indirect and direct binding assays for the optimization of the radiolodination of DF3, a monoclonal antibody directed against a human breast cancer associated antigen (1). This antibody was chosen not only because of clinical interest but also because it could not be labeled with retention of immunoreactivity using an iodogen procedure that had been successfully employed with other antibodies (2,3).

Initial attempts at labeling 50 ug of DF3 using 20 ug iodogen, while proceeding in high yield, resulted in a product with little specificity for breast tumor cell lines. This result was somewhat surprising since another antibody, B6.2 had been labeled at a 10-fold higher iodogen to protein ratio with minimal loss in reactivity (4). An indirect *in vitro* binding assay was then used to investigate the effects of various aspects of the iodogen (iodogen concentration, reaction time, presence or absence of iodide) and Bolton-Hunter (benzene residue with and without activated ester) labeling procedures on the reactivity of DF-3.

All binding assays were performed using sonicated MCF-7 human breast cancer cells. The protein concentration of the disrupted cells was measured spectrophotometrically. One hundred μ l aliquots of sonicated cells were added to 96-well microtiter plates and incubated overnight at 37°C. Plates were prepared at protein concentrations of 12.5, 25, 50, 100, 200, 400, 800 and 1600 ug per well. A set of control plates were also prepared using bovine serum albumin (BSA).

In the indirect assay, serial dilutions of DF3 antibody (both control and following exposure to each potential set of reaction conditions) in 1% BSA/PBS were added to microtiter plates containing 200 ug cellular protein per well and incubated overnight at 4°C. The wells were washed twice with 1% BSA/PBS and then incubated for 1 hr at room temperature with 125 I-labeled goat antimouse IgG. The wells were washed and the 125 I activity associated with each well was measured. By comparing the amount of antibody required to achieve the half-saturation value of 125 I-labeled goat anti-mouse binding observed with untreated DF3, the effect of each labeling parameter on the immunoreactivity of DF3 could be determined. Using the assay conditions described, half-saturation binding for untreated DF3 control occurred at 180 ng of antibody. In contrast, 580 ng and 2000 ng of DF3 were required to achieve half-max binding after exposure to 1 ug and 5-10 ug of iodogen, respectively. Similar differences were obtained with and without iodide in the reaction mixture suggesting that sensitivity of DF3 to oxidants rather than presence of a reactive tyrosine in the antigen recognition site is the more probable cause. The immunoreactivity of DF3 did not appear to be decreased significantly by the Bolton-Hunter reaction conditions.

The immunoreactivities of four different ^{125}I -labeled DF3 preparations were investigated: IgG using 1 and 10 ug Iodogen and both IgG and F(ab')₂ using the Bolton-Hunter method. Serial dilutions of each labeled antibody were added to microtiter plates containing the 8 different concentrations of MCF-7 and control protein and incubated overnight at 4°C. The wells were washed twice and then the fraction of input counts bound to the plates was determined.

Data from the direct binding measurements was analyzed in two ways. First, results obtained at the four highest antigen concentrations were used to calculate the immunoreactive fractions using the method described by Lindmo et al. (5). The immunoreactive fractions ranged from 0.13 for the 10 ug Iodogen preparation to 0.65 for DF3 IgG labeled via the Bolton-Hunter method. Second, the equilibrium binding data analysis program developed by McPherson (6) was used to generate Scatchard plots, affinity constants and the maximum amount of antibody bound (B_{max}) at each antigen concentration.

TABLE 1. Binding Data: ^{125}I -DF3 F(ab')₂ via Bolton-Hunter

MCF-7/well ug	$K_a \times 10^{-8}$ M^{-1}	B_{max} nM	$B_{\text{max}}/\text{ug Ag}$ pM/ug
800	0.38 ± 0.08	24.62 ± 0.49	30.8 ± 0.6
400	0.79 ± 0.09	10.36 ± 0.11	26.0 ± 0.3
200	1.49 ± 0.13	3.81 ± 0.25	19.1 ± 1.3
100	1.91 ± 0.15	1.73 ± 0.11	17.3 ± 1.1
50	2.13 ± 0.22	0.93 ± 0.08	18.6 ± 1.6
25	2.62 ± 0.09	0.46 ± 0.01	18.4 ± 0.4
12.5	2.37 ± 0.45	0.23 ± 0.03	18.4 ± 2.4

In all cases, data obtained at 1600 ug per well was not consistent with a saturable binding process. Lower affinity constants and higher B_{max}/ug antigenic protein were observed at higher concentrations of protein per well. Consistent values of K_a and B_{max} were generally observed with 12.5-100 ug cell-derived protein per well (See Table). Results obtained at these concentrations were averaged to obtain the following values for the K_a of ^{125}I -labeled DF-3: 10 ug Iodogen, $8.1 \times 10^7 M^{-1}$; 1 ug Iodogen, $2.1 \times 10^8 M^{-1}$; Bolton-Hunter IgG, $6.4 \times 10^8 M^{-1}$; and Bolton-Hunter F(ab')₂, $2.3 \times 10^9 M^{-1}$. When data at 12.5-100 ug protein per well were corrected for the immunoreactive fractions calculated as described above, almost identical affinity constants for DF3 IgG were obtained from the three preparations ($K_a = 1.1-1.3 \times 10^9 M^{-1}$).

In conclusion, both indirect and direct binding assays were of value in optimizing the radiolabeling of antibody DF3. When labeled by the Bolton-Hunter method, ^{125}I -labeled DF3 had a 10-fold higher affinity constant than following labeling with a relatively low concentration of Iodogen. It is important to note that the conditions used in *in vitro* assays can influence the values obtained for the affinity constant and B_{max} , particularly at high antigen concentrations. The magnitude of these effects appeared to differ among the four labeled preparations. The possibility that in some cases, radiolabeling of monoclonal antibodies creates subpopulations of proteins with nonunique affinity constants is being investigated as a contributory factor.

1. Kufe, D., Inghirami, G., Abe, M., Hayes, D., Justl-Wheeler, H. and Schlom, J., *Hybridoma*, **3**, 223 (1984).
2. Carroll, A.M., Zalutsky, M.R., Benacerraf, B., and Greene, M.I., *Surv. Synth. Path. Res.*, **3**, 189 (1984).
3. Zalutsky, M.R., Colcher, D., Kaplan, W.D., and Kufe, D.W., *Int. J. Nucl. Med. Biol.*, **12**, 227 (1985).
4. Colcher, D., Zalutsky, M., Kaplan, W., Kufe, D.W., Austin, F., and Schlom, J., *Cancer Res.*, **43**, 736 (1983).
5. Lindmo, T., Boven, E., Cuttitta, F., Fedorko, J., and Bunn, P.A., *J. Immunol. Meth.*, **72**, 77 (1984).
6. McPherson, G.A., *Computer Prog. in Biomed.*, **17**, 107 (1983).

SYNTHESIS AND RADIOIODINATIONS OF SOME ARYL TIN COMPOUNDS FOR
RADIOLABELING OF MONOCLONAL ANTIBODIES,

D.S. Wilbur, D.S. Jones, And A.R. Fritzberg
NeoRx Corporation, Seattle, WA 98119

Many labeling methods for radioiodinating proteins have been reported over the past three decades (1-3). Virtually all of the radioiodination methods previously reported have resulted in bonding of the radioiodine to a phenolic aromatic ring. This is true for radioiodination of small molecules prior to attachment to proteins, as well as direct labeling of proteins. Some examples of attaching radioiodinated small molecules to proteins have been reported by Bolton and Hunter (4), Wood et. al. (5), and Su and Jeng (6). While the phenolic ring permits rapid substitution of radioiodine onto the small molecules or proteins, it is believed that the ortho-iodo phenol that results is similar enough to iodinated thyroid hormones that deiodinases can cause loss of the radioiodine in vivo. Our interest in using monoclonal antibodies for in vivo tumor diagnosis and therapy led to an investigation of a method of attaching radioiodine to monoclonal antibodies such that the radioiodine label is metabolically and chemically stable. The method that was chosen is the bonding of radioiodine to nonactivated aromatic compounds containing appropriate functionalities such that once radioiodinated they could be attached to a protein. More specifically, the synthesis of high specific activity radioiodine labeled para-iodophenyl (PIP) compounds is being investigated. In the investigation organometallic intermediates are being studied for rapid and efficient incorporation of the radioiodine into the non-activated aromatic rings.

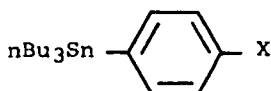
Some of the organometallic intermediates being studied for radioiodinations are shown in Table 1. The trialkyltin derivatives (e.g. SnMe₃ or SnBu₃) were of particular interest since the radioiodinations of some aryltin compounds have been reported to be quite facile (7). Two methods of synthesis have proven useful to prepare compounds 1 - 10. In one synthetic approach para-bromo compounds were lithiated by n-BuLi at -100°C (8) and subsequently transmetalated to the corresponding aryltin derivatives with n-Bu₃SnCl. A second synthetic approach that has proven to be quite useful for synthesis of compounds containing base sensitive functional groups is the use of hexamethylditin and tetrakis(triphenylphosphine)palladium (9). Using the second method it has been possible to synthesize 4 from the corresponding p-bromobenzimidate. Iodination of aryltin compounds which have different functional groups on the aryl ring have had appreciably different reaction rates. For example, the iodination of benzonitrile 1 occurs at a considerably slower rate than the succinimidyl ester 3, which itself iodinate at a rate that is much slower than the benzoic acid 2. The relative rates of radioiodinations of 2 and 3 has made it necessary to purify 3 to the extent that there is less than 0.1% of 2 present or an appreciable amount of the radioiodine is incorporated into the benzoic acid 2 in preference to the succinimidyl ester 3.

Our studies have shown that the benzoate 3 and benzimidate 4 are not as readily hydrolyzed as their alkyl congeners 6, 8 & 10. Indeed, a dilute solution of 3 in 5% HOAc/MeOH has no appreciable methanolysis over a two month period. Further

results from our studies have indicated that the lipophilicity of the tri-*n*-butyltin derivatives can be of advantage in no-carrier-added radioiodinations. Partitioning of compounds in an aqueous medium results in most of the unreacted organotin starting material coming out of solution while virtually all of the radioiodinated compound remains in solution. Thus, chromatographic separations of the radioiodinated products may not be necessary prior to conjugating the reagents to proteins.

Radioiodination and protein labeling studies are under investigation for the compounds in Table 1. Investigations with *N*-succinimidyl-4-[¹²⁵I]iodobenzoate, **11**, prepared from reaction of **3** with no-carrier-added radioiodine (I-125 or I-131) and *N*-chlorosuccinimide in MeOH at room temperature have demonstrated that it can be prepared in 65-95% radiochemical yields, and that coupling of this reagent to a monoclonal antibody can be accomplished in 35-50% yields. Furthermore, immunoreactivities of the antibody and antibody fragments labeled with **11** are measured to be 70-90% of original. However, most importantly, the *in vivo* biodistribution (in mice) of labeled antibodies and fragments shows no increase in thyroid activity from 2 hours to 72 hours sacrifice times. These results are evidence that no *in vivo* deiodination is occurring.

Table 1. Aryltin Intermediates for Radioiodinations*



<u>Compound #</u>	<u>X</u>
<u>1</u>	-CN
<u>2</u>	-COOH
<u>3</u>	-COOSucc**
<u>4</u>	-CNHOMe***
<u>5</u>	-CH ₂ CH ₂ COOH
<u>6</u>	-CH ₂ CH ₂ COOSucc**
<u>7</u>	-CH ₂ CH ₂ CN
<u>8</u>	-CH ₂ CH ₂ CNHOMe***
<u>9</u>	-CONHCH ₂ COOH
<u>10</u>	-CONHCH ₂ COOSucc**

* Ultimately to be used for radioiodinating proteins.

** Succ = *N*-succinimidyl ester

*** CNHOMe = methyl imidate

- 1.) Eckelman, W.C., Paik, C.H., and Reba, R.C., *Cancer Research*, 40, 3036 (1980).
- 2.) Osterman, L.A., *Methods of Protein and Nucleic Acid Research*. Springer-Verlag, 1984, pp 131-139
- 3.) Langone, J.J., *Methods in Enzymology*, 70, 221 (1980); *ibid* 73, 113 (1981).
- 4.) Bolton, A.E. and Hunter, W.M., *Biochem. J.* 133, 529 (1973).
- 5.) Wood, F.T., Wu, M.M., and Gerhart, J.C., *Anal. Biochem.* 69, 339 (1975).
- 6.) Su, S.N., and Jeng, I., *Anal. Biochem.* 128, 405 (1983).
- 7.) Seitz, D.E., Tonnesen, G.L., Hellman, S., Hanson, R.N., and Adelstein, S.J., *J. Organometal. Chem.* 186, C33 (1980).
- 8.) Parham, W.E. and Sayed, Y.A., *J. Org. Chem.* 39, 2051 (1974).
- 9.) Kosuyi, M., Shimizu, K., Ohtani, A., and Migita, T., *Chemistry Letters*, 829 (1981).

RADIOHALOGENATED LOW-DENSITY-LIPOPROTEIN: POTENTIAL AGENTS FOR THE VISUALIZATION OF ATHEROSCLEROTIC LESIONS

S.M. Moerlein, K.B. Dalal, Y.Yano, S. Ebbe, F.T. Lindgren, and T.F. Budinger

Donner Laboratory and Lawrence Berkeley Laboratory, University of California, Berkeley, CA 94720

The *in vivo* localization of low density lipoprotein (LDL) labeled with ^{99m}Tc (1) and ^{125}I (2,3) indicates that LDL labeled with the gamma-emitter ^{123}I or the positron-emitters ^{124}I , ^{75}Br , or ^{76}Br may be useful for imaging atherosclerotic lesions with SPECT or PET. Although the radioiodination of LDL has been reported (4), neither the radioiodination nor radiobromination of LDL has been optimized.

For convenience, these optimization experiments were conducted using commercially-available ^{131}I (1270 Ci/mmol) and ^{82}Br (240 Ci/mol) preceding application with ^{123}I , ^{124}I or ^{75}Br , ^{76}Br . LDL ($d = 1.020\text{--}1.060$ g/ml) was prepared from fresh human serum and hypercholesterolemic rabbit plasma (diet consisted of 1% cholesterol and 4% peanut oil) (5). Human and rabbit LDL were radiohalogenated using iodine monochloride and bromine/ferric chloride which had been exchange-labeled with $^{131}\text{I}^-$ and $^{82}\text{Br}^-$, respectively. The radiohalogenated LDL analogues were separated from unreacted inorganic species using gel permeation chromatography (Sephadex G-50, 0.1 M glycine pH 8.6). The eluted fractions corresponding to I- and Br-LDL were subjected to 10% SDS gel electrophoresis, and the radioactivity and staining patterns for radioiodinated and radiobrominated LDL were very similar to those of native human and rabbit LDL.

Because the overall radiochemical labeling yield for the production of radiohalogenated LDL depends on both the initial exchange reaction as well as on the subsequent halogenation of LDL, the exchange reactions ($^{131}\text{I}^-/\text{ICl}$ and $^{82}\text{Br}^-/\text{Br}_2$) were studied. The percentage of radiohalide which had exchanged with halogen was determined by quenching the exchange mixture with excess trimethylphenylstannane and analyzing for $\text{C}_6\text{H}_5^{131}\text{I}$ and $\text{C}_6\text{H}_5^{82}\text{Br}$ with radio-HPLC. $^{131}\text{I}^-$ was found to exchange with ICl with up to 95% efficiency, while a maximum of 70% of the $^{82}\text{Br}^-$ exchanged with Br_2 . The exchange efficiency was found to decrease with decreasing molarity of ICl or Br_2 , with lower limits of 0.1 mM ICl and 10 mM Br_2 for $^{131}\text{I}^-$ and $^{82}\text{Br}^-$, respectively. These differences may be due to differences in the specific activities of the radiohalides used.

Radiohalogenation of human and rabbit LDL using $^{131}\text{I}^-/\text{ICl}$ or $^{82}\text{Br}^-/\text{Br}_2/\text{FeCl}_3$ in glycine buffer (pH 8.6) reached completion within 5 min. Due to dependence on the exchange efficiency, labeling required at least 0.1 mM ICl (10 mM Br_2). However, the yield was also dependent on the relative ICl (Br_2)/LDL molar ratio R. As shown in the Figure for labeling 2 mg samples of rabbit LDL with $^{131}\text{I}^-/\text{ICl}$, yields of ^{131}I -LDL decreased as R exceeded ca. 100, after passing through a maximum for 0.2–2.0 mM ICl .

Optimum radiochemical yields of 42–48% were achieved for radioiodinated LDL, with corresponding radiobromination yields of 25–30%; each radiolabeling procedure being completed within 15 min. Preliminary *in vivo* animal distribution results will be presented for these agents.

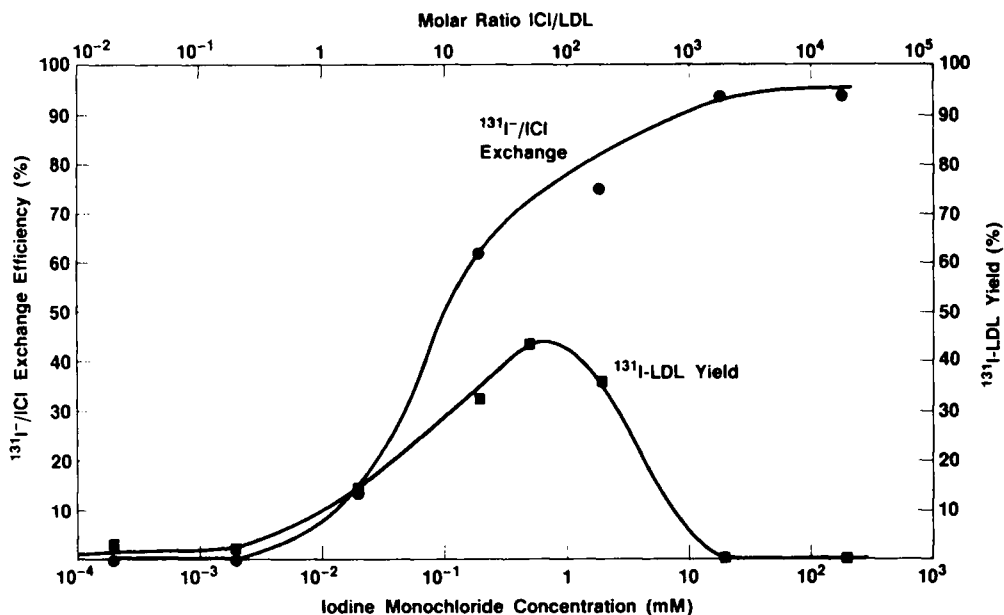
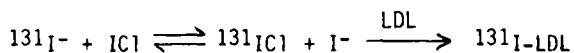


FIGURE. Effect of ICl Concentration on the Isotopic Exchange Efficiency and Radioiodination of Rabbit Low-Density Lipoprotein.



This research was supported by the U.S. Department of Energy (DE-AC03-76SF00098).

1. Lees, R.S., Garabedian, H.D., Lees, A.M., Schuhmacher, D.J., Miller, A., Isaacsohn, J.L., Derksen, A., and Strauss, H.W., *J. Nucl. Med.*, **26**, 1056 (1985).
2. Roberts, A.B., Lees, A.M., Lees, R.S., Strauss, H.W., Fallon, J.T., Taveras, J., and Kapiwoda, S., *J. Lipid Res.*, **24**, 1160 (1983).
3. Lees, R.S., Lees, A.M., and Strauss, H.W., *J. Nucl. Med.*, **24**, 154 (1983).
4. Bilheimer, D.W., Eisenberg, S., and Levy, R.I., *Biochim. Biophys. Acta*, **260**, 212 (1972).
5. Lindgren, F.T., In Perkins, E.G., ed., *Analysis of Lipids and Lipoproteins*. Champaign, American Oil Chemists Society, 1975, pp 204-224.

COMPARATIVE STUDY OF $^{123}(^{131})\text{I}$ - and $^{99\text{m}}\text{Tc}$ -LOW DENSITY LIPOPROTEINS (LDL)P. Angelberger¹, M. Hüttinger², R. Dudczak³

- 1) Research Center Seibersdorf A-2444
- 2) Inst. of Med. Chem. A-1090 Wien
- 3) 1st Med. Univ. Clinic A-1090 Wien, AUSTRIA

Presently there is great interest in early detection of atherosclerotic vessel lesions in vivo. This goal may be achieved by following lesion metabolic activity with labeled low density lipoproteins (LDL) which localize in regions of endothelial growth. Preliminary studies were undertaken with ^{125}I -, $^{99\text{m}}\text{Tc}$ - and ^{123}I -labeled LDL (1, 2, 3). This work was aimed at comparing $^{123}(^{131})\text{I}$ -LDL and $^{99\text{m}}\text{Tc}$ -LDL with regard to an optimized preparation, in vitro stability and in vivo distribution.

LDL was isolated from rabbit plasma by sequential ultracentrifugation (3). For $^{123}(^{131})\text{I}$ -labeling we studied as oxidant a) water insoluble Iodogen in suspension and b) Chloramine T. Using b), Chloramine T and LDL concentration, reaction time and amount of iodide-carrier were investigated. In case of $^{99\text{m}}\text{Tc}$ -labeling the buffer medium and pH, LDL and $\text{Na}_2\text{S}_2\text{O}_4$ reductant concentration were studied. At the end of the reaction period radiolabeled LDL was isolated from the reaction mixture by a) ultrafiltration through cellulose acetate membranes (nominal cut-off 20000 Dalton) by centrifugation, b) gel filtration on Sephadex G25M and c) preparative HPLC on size exclusion columns TSK-250 using phosphate buffered saline (pH 7.5) containing 0.001 M EDTA as eluent for b) and c).

Radiochemical purity was determined by TLC (ITLC-SG, acetone; HSA loaded SG, $\text{H}_2\text{O}:\text{EtOH}:\text{NH}_3$ 5:2:1) for $^{99\text{m}}\text{Tc}$ -LDL only, electrophoresis on paper and cellulose acetate (buffer 0.1 M barbital pH 8.6, 0.001 M EDTA, 1% albumin; 20 V/cm) and analytical HPLC (same system as prep.) for $^{99\text{m}}\text{Tc}$ - and $^{123}(^{131})\text{I}$ -LDL. Blood clearance and biodistribution were evaluated in rats and rabbits.

The Iodogen method required about 2 mg suspended Iodogen/ml reaction mixture to produce comparable (to Chloramine T) yields which dropped to zero at 50 ug/ml. Optimized labeling conditions for the Chloramine T method are summarized in Table 1 and for $^{99\text{m}}\text{Tc}$ -labeling in Table 2.

TABLE 1. Parameters for Labeling LDL with $^{123}(^{131})\text{I}$

Buffer:	0.15 M NaCl, 0.05 M PO_4 pH 7.5
LDL:	2 - 4 mg/ml $\sim 0.8 - 1.7 \times 10^{-6}$ M
Iodide:	1 - 2 $\times 10^{-6}$ M
Chloramine T:	0.0003 M
Reaction time:	5 min
Yield:	41 \pm 9% (n = 10) isolated product

TABLE 2. Parameters for Labeling LDL with $^{99\text{m}}\text{Tc}$

Buffer:	0.15 M NaCl, 0.05 M PO_4 pH 7.5
LDL:	2 - 4 mg/ml $\sim 0.8 - 1.7 \times 10^{-6}$ M
TcO_4^- :	10 - 50 mCi/ml $\sim 0.08 - 0.4 \times 10^{-6}$ M
$\text{Na}_2\text{S}_2\text{O}_4$:	0.005 M
Reaction pH:	8 ($\text{Na}_2\text{S}_2\text{O}_4$ sln. in 0.01 n NaOH)
Reaction time:	45 min
Yield:	43 \pm 8% (n = 5) isolated product

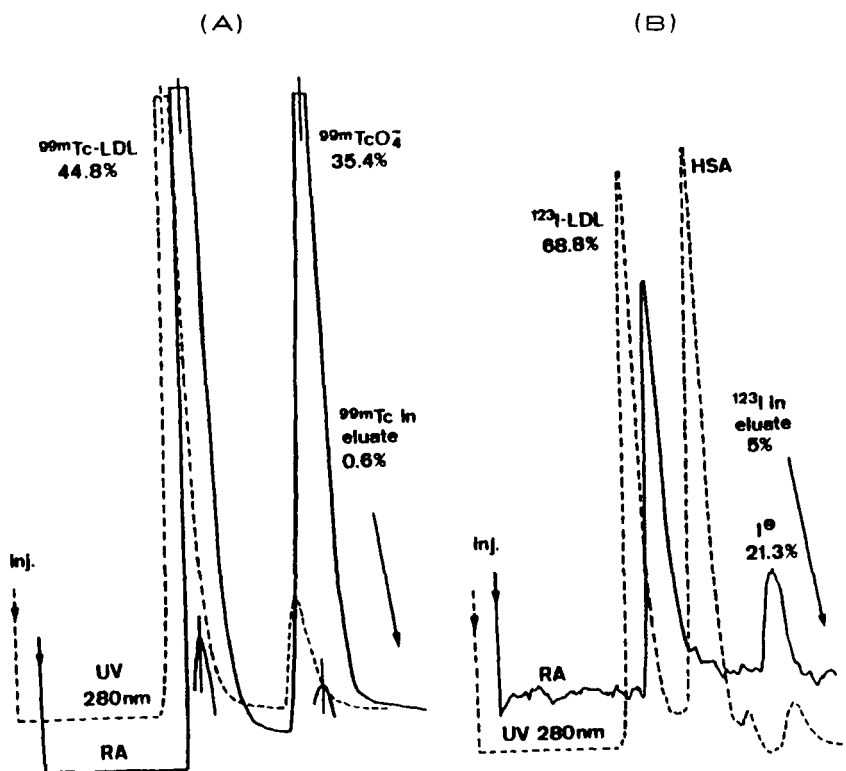


Figure 1. (A) Preparative HPLC of ^{99m}Tc -LDL reaction mixture. (B) Analytical HPLC of ^{123}I -LDL, 24 hours after labeling. A and B: SEC column TSK-250; eluent 0.15 M NaCl, 0.08 M PO_4 pH 7.5, 0.001 M EDTA; flow 1 ml/min.

Of the three separation methods ultrafiltration was most convenient and rapid but produced somewhat lower radiochemical purity than size exclusion chromatography of which the high pressure version was preferred for speed and detection efficiency. A preparative HPLC separation of ^{99m}Tc -LDL is shown in Fig. 1 (A). Radiochemical purity and in vitro stability of 123 (131) I -LDL and ^{99m}Tc -LDL are characterized in Table 3.

TABLE 3. Percentages of Impurities at various Times after Labeling

123 (131) I -LDL		^{99m}Tc -LDL		
hours	% I^-	hours	% TcO_4^-	% $\text{TcO}_2 \cdot \text{H}_2\text{O}$
0.2	0.5	0.5	5 - 12	7 - 17
1	2.7	2	9 - 22	n.d.
2	4 - 11	4	17 - 36	n.d.
4	10 - 18		(range)	
24	20 - 40			

An example of HPLC analysis for radiochemical purity (^{123}I -LDL, 24 hours after labeling) is shown in Fig. 1 (B). The increase of free I^- and TcO_4^- after labeling was not significantly reduced by addition of 20 mg albumin/ml product.

Preliminary in-vivo data are presented in Table 4.

TABLE 4. Biodistribution of labeled Rabbit-LDL

	123 (131) I-LDL	99mTc-LDL
in rats	plasma T1/2 7.6 hrs	plasma T1/2 6.2 hrs
in rabbits	" 23	" 16
rats	24 hrs p.i., % dose/g	
blood	0.09	0.07
liver	0.06	0.19
spleen	0.10	0.23
adrenals	0.09	0.15
kidneys	0.05	1.46
urine	2.21	0.83

When rabbit plasma samples were subject to trichloroacetic acid (TCA) precipitation at various times after i.v. ^{131}I -LDL and $^{99\text{m}}\text{Tc}$ -LDL (double tracer) $^{99\text{m}}\text{Tc}$ -activity in the precipitate remained about constant while ^{131}I declined.

Further biodistribution and scintigraphic studies are being conducted to evaluate ^{123}I -LDL and $^{99\text{m}}\text{Tc}$ -LDL as metabolic tracers for atherosclerotic lesions.

1. Lees R.S., Lees A.M., and Strauss H.W., *J. Nucl. Med.*, 24, 154 (1983).
2. Lees R.S., Garabedian H.D., Lees A.M., Schumacher D.J., Miller A., Isaacsohn L.J., Derksen A., and Strauss H.W., *J. Nucl. Med.*, 26, 1056 (1985).
3. Hüttinger M., Corbett J.R., Schneider W.J., Willerson J.T., Brown M.S., and Goldstein J.L., *Proc. Natl. Acad. Sci. USA*, 81, 7599 (1984).

FACTORS AFFECTING THE FORMATION OF HIGH MOLECULAR WEIGHT SPECIES AND LABELLING EFFICIENCY OF A DESFEROXAMINE-ANTIBODY CONJUGATE

J.W. Babich, M.C. Ward, K.R. Roberts, A. Bukhari, G. Coghlan, J.H. Westwood, V.R. McCready, and R.J. Ott.

Royal Marsden Hospital and Institute of Cancer Research, Surrey, England

The mouse monoclonal antibody LICR-LON-M8 has been previously labelled with In-111 (via DTPA conjugation) and used to detect bone metastases in patients with breast tumours. (1) Interest in image subtraction techniques (2) and the possibility of using antibody 'cocktails' has prompted us to produce a M8 conjugate which could be easily labelled with gallium and demonstrate good in vivo stability. Gallium-67 was the isotope of choice due to its suitable gamma energies and half-life, and its commercial availability. Desferrioxamine (DFO) was chosen as the chelating agent due to the greater stability of Ga-DFO over Ga-Transferrin. (3) The reported instability of gallium-67 labelled DTPA-antibody (4) and poor initial labelling results with DTPA-M8 also made DFO more attractive. Glutaraldehyde (GLUT) was used as the linking agent. The ability of GLUT to cross-link proteins (5) required the concentration of GLUT to be kept as low as possible in order to avoid aggregate and/or oligomer formation (high molecular weight species).

The conjugation method is, briefly, as follows. DFO (31mg/ml) and GLUT were mixed together at 4°C for 5 minutes and an aliquot of this solution was added to M8 in phosphate buffered saline (1-5 mg/ml). The mixture was incubated at 4°C for various times and the reaction quenched by adding 0.1M lysine. Unconjugated DFO was removed by extensive dialysis and gel chromatography. Labelling was carried out using Ga-67-citrate (Mallinckrodt).

The following parameters were studied in relation to labelling efficiency and high molecular weight species formation; a) GLUT:DFO molar ratios and mixture reaction time b) DFO:M8 molar ratios and mixture reaction time c) DFO/M8 reaction temperature d) M8 concentration and e) pH at time of labelling. Determination of labelling efficiency and high molecular weight species formation was performed using HPLC. A Zorbax GF-250 size exclusion column (molecular weight range 4,000 to 400,000 Daltons) and a mobile phase of 0.05M citrate/0.4M NaCl (pH 7.0) was used with a Gilson 302 HPLC pump and 111B UV flow monitor, at 280nm, connected to a strip chart recorder and a LKB 2112 fraction collector.

Our results show that HMW species formation decreased with 1) increasing DFO/M8 reaction time 2) decreasing DFO:M8 molar ratio and 3) increasing DFO:GLUT molar ratios. Labelling yield increased with increasing DFO:M8 molar ratio and increasing M8 concentration. A conjugate exhibiting high labelling yield (>90%) and low (<6%) HMW species formation has been achieved using a DFO:GLUT:M8 molar ratio of 500:150:1. Further details will be presented, including the affect of pH on labelling yield, in vivo stability data and gallium label distribution.

1. Rainsbury, R.M., Ott, R.J., Westwood, J.H., Kalirai, T.S., Coombes, R.C., McCready, V.R., Neville, A.M., Gazet, J.C., Lancet ii:934 (1983).
2. Haisma, H., Goedmans, W., DeJong, M., Hilkens, J., Hilgers, J., and DenOtter, W. Cancer Immunol. Immunother., 17, 62 (1984).
3. Sephton, R.G., and DeAbrew, S. Proc. Soc. Exp. Biol. Med., 161, 402 (1979).
4. Anderson, W.T., and Strand, M. Cancer Res., 45, 2154 (1985).

ENDOLABELING AND FRAGMENTATION OF MONOCLONAL ANTIBODIES AS RESEARCH TOOLS FOR KINETIC STUDIES

J. Shani, S. Mohd, W. Wolf, L.E. Walker and R.A. Reisfeld
Radiopharmacy Program, University of Southern California School of Pharmacy, Los Angeles, CA 90033, and Scripps Clinic and Research Foundation, La Jolla, CA 92037

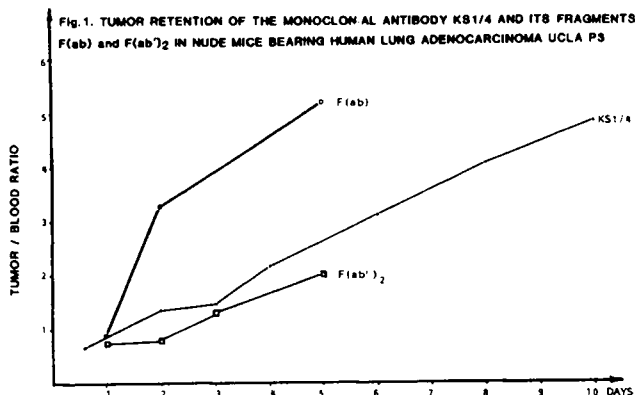
Two of us (LEW and RAR) have produced a panel of monoclonal antibodies (MoAbs) to human lung adenocarcinoma that demonstrate a high specificity for tumor cells and little, if any, reactivity with normal tissues (1). One of these monoclonal antibodies, KS1/4 reacts preferentially with an adenocarcinoma of the lungs and effectively inhibits the growth of tumors established in athymic (nu/nu) mice (2). This monoclonal antibody is an IgG2a isotype and reacts with a M_r 40,000 glycoprotein. In order to evaluate some of the key factors that may allow the optimization of radiolabeled monoclonal antibodies when used as diagnostic and therapeutic tools to detect and treat human neoplasia, we studied three approaches: (a) we compared the biodistribution of the anti-lung-tumor monoclonal antibody KS1/4, labeled with four different radionuclides, in athymic (nu/nu) mice bearing a human lung tumor; (b) we fragmented the MoAb KS1/4, labeled its two antigen-recognizing fragments and compared their biodistribution in the tumor-bearing mice and (c) set-up conditions for performing analyses that have to be considered when deciding which radionuclide should be chosen to label a given MoAb.

For studying the first approach, the following radionuclides were used: I-131, In-113m and In-111 exolabeling, and Se-75 endolabeling. The results of the localization of those labels of the intact MoAb KS1/4 in the tumored nude mice is shown in Table 1. When the mice were injected with the radioindium-labeled MoAb, both the tumor uptake and the tumor-to-blood ratio increased with time to a ratio of 4.8 at four days post injection (not shown in table). However, when the animals were treated with the iodinated MoAb, their tumors' uptake and the tumor-to-blood ratios decreased to unity approximately 60 hours after injection. High uptake of the label was also noticed in the mice treated with the Se-75-methionine labeled MoAb. However, the serum levels of the circulating MoAb were high, and therefore, even 48 hours after injection, the tumor-to-blood ratio of the intrinsically-labeled MoAb did not reach unity. Because of this, the rate of increase in uptake of the Se-75-methionine-labeled MoAb was much greater than that of the other MoAb labels. The tumor localization of the Se-75-methionine-labeled MoAb increased 8-fold over 48 hours, while that of the radioindium analog increased only 3-fold, and tumor localization of the radioiodinated compound decreased by 66%. A second injection of the In-labeled MoAb failed to increase the tumor-to-blood ratio. The 1.3-1.6-fold increase in the MoAb uptake by the tumor was negated by the corresponding 1.8-3.8-fold increase in the circulating levels of the label. The data presented in Table 1 suggest that, at least for the KS1/4 MoAb, radioiodination and intrinsic labeling with Se-75 methionine are the radiolabeling techniques of choice, since they allow attainment of the highest tumor retention, even though some loss of immunointegrity occurs following radioiodination (3).

TABLE 1. Comparative Biodistribution of KS1/4 Monoclonal Antibody Exolabeled with I-131, In-113m and In-111, or Endolabeled With Se-75, 48 h After Its Injection to Nude Mice Bearing Human Lung Adenocarcinoma UCLA P3 (results are % injected per gram; n=4).

	<u>I-131</u>	<u>In-113m</u>	<u>In-111</u>	<u>Se-75</u>
Blood	6.6	1.8	0.4	9.7
Tumor	7.6	1.7	0.8	5.3
Liver	7.1	16.4	7.2	4.4
Kidney	8.2	8.1	7.1	5.5
Spleen	6.2	3.8	4.2	2.7
Heart	4.0	0.7	0.4	2.5
Lungs	7.7	1.3	0.5	4.0
Stomach	2.1	0.3	0.1	0.8
Intestine	1.7	0.5	0.4	1.5
Muscle	1.4	0.4	0.2	1.1
Bone	1.2	0.7	0.6	2.0
Thyroid	8.1	-	-	2.7
Tumor/Blood	1.1	0.9	2.0	0.6

For the second approach, both fragments of KS1/4 were obtained: F(ab) by papain digestion and F(ab')₂ by the action of pepsin. The two fragments and the intact MoAb were conjugated to the bifunctional chelating agent DTPA and subsequently radiolabeled with In-111. Labeling yields and specific activities were determined as described in a previous paper from this laboratory (4), and the binding ability of the radiolabeled MoAb was evaluated utilizing the ELISA assay. The tumor-bearing nude mice were injected 200 μ l of about 100 μ Ci/ μ g of the MoAb-radionuclide conjugate, exhibiting over 95% labeling yield and over 90% immunointegrity. As seen from Figure 1, the retention of the labeled F(ab) fragment at five days post injection was about two-fold the retention of the intact KS1/4, and about three-fold than that of the F(ab')₂ fragment, suggesting that the penetrability of the small F(ab) fragment into the tumor is significantly more efficient than both other carriers - the F(ab')₂ and the intact MoAb.



For studying the third approach, a series of radiopharmacokinetic models have been formulated (5), where a computational method allows the determination of the model identifiability, given the outputs (measurements) to be collected. A simple analysis of structural identifiability determined that these models are observable, controllable and structurally identifiable, and therefore its parameters can be estimated from the data to be generated from the measured outputs. The most likely, general model to be tested is that represented in figure 2. Data required for testing the validity of this model include, other than the total radioactivity concentration in the whole body, the tumor, the liver and the urine, how much of the activity in the blood is that of the original antibody, how much is antigen conjugated, and how much is in the form of metabolites. Knowledge of the antibody's kinetic behaviour is critical in determining its most effective window and conditions of utilization, and how its biodistribution may be altered by proper kinetic manipulation.

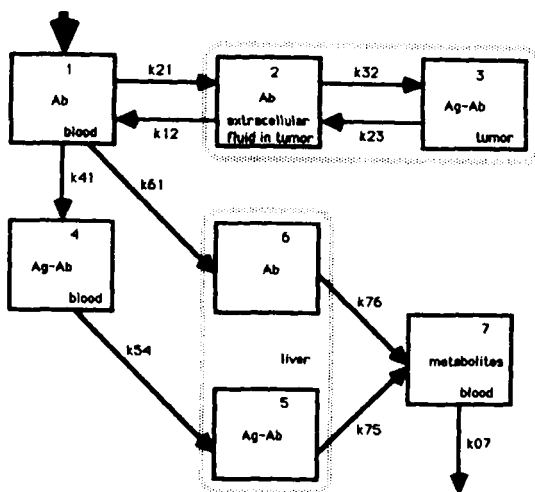


Fig. 2

Acknowledgements. This work has been supported in part by DOE grant DE-FG03-84-ER60219 to W.W. and NCI grant CA-34778 to L.E.W.

References:

1. Varki, N.M., Reisfeld, R.A. and Walker, L.E.: *Cancer Research* **44**, 681 (1984)
2. Varki, N.M., Reisfeld, R.A. and Walker, L.E. in *UCLA Symposia*, Park City, Utah, February 1985. *In Press* (1986)
3. Shani, J., Wolf, W., Chanachai, W., Mohd, S., Reisfeld, R.A., and Walker, L.E.: Labeling and comparative biodistribution of the monoclonal antibody KS1/4 in nude mice bearing human lung adenocarcinoma. *Inter. J. Nucl. Med. Biol.* *In Press* (1986)
4. Chanachai, W., Shani, J., Wolf, W., Harwig, J.F. and Nakamura, R.M., *Inter. J. Nucl. Med. Biol.* **12**, 289 (1985)
5. Wolf, W. and Shani, J.: Criteria for the selection of the most desirable radionuclide for radiolabeling MoAb. *Inter. J. Nucl. Med. Biol.* *In Press* (1986)

SCINTIGRAPHIC STUDIES AND IN VIVO DISTRIBUTION OF I-123-Fab OF ANTIMYOSIN ANTIBODY IN INFARCTED AND NORMAL DOGS. T.H. Lin, J.L. Wu, W. Hornoff*, B.W. Feldman, R.M. Baldwin, J.F. Lamb. Medi-Physics, Inc., Emeryville, CA and *University of California, Davis, CA.

The possibility of early scintigraphic detection of myocardial infarction using I-123 labeled fragments of anticardiac myosin antibody after intravenous injection was investigated in dogs.

Fragments of antimyosin antibody were labeled with I-123 using the Chloramine-T method. The viability of the I-123-Fab solution was shown by nearly quantitative trichloroacetic acid precipitation and high affinity toward canine myosin coated plate (80% binding).

The labeled antibody was administered i.v. to 1 normal dog and 2 dogs with induced myocardial infarcts. The initial scintigraphic images were that of blood pool. The activity cleared from the blood slowly such that about 27% and 10% of the initial activity in blood remained at 3 hr and 24 hr, respectively. The activity accumulated progressively in the kidneys during the first hour.

Tissue distribution study of I-123-Fab in infarcted dog at 3 and 24 hour showed that most of the activity was in the blood and viscera. Greater than 40% of the injected dose was excreted in the urine during 24 hours after injection. The ratio of the radioactivity in the center of the infarct to normal myocardium was 1.5 and 11 at 3 hr and 24 hr, respectively. The corresponding ratios for the center of infarct to blood were 0.5 and 1.8. A higher infarct to blood ratio is necessary for successful imaging of the infarcted tissue.

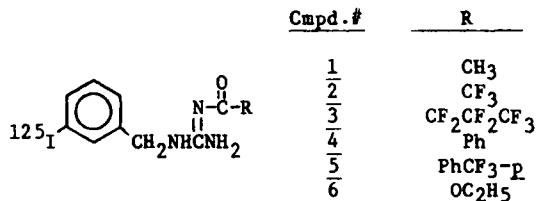
In conclusion, no infarcted myocardium was visible from the scintigrams at 3 and 24 hr after injection of I-123-Fab antimyosin. Low infarct to blood ratio, rapid and excessive in vivo deiodination, and high blood background were the possible causes of the lack of visualization of the infarct.

PROTRACERS FOR MAPPING CENTRAL CATECHOLAMINE STORES.

D.M. Wieland, T-Y. Lin, P. Arjunan, H. Lee, P.S. Sherman and S.J. Fisher.

University of Michigan Medical School, Ann Arbor, MI

Although radioiodinated *meta*-iodobenzylguanidine (MIBG) has been used to image peripheral organs and tumors based on its affinity for adrenergic neurons, application of MIBG to mapping central catecholamine stores is limited by its failure to pass the blood-brain barrier (BBB). We report here the synthesis of derivatives of MIBG that have lower pKa's and higher lipophilicities than MIBG itself. The goal was to have these derivatives serve as protracer forms that would enter the brain following i.v. injection and be quickly hydrolyzed to the parent tracer MIBG. I-125-MIBG in free base form was acylated with the appropriate anhydride, acid



chloride or ester to give 1-6. Tracers 2 and 4 exhibited 10-20 fold higher concentrations in the rat brain than MIBG 1-30 min after i.v. injection. In contrast to 4, compound 2 showed virtually no washout from the brain over the first 30 min suggesting hydrolysis to MIBG and subsequent trapping. The hydrolytic stability in phosphate (pH 7.1) buffered ethanol is $4 \gg 2$. Tracers 3 and 5, though highly lipophilic, gave low brain uptakes due likely to enhanced blood binding. These initial experiments show that a protracer form of MIBG can penetrate the BBB and that in certain cases (ie., 2) intra-brain hydrolysis may occur.

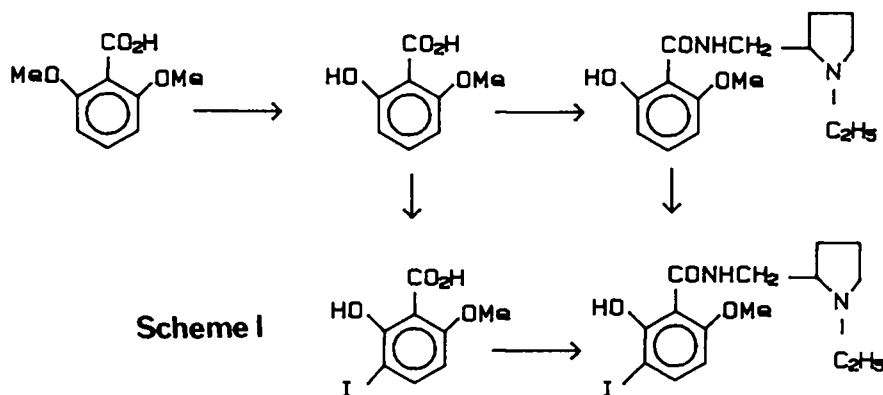
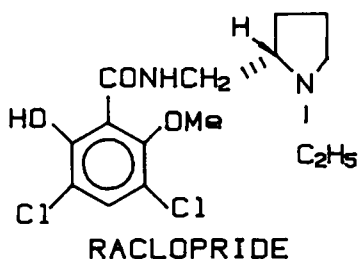
PREPARATION AND RADIOLABELING OF IBZM: A POTENTIAL D-2
SPECIFIC BRAIN IMAGING AGENTS FOR SPECT

HF Kung, X-J Xu, Y-Z. Guo.

Department of Nuclear Medicine, SUNY at Buffalo, USA

Recently, *in vivo* imaging of dopamine receptors in human brain using positron emission computed tomography (PET) has been reported. Two D-2 specific radiopharmaceuticals [^{11}C] N-methyl-spiperone¹ and [^{11}C] raclopride² have been employed for PET imaging. As expected these two agents showed specific concentration in basal ganglia, a region known to have high concentration of dopamine receptors. Raclopride has a higher selectivity and affinity for central D-2 receptors and negligible affinity for D-1, S-2 serotonin and alpha-1 adrenergic receptors³.

In developing new receptor-site specific brain imaging agents labeled with I-123 for single photon emission computed tomography (SPECT), an analog of raclopride, 3-[^{125}I]-iodo-N-[(1-ethyl-2-pyrrolidinyl)-methyl]-2-hydroxy-6-methoxybenzamide (IBZM), was prepared using a method similar to that reported for raclopride and its derivatives⁴. Monodemethylation of 2,6-dimethoxybenzoic acid by one equivalent of hydrobromic acid gave 6-methoxybenzoic acid. Subsequent iodination with iodine monochloride in glacial acetic acid produced 4-iodo-6-methoxysalicylic acid. Both of the iodinated and noniodinated benzoic acid derivatives can be transformed to the corresponding benzamide by an one pot reaction (Scheme 1).



Radioactive labeling of IBZM was accomplished by either a simple exchange reaction or by a chloramine-T method. The labeling yield of the exchange reaction was dependent on the reaction temperature, after heating for 2 hrs the labeling yield was 86, 73 and 59% for 100, 85 and 65 °C, respectively. An increasing quantity of impurity was produced during the exchange reaction, especially at lower pHs and after prolonged heating. When undiodinated IBZM was treated with a mixture of chloramine-T and I-125 sodium iodide, the labeling reaction was instantaneous. The reaction pH and the concentration of the oxidant, chloramine-T showed significant effect on the labeling yield. The optimal condition for labeling was at pH 2 and 20 ug of chloramine-T in 0.2 ml of buffer (labeling yield >90%). The major difference between these two labeling methods is the specific activity of the final product. The exchange reaction gives I-125 IBZM with lower specific activity, while the chloramine-T method can be used to prepared no carrier-added product. The desired product labeled by either methods can be purified by HPLC using a reverse-phase column and a acetonitrile-buffer solvent mixture (radiochemical purity >95%). Biodistribution of the carrier-free [¹²⁵I]-IBZM in rats showed good initial brain uptake and retention, total brain uptake was 3.8, 2.7 and 1.5 % dose at 2min 15min and 30 min, respectively. Autoradiographic studies of rat brain sections suggested that the agent localized in dopamine rich regions and the localization can be blocked by (+)-butaclamol, a dopamine blocker. When labeled with I-123, IBZM may be a useful agent for SPECT imaging of central dopamine receptors.

References

1. Wagner HN, Burns HD, Dannals RF, et al Science **222** 1264-1266, 1983.
2. Farde L, Ehrin E, Eriksson, et al Proc Natl Acad Sci USA **82**, 3863-3867, 1985.
3. Farde L, Hall H, Ehrin E, et al Science, **231**, 258-261, 1986.
4. de Paulis T, Kumar Y, Johnsson L, et al J Med Chem, **28**, 1263-1269, 1985.

NEW POTENT RADIOIODINATED LIGAND FOR DOPAMINE RECEPTOR STUDY :
SYNTHESIS AND IN VITRO EVALUATION.

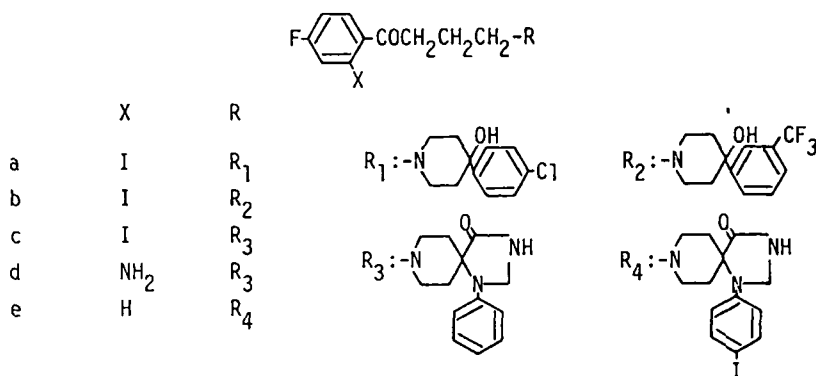
I.Nakatsuka, M.Okuno, A.Yoshitake, H.Saji* and A.Yokoyama*
Takarazuka Research Center, Sumitomo Chemical Co., Ltd.,
Takarazuka 665, *Faculty of Pharmaceutical Sciences and School of
Medicine, Kyoto University, Kyoto 606, Japan

Several neuropsychiatric diseases such as schizophrenia, Huntington's chorea and Parkinson's disease are thought to be associated with abnormalities of the dopamine receptor in the brain (1-3). There have been many attempts to develop radioligands labeled with positron emitters for the external detection of dopamine receptors in the brain (4-6). However, radioiodinated ligand constitutes nowadays a field of great interest as for dopamine receptor binding assay and ultimately as for the single photon emitting CT (SPECT) studies.

In a search for iodinated neuroleptic butyrophenones, various amino butyrophenones were synthesized from the cyclopropyl-phenyl ketone derivative via the reaction with benzylamine. Then, through diazonium intermediates, the iodination at ortho position was selectively carried out. The synthesized butyrophenone (a,b,c) were confirmed by IR, NMR and mass spectra.

A preliminary dopamine receptor affinity was measured from the ability to inhibit specific ^3H -spiroperidol (SP) binding to rat striatal membranes. Among the tested derivatives, only the 2'-iodospiroperidol (2'-ISP) (c) showed the highest affinity. In comparison with 4-iodospiroperidol (4-ISP) (e)*, which has been reported as a potent ligand for the dopamine receptor (7), 2'-ISP showed about 7 times more potency than that of 4-ISP (Table 1). Since binding of SP to the serotonin receptor has been also reported (8), interaction of 2'-ISP with serotonin receptor was examined by the in vitro binding assay using ^3H -ketanserin in the rat cortical membranes. 2'-ISP was found to have the lowest affinity among the tested compounds (Table 1). These results indicated the high affinity and high selectivity of 2'-ISP for the dopamine receptors, especially to the D-2 receptor.

Figure 1.



* Gift of NEN Products.

Table 1. K_i -values and Relative Affinities of The Iodinated Butyrophenones to The Dopamine and Serotonin Receptors

Compounds	Dopamine Receptor		Serotonin Receptor	
	K_i (nM)	%	K_i (nM)	%
Spiroperidol	0.300	100	0.300	100
Haloperidol	4.23	7.1	ND	ND
a	27.3	1.1	ND	ND
b	42.8	0.7	ND	ND
c	1.00	28	16.5	1.8
e	7.23	4.0	5.40	5.6

ND: non determined

Then, the radioiodination of 2'-ISP as for its utilization in receptor assay was carried out by radioisotopic exchange reaction with ^{125}I (specific activity : 25-30 Ci/mmol). Binding of ^{125}I -2'-ISP to rat striatal membranes was saturable and Scatchard analysis revealed a homogenous population of binding sites with an apparent dissociation constant (K_d) of 0.25 nM and a number of binding sites (B_{max}) of 210 fmol/mg protein.

In conclusion, among the tested compounds, the spirodecane containing butyrophenone derivative (c), the 2'-ISP showed the highest dopamine receptor affinity. Also, iodination through the diazonium intermediate yielded a highly selective introduction of the iodine in the ortho position, generating an appropriate, easy to radioiodinate ligand, for the in vitro dopamine D-2 receptor assay. This new ligand, 2'-ISP constitutes a very promising candidate for the in vivo dopamine receptor imaging, should the ^{123}I , becomes available (9).

1. Reisine T.D., Fields J.Z. and Yamamura H.I., *Life Sci.*, 21, 335 (1977)
2. Reisine T.D., Fields J.Z., Stern L.Z., et al., *ibid*, 21, 1123 (1977)
3. Lee I., Seeman P., Tourtelotte W., et al., *Nature*, 274, 897 (1978)
4. Welch M.J., Kilbourn M.R., Mathias C.J., et al., *Life Sci.*, 33, 1687 (1983)
5. Wagner H.N., Burns H.D., Dannals R.F., et al., *Sci.*, 221, 1264 (1983)
6. Farde L., Hall H., Ehrin E. and Sedvall G., *Sci.*, 231, 258 (1986)
7. Gundlach A.L., Largent B.L. and Snyder S.H., *Life Sci.*, 33, 1981 (1984)
8. Creese I. and Snyder S.H., *Eur. J. Pharmacol.*, 49, 201 (1978)
9. Saji H., Tokui T., Saiga A., et al., To be presented in this symposium.

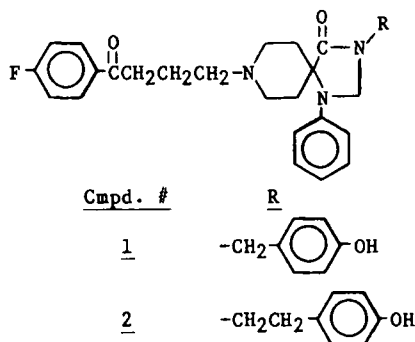
RADIOIODINATED N-PHENALKYLSPIPERONES FOR SPECT ANALYSIS OF DOPAMINE RECEPTORS

S.G. Mislankar, D.L. Gildersleeve, and D.M. Wieland

University of Michigan Medical Center, Ann Arbor, MI 48109

A number of laboratories have synthesized ^{18}F - and ^{11}C -labeled spiperone and spiperone analogs for possible use in quantifying dopamine receptor concentrations in the brain. To date a single photon emitting agent has not been developed for SPECT analysis of central D_2 receptors. Recently, photoaffinity probes derived from N-phenethyl derivatives of spiperone have been successfully used to characterize the D_2 receptor (1,2). This work has prompted us to evaluate N-phenalkyl substituents as possible platforms for incorporating ^{123}I into spiperone.

Compound 1 was synthesized by alkylation of the ethylene ketal of spiperone with p-methoxybenzyl bromide/NaH followed by simultaneous removal of the ethylene ketal and O-methyl group with BBr_3 . Compound 2 was obtained by alkylation of the ethylene ketal of spiperone with p-methoxyphenacylbromide/NaH, reduction of the keto function with hydrazine/ K_2CO_3 and removal of the protecting groups with BBr_3 . Compounds 1 and 2 were radiolabeled by reaction with $\text{NaI-}^{125}\text{I}$ and chloramine-T in



pH 7.0 phosphate buffer. Following extraction into ethyl ether, the compounds were purified by passage through silica SEP-PAK cartridges. Effective specific activities ranged from 20-40 Ci/mm; radiochemical yields were 50-70%. Radio-HPLC analysis of I-125-1 and I-125-2 was performed on an Ultrasphere silica column using $\text{CH}_2\text{Cl}_2/\text{CH}_3\text{OH}/\text{Et}_3\text{N}$ (975/25/0.2); radiochemical purities were > 95%. The D_2 receptor binding affinities and in vivo striatum-to-cerebellum concentration ratios of I-125 labeled 1 and 2 are presently being evaluated.

HPLC Data for Compounds 1 and 2*

Compound	t_R
<u>1</u>	11.5
I-125- <u>1</u>	10.9
<u>2</u>	12.7
I-125- <u>2</u>	9.9

*Flow rate: 1 ml/min; column size:

4.6 x 250 mm

1. Amlaiky, N., Kilpatrick, B.F., and Caron, M.G., FEBS Lett., 176, 436 (1984).
2. Amlaiky, N., and Caron, M.G., J. Biol. Chem., 266, 1983 (1985).

IN VIVO EVALUATION OF RADIOIODINATED SPIROPERIDOL DERIVATIVES AS RADIOPHARMACEUTICAL FOR DOPAMINE RECEPTOR STUDY.

H.Saji, T.Tokui, A.Saiga, Y.Kuge, I.Nakatsuka*, M.Okuno*, A.Yoshitake*, K.Torizuka, and A.Yokoyama.

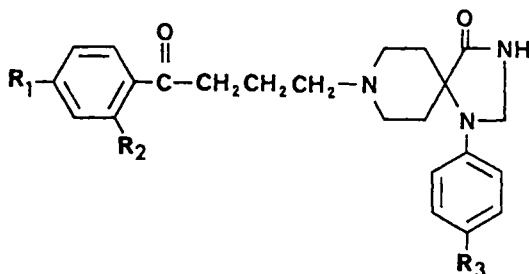
Faculty of Pharmaceutical Sciences and School of Medicine, Kyoto University, Kyoto 606, *Takarazuka Research Center, Sumitomo Chemical Co., Ltd., Takarazuka 665, Japan.

The usefulness of ^{11}C and ^{18}F labeled butyrophenone neuroleptic drugs for the detection of dopamine receptors is at present a field of great interest (1-4). Being aware of the prompt availability of ^{123}I , our effort was directed to the development of iodinated dopamine receptor binding butyrophenones. Among various iodinated butyrophenones synthesized, 2'-iodospiroperidol (2'-ISP) has shown in vitro, high binding affinity for cerebral striatal dopamine receptors, as described elsewhere (5). This very interesting in vitro result called for an in vivo evaluation of 2'-ISP as a dopamine receptor imaging radiopharmaceutical and for a in vivo study on the validity of iodination at ortho position of the phenyl ring of butyrophenone group in its dopamine receptor binding. In the present work, biodistribution of 2'-ISP in various regions of the brain was screened by comparative studies with an iodinated derivative in N-phenyl ring of spirodecane group (4-iodospiroperidol(4-ISP)) and with an iodinated derivative at the para position of the phenyl ring of the butyrophenone (4'-iodospiroperidol(4'-ISP)). Paralleled study of saturability and affinity were also carried out.

The labeling of ^{125}I -2'-ISP was carried out by radioiodine exchange reaction; that of ^{125}I -4'-ISP, by acid decomposition of aryl piperidine triazene. ^{125}I -4-ISP was purchased from NEN Products.

ISP, appears as offering the requisites for a dopamine receptor radiopharmaceutical to be used in SPECT studies, provided the ^{123}I becomes readily available. The effect of iodination at ortho position of butyrophenone phenyl ring is discussed as the plausible cause for less alteration in the in vivo dopamine receptor binding environment.

Figure 1.



	R ₁	R ₂	R ₃
2'-Iodospiroperidol	F	I	H
4-Iodospiroperidol	F	H	I
4'-Iodospiroperidol	I	H	H

The radioactivities accumulated in various regions of the mouse brain after intravenous injection of these three compounds, are shown in Fig.2. Although ^{125}I -4'-ISP accumulated in the striatum at the initial stage, its radioactivity cleared rapidly as in the cerebral cortex and the cerebellum. By contrast, both ^{125}I -2'-ISP and ^{125}I -4-ISP showed specific regional localization: high radioactivity concentration in the striatum and low concentration in the cerebral cortex and the cerebellum. However, striatal uptake of ^{125}I -2'-ISP was found to be greater than that of ^{125}I -4-ISP. Therefore, the striatum to cerebellum ratio and the relative in vivo affinity for dopaminergic binding of ^{125}I -2'-ISP was substantially higher than that for ^{125}I -4-ISP. In the autoradiographic studies, regional localization of ^{125}I -2'-ISP in brain was well comparable with ^3H -spiroperidol.

Furthermore, striatal binding of 2'-ISP was saturable and displaced by the administration of spiroperidol, haloperidol and (+)-butaclamol, potent antagonists, but unaffected by (-)-butaclamol, a drug without dopamine receptor activity.

Thus, in vivo results assessed the in vitro dopamine binding affinity data. The relative in vivo affinity reached by ^{125}I -2'-

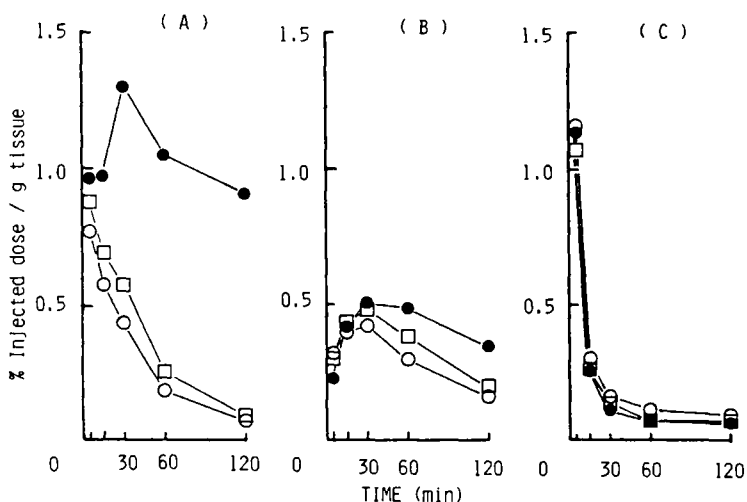


Figure 2. Distribution time-course of ^{125}I labeled iodinated spiroperidol derivatives in striatum, cerebral cortex and cerebellum.

A: [^{125}I]-2'-Iodospiroperidol ●: Striatum
 B: [^{125}I]-4-Iodospiroperidol □: Cortex
 C: [^{125}I]-4'-Iodospiroperidol ○: Cerebellum

1. Welch M.J., Kilbourn M.R., Mathias C.J., et al., Life Sci., 33, 1687 (1983)
2. Wagner H.N., Burns H.D., Dannals R.F., et al., Science, 221, 1264 (1983)
3. Arnett C.D., Fowler J.S., Wolf A.P., et al., Life Sci., 36, 1359 (1985)
4. Arnett C.D., Shiu C.Y., Wolf A.P., et al., J. Neurochem., 44, 835 (1985)
5. Nakatsuka I., Okuno M., A.Yoshitake, Saji H. and Yokoyama A., To be presented in this symposium.

STUDIES ON THE CHEMISTRY OF TECHNETIUM HM-PAO

L.R. Canning, G. Nechvatal, I.M. Piper, D.P. Nowotnik, B. Higley, A.M. Forster and R.D. Neirinckx.

Pharmaceuticals Development, Amersham International, Amersham, Buckinghamshire, England.

From a research program which involved the synthesis and evaluation of over 100 derivatives of the ligand PnAO (1), Tc99m HM-PAO was selected as the agent of choice for rCBF imaging (2). Separation of HM-PAO into the meso and d,l-diastereoisomers and to the d- and l-enantiomers was achieved by standard methods.

Tc99m labelling of each of the stereoisomers was achieved using freeze dried formulations of the ligand and a stannous salt.

Biodistribution studies in rats have shown that each diastereoisomer complex has similar brain uptake (~2.3% id at 30 sec pi), but retention in the brain varies considerably, with dl > meso. In preliminary clinical studies (3) the superiority of the d,l-diastereoisomer was confirmed. This complex displayed good uptake and retention in brain, and provided high quality tomographic images. d,l HM-PAO was selected for further clinical trials.

It was observed that the lipophilic Tc99m complex of d,l-HM-PAO converts in vitro to a more hydrophilic complex. It has been proposed (4) that this secondary complex results from isomerisation of the oxime groups in the lipophilic complex. Formation of the lipophilic Tc99m complex of d,l-HM-PAO requires the oxime groups to adopt the E,E-configuration. While this is the most favoured orientation of the oximes of the ligand in solution, isomerisation to the E,Z and Z,Z forms has been observed. The E,Z oxime isomer was isolated by HPLC, and labelled with Tc99m. This complex was shown by chromatography, to convert slowly to the E,E-oxime isomer complex. Thus, it appears unlikely that the secondary complex of Tc99m d,l-HM-PAO results from oxime isomerisation as thought previously.

1. Cumming, S.A. Nechvatal, G., Canning, L.R. et al., Eur.J.Nucl.Med., 11, A5, 1985.
2. Nowotnik, D.P., Canning, L.R., Cumming, S.A., et al., Nucl.Med.Comm., 6, 499-506, 1985.
3. Sharp, P.F., Smith, F.W., Gemmell, H.G., et al., J.Nucl.Chem., 27, 171-177, 1986.
4. Nowotnik, D.P., Canning, L.R., Cumming, S.A., et al., J.Nucl.Med.Allied.Sci., 29, 209, 1985.

REGIONAL CEREBRAL UPTAKE OF Tc-99m-d,l-HM-PAO COMPARED TO OTHER rCBF TRACERS

W. A. Volkerl, T. J. Hoffman, E. H. McKenzie, R. A. Holmes, D. P. Nowotnik* and R. D. Neirinckx*

Department of Radiology, University of Missouri and Research Service, H. S. Truman Veterans Hospital, Columbia, MO and Amersham International*, UK

Tc-99m forms a neutral-lipophilic chelate with d,l-4,8-diaza-3,6,6,9-tetramethylundecane-2,10-dione bis oxime (d,l-HM-PAO) that has excellent cerebral uptake and retention properties [1,2]. Studies in humans and animals suggest that the regional cerebral uptake (rCU) of Tc-99m-d,l-HM-PAO is proportional to the regional cerebral blood flow (rCBF) and that there is minimal intracerebral redistribution [1,2]. For this reason, this chelate is being used in conjunction with SPECT to evaluate patients with rCBF disorders. The applicability of this chelate as an rCBF agent must, however, be evaluated further. For this reason, the rCU of Tc-99m-d,l-HM-PAO was compared to three other tracers commonly used to assess rCBF in laboratory animals.

The rCU of two tracers (C-14-iodo-antipyrine or C-14-IAP and I-125-N-isopropylidoamphetamine or I-125-IMP) were compared with Tc-99m-d,l-HM-PAO using dual-isotope autoradiography (ARG). Tc-99m-d,l-HM-PAO was made using a freeze-dried kit.* Paper and TLC chromatography were performed immediately prior to administration to insure that the radiochemical purity of the lipophilic chelate was >90%. Anesthetized Sprague-Dawley rats (50 mg/kg Na-pentobarbital, ip) were injected with 1 ml of saline containing Tc-99m-d,l-HM-PAO and either C-14-IAP or I-125-IMP). The blood flow to the brain was stopped at either 15 sec or at 60 min PI (only with I-125-IMP), the brains were removed and frozen in liquid nitrogen and 20 micron thick sections were obtained at -24C. The sections were air dried and placed on DuPont MRF 31 CT film (18-24 hr for Tc-99m and subsequently 10-14 days for C-14 or I-125) for development of the ARGs.

Visual comparison of the digitized images in Figure 1 shows that the initial brain uptake pattern of Tc-99m-d,l-HM-PAO is similar to C-14-IAP at 15 sec PI. In both cases, grey matter contains the highest activity of the tracers and this is most pronounced in the auditory cortex and the nuclei of the auditory and visual pathways in the pons, midbrain and thalamus which are structures with high flow in the rat [3]. The Tc-99m chelate exhibits considerable sub-structural detail while C-14-IAP exhibits a more diffuse pattern of uptake which must be due to the diffusability of C-14-IAP in brain. These data provide evidence that the rCU of Tc-99m-d,l-HM-PAO is related to rCBF.

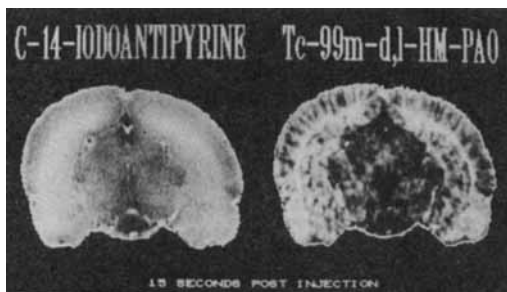


Figure 1. Dual isotope ARG study showing digitized images of rCU of C-14-IAP and Tc-99m-d,l-HM-PAO in same rat brain section.

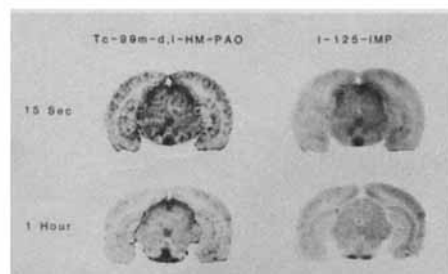


Figure 2. Dual isotope ARG showing rCU of tracers in sections of rat brain at 15 sec and 1 hr.

*Ceretek, Amersham International

Table 1. Tc-99m-d,l-HM-PAO to Sn-113 microsphere uptake ratios in localized regions in the brain of anesthetized rabbits.

	<u>5 Minutes Post Injection</u>		<u>1 Hour Post Injection</u>	
	<u>Tc-99m/Sn-113m</u> <u>Ratio</u>	<u>Flow Range In</u> <u>ML/Min/</u> <u>100 gm Tissue</u>	<u>Tc-99m/Sn-113m</u> <u>Ratio</u>	<u>Flow Range In</u> <u>ML/Min/</u> <u>100 gm -Tissue</u>
	<u>MEAN±S.D.</u> <u>(RANGE)</u>		<u>MEAN±S.D.</u> <u>(RANGE)</u>	
CEREBRUM	.935±.123 (.800-1.200)	23.0 -183.5	.818±.094 (.700-1.020)	52.7 - 203.9
GREY MATTER	1.001±.212 (.720-1.290)	32.3 -256.1	.967±.112 (.790-1.090)	58.6 - 259.4
WHITE MATTER	1.522±.589 (.620-2.390)	14.9 -57.6	1.194±.291 (.830-1.710)	26.2 - 113.1
DIENCEPHALON	1.120±.361 (.640-1.660)	17.4 -200.7	1.065±.223 (.770-1.560)	28.6 - 145.4
PONS	1.366±.282 (.930-1.830)	14.1 -139.2	1.115±.201 (.900-1.580)	25.7 - 140.5
MEDULLA	1.729±.601 (.900-2.570)	13.9 -118.3	1.265±.201 (.890-1.620)	26.9 - 95.9
MIDBRAIN	1.074±.078 (.820-1.370)	39.5 -190.4	.967±.196 (.680-1.400)	52.1 - 158.8
CEREBELLUM	1.072±.178 (.960-1.180)	19.8 -148.0	.964±.085 (.850-1.070)	47.1 - 138.2

The rCU of I-125-IMP at 15 sec PI is also qualitatively similar to that observed with Tc-99m-d,l-HM-PAO (Figure 2). The sub-structural detail with this Tc-99m-chelate is superior to the I-125 amine. The Tc-99m-d,l-HM-PAO ARG at 60 min PI shows little change (other than the later image has a lower exposure) from the 15 sec PI ARG indicating minimal movement or clearance of Tc-99m-activity from the initial sites of uptake (Figure 2). In contrast, the later I-125-IMP ARG has undergone noticeable changes when compared to the early image. These results are consistent with other findings that demonstrate significant intracerebral redistribution of this I-125-amine by 60 min PI [4,5]. Sn-113 microspheres (15 ± 0.9 microns) with Tc-99m-d,l-HM-PAO were injected into the left-ventricle of anesthetized rabbits (via a left carotid cannula). Blood samples were obtained from a femoral artery during injection for use in calculating the blood flow in each weighed tissue sample. Sections of the brains excised from the rabbits (n=5 in each group) weighed and counted (for both isotopes). Tc-99m-d,l-HM-PAO/Sn-113m microsphere ratios were obtained for 8 discrete cerebral tissue samples by first normalizing the total Tc-99m-d,l-HM-PAO cerebral uptake to the uptake of Sn-

113m microspheres. Subsequently, paired samples of cerebrum, grey matter, white matter, diencephalon, pons, medulla, midbrain, and cerebellum were counted to determine individual Tc-99m-d,l-HM-PAO/Sn-113m microsphere ratios (See Table 1). Pure grey matter tissue samples obtained over a wide flow range correlated well with microsphere deposition at both 5 minutes and 1 hour P.I., while pure white matter tissue samples revealed a higher uptake of Tc-99m-d,l-HM-PAO compared to microspheres at both 5 minutes and 1 hour P.I. The statistical variability in the ratios in tissues with a high white matter content are large, particularly in the 5 min P.I. data, which is in part due to the low weights of the tissue sections. The overall weighted Tc-99m-d,l-HM-PAO/Sn-113m microsphere mean ratios are 1.06 at 5 min P.I. and 0.93 at 1 hour P.I. (Weighting Factor = Tissue Sample Weight). This data indicates that although uptake of Tc-99m-d,l-HM-PAO in white matter tends to be an overestimation of microsphere deposition, there is a high overall correlation of Tc-99m-d,l-HM-PAO uptake to microsphere deposition (or rCBF) at both 5 min and 1 hour P.I.

In summary, the rCU of Tc-99m-d,l-HM-PAO correlates well with the rCU of both C-14-IAP and I-125-IMP at 15 sec P.I. The ARG study shows minimal intracerebral redistribution of Tc-99m-d,l-HM-PAO at 1 hr P.I. while there are observable changes in rCU of I-125-IMP at 1 hr P.I. There is a good correlation of rCU of Tc-99m-d,l-HM-PAO with Sn-113m-microsphere deposition in cerebral tissues at both 5 min and 1 hr P.I. The results using these techniques indicate that the rCU of Tc-99m-d,l-HM-PAO correlates well with rCBF both shortly after injection and at 1 hr P.I.

References

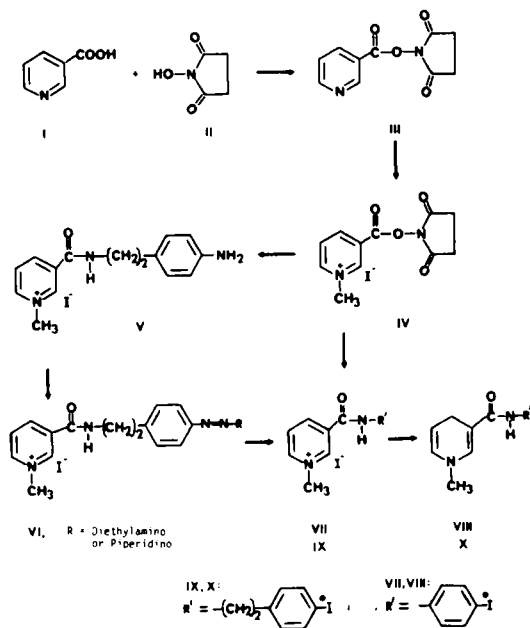
1. Holmes, R.A., J. Nucl. Med., 27, 299, 1986.
2. Sharp, P. F., Smith, F. W., Gemmell, H. G., Lyall, D., Evans, N.T.S., Gvozdanovic, D., Davidson, J., Tyrrell, D. a., Pickett, R. D., Neirinckx, R. D., J. Nucl. Med., 27:2:171, 1986.
3. Sakurada, O., Kennedy, C., Jehle, J., Brown, J. D., Corbin, G. L. and Sokoloff, L., Am. J. Physiol. 238, H776, 1980.
4. Rapir, J. R., LePoncin-Lafitte, M., Duterte, D., Rips, r., Morier, E. and Lassen, N. A., J. Cereb. Blood Flow Metab., 4, 270, 1984.
5. Crentzig, H., Schober, O., Gielow, P., Freidrich, R., Becker, H., Dietz, H., and Hundeshagen, H., J. Nucl. Med., 27, 178, 1986.

DESIGN, SYNTHESIS AND EVALUATION OF REDOX RADIOPHARMACEUTICALS: A POTENTIAL NEW APPROACH FOR THE DEVELOPMENT OF BRAIN IMAGING AGENTS P. C. Srivastava and F. F. Knapp, Jr., Nuclear Medicine Group, Oak Ridge National Laboratory, Oak Ridge, TN 37831, USA.

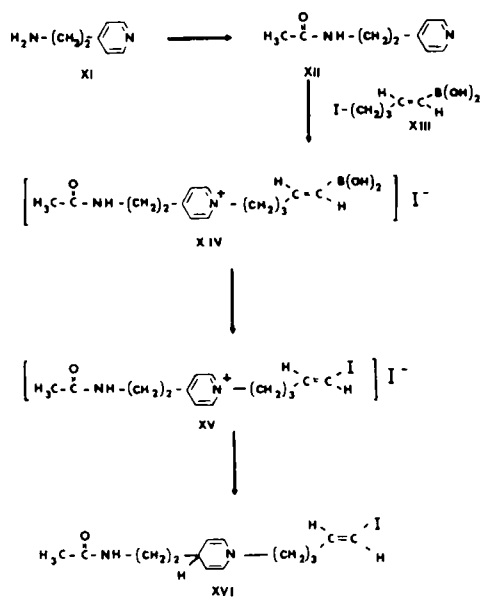
^{123}I -labeled lipophilic radiopharmaceuticals which cross the intact blood-brain barrier and mimic regional blood flow (1) can potentially be used for scanning brain lesions by either planar or single photon computerized tomographic (SPECT) techniques (2). The strategies that have been pursued to develop brain imaging agents include the screening of a variety of radioiodinated amphetamines (3) resulting in the development of p -[^{123}I]iodo- N -isopropylamphetamine (IMP) for SPECT studies in humans (4), and "pH shift" agents (5) resulting in the development of N,N,N' -trimethyl- N' -[2-hydroxy-3-methyl-[^{123}I]iodobenzyl]-1,3-propanediamine (HIPDM) which also shows excellent properties in human studies (6). Other promising recent advances in this area include the development of p -[^{123}I]iodophentertine (7), radioiodinated piperazine analogues (8), and ^{201}Tl complex of diethyldithiocarbamic acid (9) as potential brain imaging agents.

The goals of this paper are to describe the fabrication (Scheme I) and complete evaluation of a dihydropyridine \rightleftharpoons pyridinium salt type redox system (10) for the delivery of radioiodinated agents to the brain. The work in part has been described recently (11). For preliminary evaluation, the pivotal intermediate, N -succinimidyl (1-methylpyridinium iodide)-3-carboxylate (IV) was prepared by condensation of nicotinic acid (I) and N -hydroxysuccinimide (II) in the presence of dicyclohexylcarbodiimide, followed by quaternization of III with methyl iodide. Coupling of IV with 4-[^{125}I]iodoaniline, prepared by ^{125}I - I_2 treatment of 4-aminophenylmercuric acetate, gave 1-methyl-3-[N -(4-iodophenyl)carbamoyl]-pyridinium iodide (VII) which after sodium dithionite reduction gave 1-methyl-3-[N -(4-iodophenyl)carbamoyl]-1,4-dihydropyridine (VIII). Compound IV was also coupled with (4-aminophenyl)ethylamine to give V which was diazotized and sequentially transformed into triazines VI, 1-methyl-3-[N -[β -(4-[^{125}I]iodophenyl)ethyl]carbamoyl]pyridinium iodide (IX) and 1-methyl-3-[N -[β -(4-[^{125}I]iodophenyl)ethyl]carbamoyl]-1,4-dihydropyridine (X) (Scheme I). Compounds, 1-(E -1-[^{125}I]iodo-1-penten-5-yl)-4-(2- N -acetylaminoethyl)pyridinium iodide (XV) and 1-(E -1-[^{125}I]iodo-1-penten-5yl)-4-(2- N -acetylaminoethyl)-1,4-dihydropyridine (XVI), were also prepared via the synthesis and $\text{Na}[^{125}\text{I}]$ -chloramine-T iodination of XIV as shown in Scheme II in order to determine the relative redox properties and brain specificities of new structurally modified dihydropyridine \rightleftharpoons pyridinium agents.

Tissue distribution studies of ^{125}I -labeled 4-iodoaniline and the redox agents were performed in rats. [^{125}I]Iodoaniline initially showed moderate (0.58% dose/gm) brain uptake with subsequent release of the radioactivity from the brain. [^{125}I]Iodoaniline, however, when coupled to a dihydropyridine carrier (VIII) showed significantly higher (>1% dose/gm) uptake and retention in the brain (Fig. 1). The [^{125}I]iodophenylethyl analogue X showed uptake (>1% dose/gm) and retention in the brain very similar to VIII. Apparently the lipophilic agents, VIII and X, cross the blood-brain barrier and are oxidized (quaternized) within the brain. The blood-brain barrier then prevents their release resulting in high uptake and retention in the brain and high brain: blood ratios (Fig. 2). The nonlipophilic quaternary compounds VII and IX do not cross the blood-brain barrier and, therefore, do not show brain uptake. Compound XVI showed initial moderate (0.49% dose/gm) brain uptake and quick washout from the brain. The differences in the properties of XVI as compared to VIII and X could apparently be due to the different structural features and inability of XVI to undergo facile oxidation in the brain.



Scheme I



Scheme II

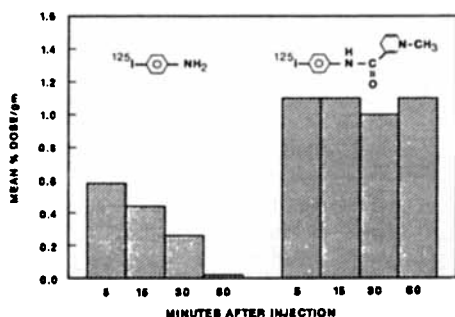


Fig. 1. Dihydropyridine coupled 4-[¹²⁵I]-iodoaniline agent (VIII) shows significantly higher uptake and retention in the brain as compared to the parent 4-[¹²⁵I]-iodoaniline independently. Agent X shows properties similar to VIII.

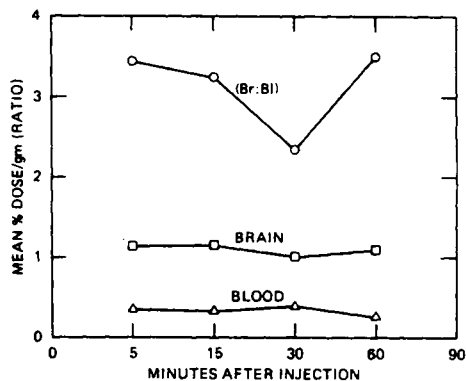


Fig. 2. High uptake and retention in the brain and low blood levels of VIII result in high brain:blood ratios. Agents VIII and X show similar properties.

Research supported by the Office of Health and Environmental Research, U.S. Department of Energy, under contract DE-AC05-84OR21400 with Martin Marietta Energy Systems, Inc.

1. Oldendorf, W. H., *Proc. Soc. Exp. Biol. Med.*, **19**, 1182 (1974).
2. Budinger, T. F., *J. Nucl. Med.*, **21**, 279 (1980).
3. Winchell, H. S., Baldwin, R. M., Lin, T. H., *J. Nucl. Med.*, **21**, 940 (1982).
4. Kuhl, D. E., Barrio, J. R., Huang, S. C., Selin, C., Ackerman, R. F., Lear, J. L., Wu, J. L., Lin, T. H., Phelps, M. E., *J. Nucl. Med.*, **23**, 196 (1982).
5. Kung, H. F., Blau, M., *J. Nucl. Med.*, **21**, 147 (1980a).
6. Polak, J. F., Holman, B. L., Moretti, J. L., Eisner, R. C., Lister-James, J., English, R. J., *J. Nucl. Med.*, **25**, 495 (1984).
7. Elmaleh, D. R., Kuzuka, H., Boudreaux, G., Hanson, R. N., *Proceedings of the 5th International Radiopharmaceutical Chemistry Symposium, Tokyo, Japan, July 1984. J. Lab. Compds. and Radiopharm.* **XXI**, p. 88, 1078 (1984).
8. Hanson, R. N., El-Shounbagy, T., Hasson, M., *Proceedings of the 5th International Radiopharmaceutical Chemistry Symposium, Tokyo, Japan, July 1984. J. Lab. Compds. and Radiopharm.* **XXI**, p. 92 (1984).
9. Vyth, A., Fennema, P. J., van der Schoot, J. B., *Pharm. Weekblad Sci. Ed.*, **5**, 213 (1983).
10. Bodor, N. J., Simpkins, W., *Science*, **221**, 65 (1983).
11. Tedjamulia, M. L., Srivastava, P. C., Knapp, F. F. Jr., *J. Med. Chem.*, **28**, 1574 (1985).

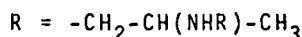
BRAIN AFFINITY OF THE RUTHENOCENE ANALOGUE OF AMPHETAMINE
LABELLED WITH γ -EMITTERS

M. Wenzel and D. Preiss

Freie Universität Berlin, Pharmazeutisches Institut,
 Berlin-Dahlem, Königin-Luise-Str. 2+4, (Germany)

In nuclear medicine there is a great demand for compounds labelled with short lived γ -emitters which have an affinity for the living human brain. For brain imaging iodo labelled amphetamine derivatives are used, e.g. p-Iodo-isopropyl-amphetamine (1,2), although there are significant drawbacks of the radioisotopes of iodine (3).

The paper describes the synthesis and the organ distribution of amphetamine analogues substituted ruthenocenes (Rc) derived from the structure:



Ruthenocene analogues of amphetamine

The ruthenocene amphetamine analogues were labelled with Ru-103 (4,5) starting from the analogous ferrocene compounds. The ferrocene compound was prepared by the condensation of ferrocene carboxaldehyde and nitroethane following by the reduction of the intermediate to ferrocenyl-isopropylamine. The iron was replaced by Ru-103 by a standard procedure (6,7). The labelled ruthenocene amphetamines were separated from by-products by thin layer-chromatography, yielding the pure metallocene amphetamine (mixture of ruthenocene and ferrocene compound, which have almost the same R_f-values), Radiochemical yield ~ 20-30 %. Spec. act. ~100 μ Ci/ μ Mol ruthenocene.

In Table 1 the organ distribution in rats of the Ru-103 labelled ruthenocene amphetamine analogue is summarized. The organs with the highest Ru-103 concentration are lung, adrenal, kidney and brain. The Ru-103 concentration in brain peaked between 3,5-2,5 %/% body weight. The background radioactivity resulting mainly from the blood, decreases quicker than the radioactivity in the above mentioned organs. The concentration ratios organ/blood in rats are reaching ratios for the brain up to 19:1, 20' after i.v. injection of N-isopropyl-Rc-amphetamine. The brain/blood ratios with ruthenocene derivative are the same or greater than that reported for the iodo-labelled amphetamine derivatives (maximal brain/blood ratio in rats for I-123 N-isopropyl-amphetamine according to Biersack (2) 9:1 (n=5) and Winchell (1) 20:1 (n=2)). Therefore the Ru-103 labelled ruthenocene amphetamine derivatives show a higher brain index than iodo labelled amphetamines.

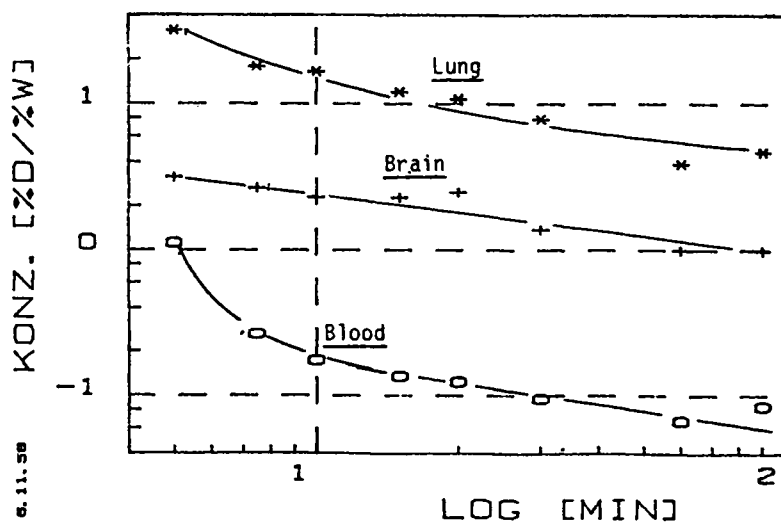
Tab. Organ-Distribution of ^{103}Ru -labelled Ruthenocene-Amphetamines

5 Mice or 4 rats received $1\ \mu\text{Mol/kg}$ of the labelled ruthenocene compound i.v.. After 15 min. the animals were killed; weight and ^{103}Ru -activity of the different organs determined (7).

$\bar{x} + \sigma$; M = Mice K = Rats.

Ruthenocene-Derivatives	^{103}Ru -Conc. [% injected dose/%weight] x 100										Ratio		
	Muscle	Blood	Lung	Liver	Kidney	Adrenal	Brain	Brain Blood	Lung Blood				
Rc- $\text{CH}_2\text{-CH}(\text{NH}_2)\text{-CH}_3$	M	87±20	46±7	1033±414	316±57	906±69	-	248±47				5,4	22,5
	R	58±17	17±3	1434±380	146±380	146±62	529±67	197±73				11,6	84
N-methyl-	M	64±10	35±15	737±169	341±92	857±62	210±54	220±54				6,3	21,1
	R	50±8	18±1	902±157	172±82	652±169	471±60	228±63				12,7	50
N,N-dimethyl-	M	60±14	26±5	436±120	253±179	632±49	781±188	271±27				10,4	16,8
	R	49±10	19±4	860±289	170±26	822±139	575±148	219±49				11,5	45,2
N-isopropyl-	M	62±12	33±7	645±111	337±36	816±179	1052±256	190±11				5,8	19,5
	R	42±18	15±6	1224±553	157±91	780±142	884±155	205±49				13,7	82
Rc- $\text{CH}_2\text{-CH}(\text{NH}_2)\text{-C}_2\text{H}_5$	M	64±7	74±17	712±76	449±21	588±14	845±136	184±6				2,5	9,6
	R	69±9	27±9	1675±389	170±55	640±108	866±330	222±35				8,2	62

Fig. Concentration of N-isopropyl-Rc-amphetamin in Rats



Literature:

1. Winchell, J., Baldwin, R.M. and Lin, T.H.,
J.Nucl.Med. 21, 940 (1980)
2. Biersack, H.J., Zschachlitz, L., Klüenberg, H.,
Breulel, H.P., Oehr, P. and Winkler, C.,
Nuc Compact 15, 13 (1984)
3. Bremer, K.H. and Kloss, G.,
in Nuklearmedizin, Funktionsdiagnostik und Therapie
(1979) p. 65 Georg Thieme Verlag Stuttgart
4. Hanzlik, R.P. and Kishore, V.,
Xenobiotica 8, 753 (1978)
5. Wenzel, M. and Preiss, S.,
Fortschr. Röntgenstr. 144, 105 (1986)
6. Langheim, D., Wenzel, M. and Nipper, E.,
Chem.Ber. 108, 146 (1975)
7. Schneider, M. and Wenzel, M.,
J.Labelled Comp. Radiopharmaceuticals 19, 625 (1981)

THE CYCLOTRON PRODUCTION OF SHORT HALF-LIVED RADIOACTIVE NOBLE GASES FOR BIO-MEDICAL USE

J.R. Dahl, W.G. Myers, M.C. Graham

Biophysics Laboratory, Memorial Sloan-Kettering Cancer Center, 1275 York Ave., New York, New York 10021

We present a general method for the preparation of ^{19}Ne , ^{79}Kr , and ^{127}Xe . Radioisotopes of the noble gases have been used for bio-medical studies for many years. For instance, ^{133}Xe has been used for cerebral blood flow studies(1) and for lung function studies(2), ^{127}Xe and ^{81}Kr have been used for the evaluation of pulmonary disease(3), ^{81}Kr has been used for ventilation studies, and ^{19}Ne has been proposed as a tracer for the determination of region cerebral blood flow(4). Table 1 presents a survey of the very short-lived noble gases and of the principal advantages and disadvantages of each. The commonly used, longer lived, radioactive noble gases are commercially available. The increasing number of small medical cyclotrons may provide the opportunity to utilize the advantages of routine, on-line availability, improved image quality, and the shorter half-lives offered by very short-lived noble gases in studies deriving from established Nuclear Medicine procedures.

TABLE 1.
SOME PROPERTIES OF THE VERY SHORT-LIVED NOBLE GASES

NUCLIDE	HALF-LIFE (seconds)	DECAY MODE	GAMMA ENERGY (keV)	GAMMA ABUNDANCE (photons out per 100 decays)
^{19}Ne	17.5	positron	511 anhil	200
^{79}Kr	50	IT	130	27
^{127}Xe	69	IT	125 173	68 35

The method we have developed consists in the proton bombardment of nearly saturated solutions of the appropriate alkali metal halide in a target chamber which allows the solution to be sparged with helium gas during bombardment. The target solution (50ml) is contained in a recess 1.27cm thick on the beam axis and 5cm diameter, with access passages at the top and bottom, in a titanium plate. The target chamber is a modified version of one previously used for ^{18}F and ^{13}N production(5). As the helium sweeps upward through the target solution, it removes the very short-lived noble gas as it is formed. A glass adapter on top of the target chamber removes most of the target solution from the sweep gas stream. Aerosols and radiolysis products are removed from the stream of helium containing the radioactive noble gas by a tube containing NaOH pellets placed in the gas line immediately after the adapter on the top of the target chamber. From the target chamber the sweep gas flows through about 18 M of 1.5mm ID teflon tube to apparatus for quality control analysis and mixing with air for breathing and oxygen before transmission to the scanning suite. A measure of the radiochemical purity of the very short-lived noble gas was made by trapping 125ml of the sweep gas in a bottle and observing its gamma spectrum with a Ge(Li) detector coupled to a 1024 channel analyzer or by measuring the half-life of the radioactivity when the bottle was placed in an ionization chamber.

The (p,n) production reaction was used in all of the preparations. Target solutions were prepared by diluting saturated alkali metal

halide solutions (9 parts) with de-ionized water (one part). Other activities generated in the target solution, notably ^{13}N , were not carried beyond the NaOH trap by the helium sweep gas. Strong oxidizing species were generated rapidly in the target solution and presumably the principal form of ^{13}N was as $^{13}\text{NO}_3$ all of which remained in the aqueous solution. The bromide target solutions from which ^{79}mKr was prepared and the iodide solutions used for preparing ^{127}mXe , became strongly discolored during bombardment, presumably through generation of elemental halide dissolved in the target solution. The fluoride solutions used in the preparation of ^{19}Ne remained colorless. There was little change in the pH of the target solutions during bombardment. In the case of ^{127}mXe and ^{19}Ne , the only peaks observed in the gamma ray spectra of the flowing gas were attributable to the product isotope. In the case of ^{79}mKr , it was possible to detect both ^{81}mKr and ^{79}Kr in the sweep gas stream under certain conditions of flow. The ^{81}mKr was reduced below detectable levels and the ^{79}Kr was maintained below 1% by using a flow rate of about 1/4 l/min of sweep gas. The helium sweep gas required about 1 minute for transmission from the target chamber to the counting room. Within the limits of our measurements, the half-lives of each of the product radionuclides matched the published values and were measured for at least 7 half-lives in all cases. After subtraction of the background, the only component in any of the decay curves was that of the product radionuclide. The yields of each product are presented in Table 2.

TARGET AND YIELD DATA

TARGET SOLUTION	PRODUCT	SWEEP GAS		mCi/litre IN SWEEP GAS	BEAM CURRENT (micro-amp)
		PRESSURE (psig)	FLOW RATE (ml/min)		
KF	^{19}Ne	12	800	4	5
NaBr	^{79}mKr	11.8	175	32	20
KI	^{127}mXe	13	250	9.8	6

This work was supported in part by DOE Grant #DE-FG02-86ER60407.

- Buell, U., Moser, E.A., Schmiedek, P., Leinsinger, G., Kreisig, T., Krisch, C.M., Einhaupl, K. *J. Nucl. Med.* 25:4, 441 (1984).
- Chilcoat, R.T., Thomas, F.D., Gerson, J.I., *J. Nucl. Med.* 25:7, 810 (1984).
- Susskind, H., Atkins, H.L., Goldman, A.G., Acevedo, J.C., Pate, H.R., Richards, P., Brill, A.B., *J. Nucl. Med.* 22:9, 781, (1981).
- Tilbury, R.S., Rottenberg, D.A., McDonald, J.M., Levy, D.E., *J. Lab Compnds & Radiphar.* 18: 34, (1981).
- Tilbury, R.S., Dahl, J.R., Mamacos, J.P., and Laughlin, J.S., *Int. J. App. Rad. and Isot.*, 21:277-281, 1970.

FACTORS INFLUENCING THE ROUTINE USE OF ISOTOPICALLY ENRICHED ZINC-68 FOR THE PREPARATION OF GALLIUM-67

T.E. Boothe, R.D. Finn*, J.S. Sinnreich, E. Tavano, A. Rodon, P.J. Kothari and J.P. Dwyer.

Cyclotron Facility, Mount Sinai Medical Center, Miami Beach, FL 33140; *Division of Nuclear Medicine, National Institutes of Health, Bethesda, MD 20205

Gallium-67 ($t_{1/2} = 78.3\text{h}$), an important radionuclide in clinical evaluation in Nuclear Medicine, is usually prepared by the (p,2n) reaction on isotopically enriched zinc-68. Limited availability and increasing costs of Zn-68 necessitate that cyclotron operations be as efficient as possible. The steps involved in a normal production cycle include target preparation, proton irradiation, chemical separation of Ga-67 from the Zn-68, and recovery of Zn-68 in a chemical form suitable for subsequent target preparation. To minimize losses and to provide an accurate accounting of the enriched material, various stages of the production cycle have been carefully monitored over the past 3.5 years. This represents several hundred cyclotron irradiations and the handling of a combined total of approximately 200 grams of Zn-68.

Once irradiated, the Zn-68 contains Zn-65 ($t_{1/2} = 244.1\text{d}$) produced primarily by the (p,n) reaction on Cu-65. The Zn-65 allows one to follow the Zn material through the chemical processing, recovery, and target preparation. The losses attributed to each step are approximately 1%, 2%, and 2%, respectively, with another 1% lost during target irradiation. The chemical processing procedure involves etching the Zn from the target with HCl and subsequent separation of Ga-67 by liquid-liquid extraction (1,2); the recovery procedure involves the separation of Zn-68 from iron and copper using HCl and an AG1-X8 (Cl⁻ form) column.

To follow the mass of Zn-68 through the various steps, a high performance liquid chromatography method (3) has been adapted which utilizes only μg amounts of Zn and can determine other trace metals which may be present (TABLE 1).

TABLE 1. Cation Analysis Using HPLC

Cation (retention time in min)

Ga³⁺ (1.1), Cu²⁺ (1.7), Pb²⁺ (2.2), Zn²⁺ (3.7)Ti⁴⁺ (3.8), Ni²⁺ (4.1), Cd²⁺ (7.3), Fe³⁺ (7.8)

Altex Ultrasphere-ODS (5 μ , 25cm x 4.6mm); 0.01M sodium hexane-sulfonate, 0.04M tartaric acid, pH = 3.4 (NaOH) at a flow rate of 2.0 ml/min. Detection was UV - vis. at 520nm using post-column reaction with 0.2mM 4-(2-pyridylazo)resorcinol (PAR), 2M NH₄OH and 1M NH₄OAc at a flow rate of 2.0ml/min.

Another factor to be considered is the extent of isotopic dilution of the enriched Zn-68 with naturally abundant Zn. It has been observed that after several years of cycling the Zn-68 through the production processes, the enrichment drops from >98% to 95-96%. This results in the preparation of larger amounts of Ga-68 ($t_{1/2} = 68.1\text{m}$) and Ga-66 ($t_{1/2} = 9.4\text{h}$), increases risk of radiation exposure to personnel, and influences transportation and shipping characteristics.

Further details of the various parameters influencing Zn-68 inventory and their effects on Ga-67 production will be presented.

1. Hupf, H.B., and Beaver J.E., *Int. J. Appl. Radiat. Isot.*, **21**, 75 (1970).
2. Brown, L.C., *Int. J. Appl. Radiat. Isot.*, **22**, 710 (1971).
3. Boothe, T.E., Finn, R.D., Vora, M.M., Emran, A.M., Kothari, P.J., and Wukovnic, S., In Muccino, R.R., ed., *Synthesis and Applications of Isotopically Labeled Compounds-1985*, Elsevier Science Publishers, 1986, pp 453-458.

Production of ^{81}Rb using a 60 MeV proton beam. Target development and aspects of recovery.

S.L. Waters¹, J.C. Clark¹, P.L. Horlock¹, C. Brown¹, R. Bett² and H.E. Sims²

¹MRC Cyclotron Unit, Hammersmith Hospital, London W12 0HS UK.

²AERE Harwell, Didcot, Oxon OX11 0RA UK.

The use of the 60 MeV proton beam from the Variable Energy Cyclotron (VEC) at the Atomic Energy Research Establishment (AERE) Harwell, has been investigated for the production of ^{81}Rb ($t_{1/2}$ 4.58h) which is used in the preparation of $^{81}\text{Rb}/^{81}\text{Kr}^m$ generators. Previously, proton energies up to 42 MeV have been proposed for this purpose utilising the $^{nat}\text{Kr}(p,xn)$ reactions.⁽¹⁾ As the need to make ^{81}Rb with lower energy cyclotrons has been important, most attention has focused on using enriched Krypton to optimise the yield of the $^{82}\text{Kr}(p,2n)$ reaction (Q value 14 MeV)⁽²⁾. In the studies reported here, natural krypton was used in order to take full advantage of the contributions from the $^{84}\text{Kr}(p,4n)$ and $^{86}\text{Kr}(p,6n)$ routes (Q values 32 and 49 MeV respectively).

Initial experiments to measure the potential yield were carried out using an uncooled stainless steel target (50 mm internal diameter, 530 mm long), lined with removable 0.05 mm aluminium foil. The target filling pressure of 14 bar was held by a 0.125 mm Cu/2% Be foil window (Goodfellow metals) with an entrance diameter of 25 mm. By using this pressure of krypton the target was "thick" enough to degrade the beam from 60 to 40 MeV. Following 20 min irradiations of a 58.9 MeV proton beam with a current of 100 nA, the krypton gas was released through two 0.22 μm membrane filters, a soda lime trap and an ion exchange trap. The aluminium liner was dissolved in NaOH and finally the target was washed out with dilute NaOH. By radioassaying all the various components, (using a Ge(Li) detector) the potential yield of ^{81}Rb and the other radionuclides present were calculated. A summary of these results appear in the table below.

Yield of ^{81}Rb and $^{82}\text{Rb}^m$ from the irradiation of natural krypton with 58.9 MeV protons

Radionuclide	$t_{1/2}$	Yield at end of irradiation	
^{81}Rb	4.58 h	2.38 GBq μAh^{-1}	(64 mCi μAh^{-1})
$^{82}\text{Rb}^m$	6.3 h	0.91 GBq μAh^{-1}	(38% of ^{81}Rb)

A significant finding from these experiments was that > 70% of the rubidium activities produced during these irradiations remained in the gas phase for at least 2 hrs after the end of bombardment and were subsequently trapped by the first membrane filter. This phenomenon has also been observed to a lesser extent by ACERBI et al⁽¹⁾ and by SOLIN et al⁽³⁾. In contrast, the bromine radionuclides also produced during the irradiation, were quantitatively retained by the target walls. From the results of these and other experiments with noble gas irradiations, a target was designed which enabled the recovery of around 40 GBq (1 Curie) of ^{81}Rb in solution suitable for the preparation of $^{81}\text{Kr}^m$ generators. The design was similar to the experimental stainless steel target (i.e. 530 mm long, with beam entrance window of 30 mm, filled with natural krypton to 14 bar) and took full advantage of the beam energy degradation (60-40 MeV). A target diameter of 150 mm was incorporated to reduce interactions of the proton beam with the walls of the target due to multiple scattering. This effect is most prominent with proton irradiations of medium to high Z materials.⁽⁴⁾ The target, which was constructed from aluminium in order to reduce the effects of activation, was surrounded by a flowing water cooling jacket and incorporated a pure aluminium beamstop to absorb the residual proton

energy. The front plate assembly contained a 0.125 mm Cu/Be target foil and a 0.05 mm Cu/Be vacuum foil both cooled by jets directing a flow of Helium. An illustration of the principles of this design are schematically presented in Figure 1. This target has been extensively used for full production purposes and the yield from an hour irradiation with 20 μ A's of 58.9 MeV protons has confirmed our previous findings summarised in the Table above.

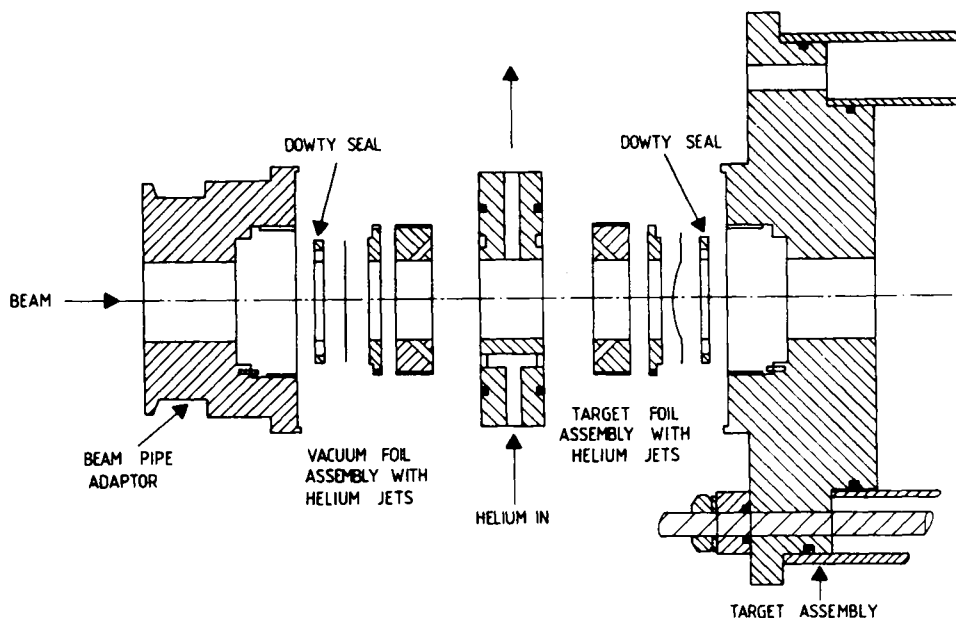


Figure 1 SKETCH OF FOIL ASSEMBLY AND ARRANGEMENT OF HELIUM COOLING

Because of the large volume of krypton within this target (125 litres) it was necessary to devise a recovery system for the gas following the irradiation. This was carried out remotely using a cryopumping system under computer control (Apple II). An illustration of the computer graphics used to operate this system is shown in Figure 2, where the remotely operated pneumatic valves (Nupro and Whitey) are clearly seen.

Another consequence of the large target size was the impracticability of recovering the ^{81}Rb by just filling or rinsing the target with solution(2,3,5). The technique of spraying was also discounted because of the possible variability in the recovery of the rubidium due to the inefficient wetting of the target walls. An alternative approach which has been successful in routinely recovering 100% of the radioactivity in about 500 ml of water, has been that of steaming the target(6). To ensure that all the rubidium produced during the irradiation is recovered, a filter is used on the gas outlet to the target to capture the rubidium in the gas phase (Figure 2). By using a silver membrane (0.45 μm) (Millipore AG45 02500) it is possible to steam the target through this filter.

The target walls were initially treated by steam to produce a film of boehmite (or complex hydroxide) in order to reduce the corrosive effects of regularly condensing steam on to the aluminium walls, and leaving them partially wet between irradiations(7). Some other groups interested in radionuclide production

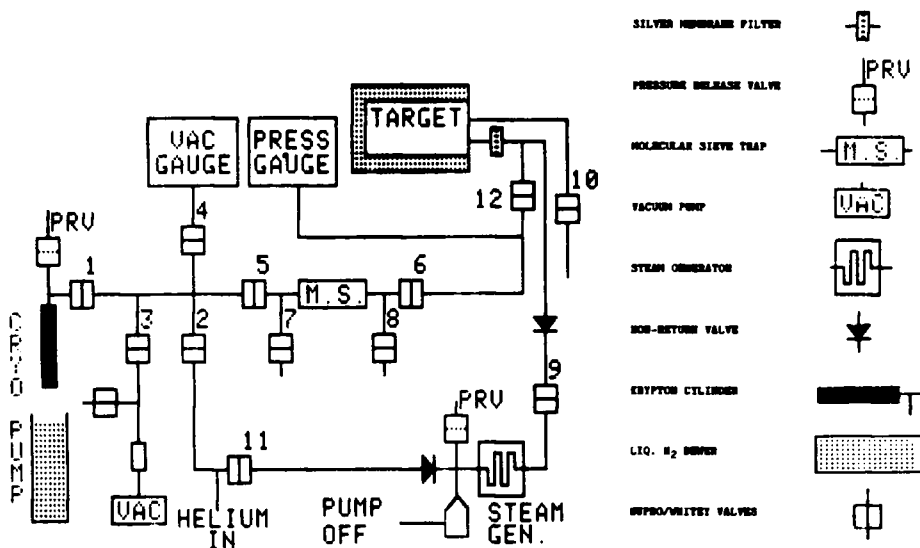


Figure 2 COMPUTER GRAPHICS DISPLAY OF REMOTE PROCESSING SYSTEM FOR RECOVERY OF ⁸¹Rb

using this gas target approach have tackled the problem of corrosion by drying the target between irradiations⁽⁸⁾. Others have used targets such as stainless steel, chromium and nickel but have had to suffer the disadvantage of the target body becoming activated. The compromise of producing an aluminium target which has electrochemically deposited walls [such as chromium or nickel⁽⁹⁾] may be the most suitable solution in this situation.

References

1. Acerbi E., Birattari C., Bonardi M., De Martinis C., and Salomone A. *Int. J. Appl. Rad. Isot.* **32**, 465 (1981).
2. Philp M.S., Ramsey C.I., Ma. J.M., and Lamb J.F. In Knapp F.F., and Butler T.A. Eds. "Radionuclide Generators". ACS Sym. Series. No. 241. Am. Chem. Soc. Washington. 1984. pp 67-73.
3. Solin O., Heselius S-J., Lindblom P., and Manngard P. J. *Labelled Compds. Radiopharm.* **21**, 1275 (1984).
4. Millburn G.P., and Schecter L. Report-UCRL-2234. University of California. Berkeley. (1954)
5. Ruth T.J., Lambrecht R.M., Wolf A.P., and Thakur M.L. *Int. J. Appl. Rad. Isot.* **31**, 51. (1980).
6. Friedman A.M., De Jesus O.J., Harper P., and Armstrong C. J. *Labelled Compds. Radiopharm.* **19**, 1427. (1982).
7. Van Lancker M. *Metallurgy of Aluminium Alloys*. London, Chapman and Hall, 1967, pp 364-412.
8. Personal communication.
9. (i) Cimetièrre C and Leger J. *Ann. Report of Service du Cyclotron, Centre National de la Recherche Scientifique, Orléans* (1983) p144.
(ii) Brenner A., In Lowenheim F.A., Ed. "Modern Electroplating". New York. John Wiley and Sons, Inc., 1942, pp 698-713.

CHEMICAL CONSIDERATIONS OF ^{153}Sm -EDTMP, A NEW THERAPEUTIC BONE AGENT

J. R. Garlich, S. A. Baughman, Jaime Simon, K. McMillan, Dow Chemical Company, Freeport, Texas. A. R. Ketring, W. A. Volkert, *W. F. Goeckeler and *D. E. Troutner, University of Missouri Dept. of Radiology and *Chemistry.

Samarium-153-Ethylenediaminetetramethylenephosphonic acid (^{153}Sm -EDTMP) has shown promise for the treatment of bone cancer. This paper describes the synthesis and purification of the ligand EDTMP, the ability of ^{153}Sm to complex EDTMP, and the nature of the ^{153}Sm -EDTMP complex. In addition, a "kit" formulation is described.

Synthesis of EDTMP was accomplished by slow addition of formaldehyde to an acidic ethylenediamine phosphorous acid mixture. The major impurity was N-methylethylenediaminetrimethylenephosphonic acid (N-methyl-EDTMP). Several other impurities were identified. Purification yielded 99.9% EDTMP. Figure 1 compares EDTMP before and after purification. The superior ability of EDTMP to complex ^{153}Sm over N-methyl-EDTMP was demonstrated using an HPLC coupled to a NaI crystal for detection. (See Figure 2.)

Gravimetric experiments were performed with non-radioactive ^{153}Sm . The results, summarized in Table 1, indicated a 1:1 complex was formed. Further confirmation of a 1:1 complex was obtained by Fab Mass-spec.

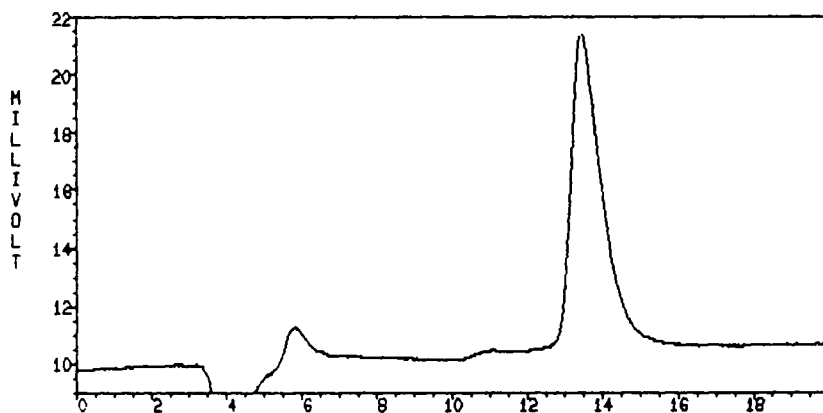


FIGURE 1. a. HPLC of EDTMP Prior to Purification

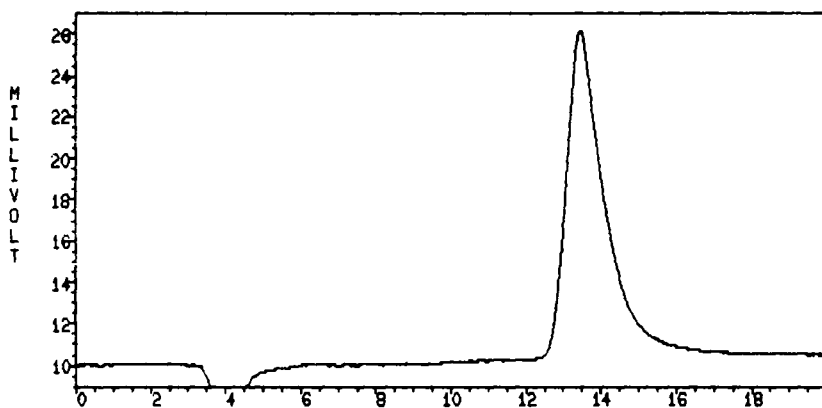


FIGURE 1. b. HPLC of EDTMP After Purification

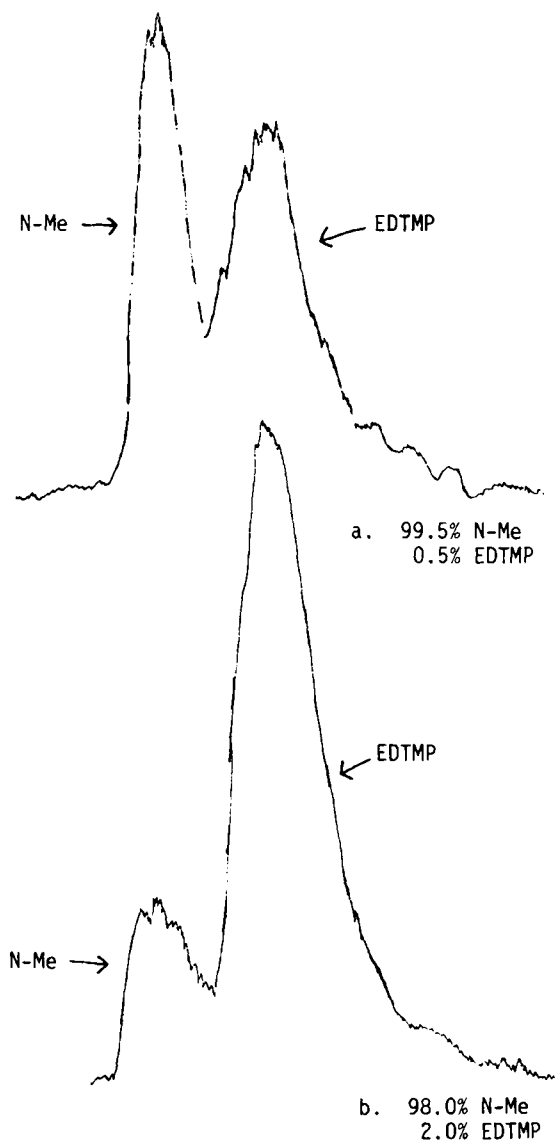


FIGURE 2. Reverse Phase HPLC of Sm-153 Complexed to a Mixture of EDTMP and N-Methyl-EDTMP

TABLE 1. Gravimetric Experimental Results for the Ratio of Sm:EDTMP

Weight EDTMP	Ml of 0.26M Samarium	Molar Ratio Sm:EDTMP	Weight of PPT	Weight if 1:1 Ratio
1.0g	2.2	0.25	0.30g	0.33g
1.0g	4.4	0.50	0.61g	0.67g
1.0g	8.8	1.0	1.34g	1.33g

A "kit" formulation was developed for EDTMP. The kits consist of 210 mg of EDTMP titrated with base to pH = 10.3. Addition of 6 ml of a Sm-153 solution in 0.1 N HCl yielded an injectable solution with a pH of 7.5–8. The complex was shown to be stable for at least seven days after reconstitution of the kits. Table 2 summarizes the complex stability over time.

TABLE 2. Complex Stability Tests

Kit #	% Complex Yield				
	Day 1	Day 2	Day 4	Day 9	Day 12
3	99.62	99.59	99.82	99.17	98.61
6	99.77	99.65	99.86	99.13	97.66
18	99.56	99.70	98.91	99.01	99.02

153 Sm-EDTMP, A POTENTIAL THERAPEUTIC BONE AGENT

J. Simon and W. F. Goeckeler, Dow Chemical Company, Freeport, Texas
 *B. Edwards, *L. Stringham, **W. A. Volkert, ***D. E. Troutner, and *R. A. Holmes, *Harry S. Truman Memorial Veterans Hospital, University of Missouri Department of **Radiology and ***Chemistry

Ethylenediaminetetramethylenephosphonic acid (EDTMP) forms a stable complex with Sm-153. Biodistributions in rats and rabbits show the complex to be an excellent bone agent. The nuclear properties of Sm-153 make it an ideal candidate for therapy. This paper discusses pre-clinical development of Sm-153-EDTMP as a therapeutic bone agent.

Evidence for complex formation includes HPLC, paper chromatography, ion exchange and electrophoresis. Figure 1 shows a single radioactive species on reverse phase HPLC. Complex formation occurs in high yields at pH's ranging from slightly acidic to very basic. The ratio of metal to ligand appears to be 1:1 for the complex.

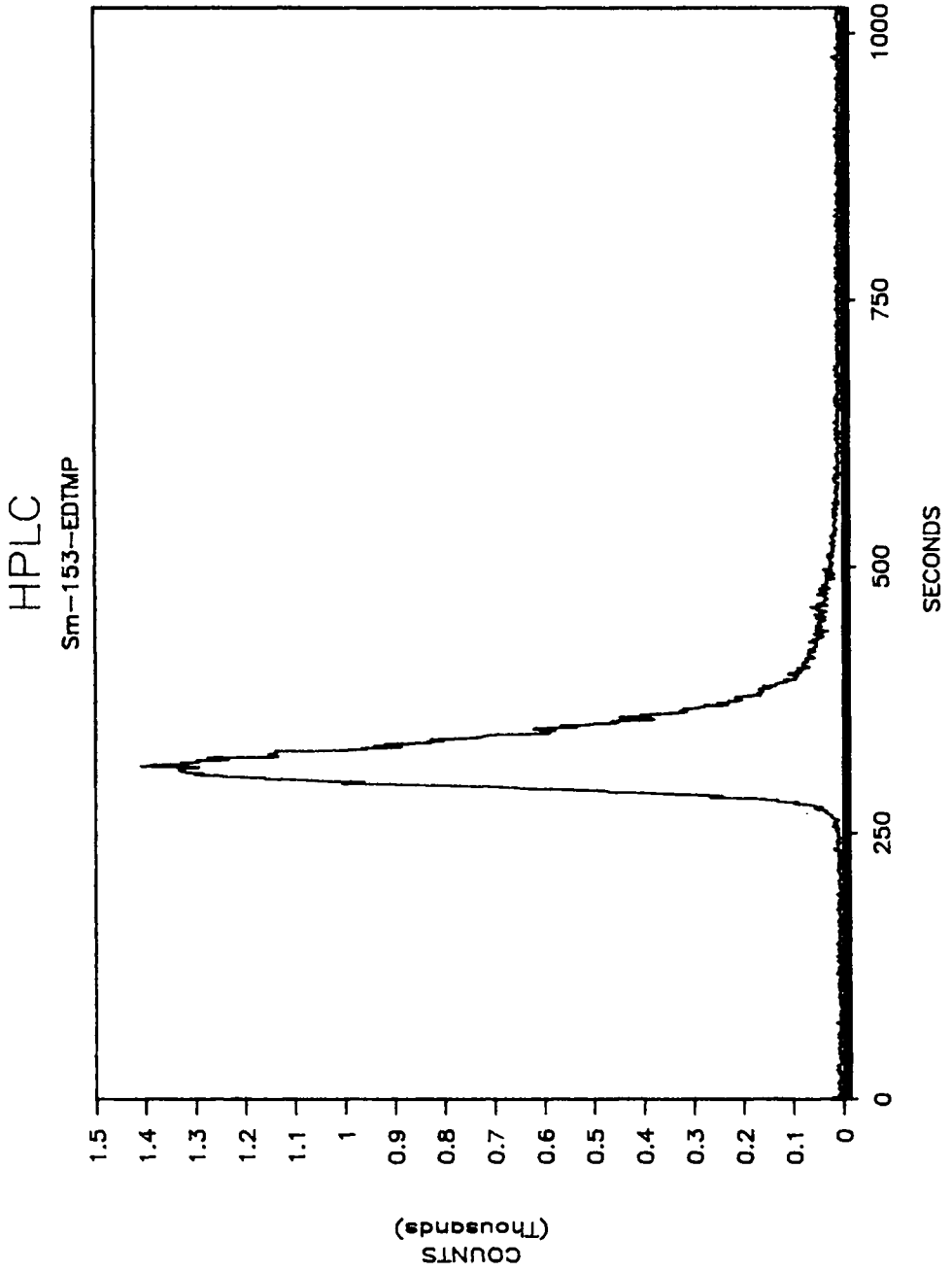
Biodistributions in rats show high skeletal uptake, fast blood clearance, low soft tissue uptake, and a lesion to normal bone ratio equal to Tc-99m-MDP. (See Table 1 below.)

TABLE 1. Biodistribution of Sm-153-EDTMP in Rats
 (S.D.) of 5 Animals

Organ	15 Min.	2 Hrs.	24 Hrs.
Blood	5.8 (0.5)	0.03 (0.02)	0.007 (0.002)
Liver	0.96 (0.14)	0.25 (0.04)	0.35 (0.02)
Spleen	0.055 (0.004)	0.006 (0.004)	0.007 (0.006)
Lg. Intestine	0.62 (0.08)	0.09 (0.02)	0.06 (0.01)
Sm. Intestine	0.79 (0.07)	0.75 (0.39)	0.05 (0.01)
Kidneys	1.75 (.33)	0.25 (0.04)	0.25 (0.09)
Muscle	8.85 (0.85)	0.22 (0.07)	0.13 (0.04)
Femur	1.90 (0.15)	2.31 (0.16)	2.08 (0.12)
Urine	28.38 (3.10)	49.11 (3.92)	54.68 (2.42)
Skeleton*	47.56 (3.70)	57.71 (4.04)	52.04 (2.90)

*Based on % dose femur x 25.

FIGURE 1. Reverse Phase HPLC of ^{153}Sm -EDTMP Using Radiometric Detection



Ratios of bone to soft tissue uptake are extremely high due to the specificity for the skeletal system and the efficient blood clearance. In animals where renal clearance has been blocked, much higher uptake in the bone is observed with slightly higher soft tissue uptake (see Table 2).

TABLE 2. Biodistribution of Sm-153-EDTMP
3 Hours Post Injection of Rabbits with Excised Kidneys
% Administered Dose (S.D.) of 5 Animals

Organ	% Renal Function		
	100%	50%	0%
Blood	0.176 (.099)	.226 (.045)	1.109 (.410)
Muscle	.321 (.112)	.332 (.132)	1.334 (.849)
Marrow	.172 (.070)	.104 (.032)	.242 (.179)
Liver	.483 (.084)	.636 (.223)	1.323 (.359)
Kidneys	.611 (.109)	.521 (.596)	
Urine	37.382 (8.150) N=3	28.777 (7.278)	.058 (.064) N=3
Femur	2.686 (.342)	3.449 (.345)	4.32 (.262)
Skeletal	54.001 (6.889)	69.325 (6.917)	92.871 (6.728)

A series of normal dogs have been treated with up to 2 mci/kg of Sm-153-EDTMP. The only observable effect was to the bone marrow. This was measured by white blood cell and platelet count. In all cases, the blood values returned to normal. Dogs with spontaneous bone tumors were treated with 0.5-1.0 mci/kg of Sm-153-EDTMP. Images compared favorably with corresponding Tc-MDP scans.

Evidence of pain reduction was observed by the animals' use of limbs which were non-weight bearing prior to treatment. Radiographs before and after treatment showed tumor shrinkage.

Also, in several cases, complete absence of disease was proven.

Data obtained from rats have been used to calculate radiation dose into human subjects following the administration of Sm-153-EDTMP.⁽¹⁾ The data were favorable for the proposed use. Thus, all data point toward this agent as an excellent candidate for the treatment of calcific tumors.

1. Logan, et. al., K. W., Radiation Dose Calculations in Persons Receiving Injection of Sm-153-EDTMP, submitted to Journal of Nuclear Medicine.

PHARMACOKINETICS AND METABOLISM OF ^{153}Gd -GADOLINIUM CHELATES

Tweedle, M.F., W.C. Eckelman, P. Wedeking

Contrast Media Research Department, Squibb Institute for Medical Research, New Brunswick, NJ, 08903

First generation NMR imaging agents will have *in vivo* distribution, kinetics, and excretion similar to x-ray contrast agents and to $^{99\text{m}}\text{Tc}$ -DTPA; they will be used initially in NMR imaging for the same indications that diatrizoic acid and iopamidol are currently used for in x-ray CT.

Gadolinium(III) (Gd) is a highly paramagnetic rare earth ion ($\mu_{\text{eff}}^2 = 63 \text{ B.M.}$) and is effective at creating NMR image enhancement through enhancement of the proton relaxation rate (1). Approximately 10^{-4} molal Gd^{3+} is required in tissues to create substantial contrast in the images, making the i.v. dose for a widely distributed agent on the order of 0.1 mmol/kg, compared to 3 mmol I/kg for CT, and <1 mg/kg (of ligand) for most $^{99\text{m}}\text{Tc}$ radiopharmaceutical kits. Consequently, acute toxicity is a major concern. Gd^{3+} is poorly tolerated *in vivo* as the free ion. The i.v. LD_{50} 's in mice for GdCl_3 and $\text{Gd}(\text{OH})_3$ were found to be 0.3 and 0.1 mmol/kg, respectively. LD_{50} 's >10 mmol/kg (no deaths at 10 mmol/kg) were found for Gd^{3+} chelates of DOTA and DTPA. LD_{50} for $\text{Na}[\text{Gd}(\text{EDTA})]$ in mice was >1 mmol/kg.

The dynamics of blood clearance and urine accumulation were determined and compared for four Gd-chelates administered to anesthetized dogs and rats; we also looked for metabolites of the Gd-chelates injected. The studies were done by co-injecting ^{153}Gd -labeled Gd(ligand) and carrier-free $^{99\text{m}}\text{Tc}$ (DTPA). HPLC was used to determine the purity of the radiolabeled compounds and the degree to which replacement reactions (metals trading ligands) occurred. TLC was used to determine the amount of unchelated metals. The ligands tested were DTPA (diethylenetriaminepentaacetic acid), DOTA (1,4,7,10-tetraazacyclododecane tetraacetic acid), TETA (1,4,8,11-tetraazacyclotetradecane tetraacetic acid), EDTA (ethylenediaminetetraacetic acid). $^{153}\text{Gd}(\text{acetate})_3$ was also tested along with unlabelled $\text{Gd}(\text{DOTA})^-$ in order to determine the extent to which weakly chelated Gd affected the results.

Following an i.v. co-injection of 0.05 to 0.25 mmol/kg of Gd(ligand) at $^{153}\text{Gd} = 4 \text{ uCi mmol}^{-1}$ and $0.3 \text{ mCi } ^{99\text{m}}\text{Tc}(\text{DTPA})$, serial (arterial) blood and urine samples were collected and counted. Four days later, the samples were recounted to obtain data for ^{153}Gd , and the initial data corrected for the ^{153}Gd . The data were reduced using standard curve stripping methods. Theoretical Area Under the blood clearance Curves (AUC) were compared with AUC's calculated assuming a two compartment model. Data were paired by calculating ratios to the $^{99\text{m}}\text{Tc}(\text{DTPA})$ data.

Data from six dogs dosed with $^{153}\text{Gd}(\text{DTPA})$ (<0.3 % unchelated ^{153}Gd to 95 % confidence) are summarized in Tables 1 and 2. These data fit a two compartment model. The elimination phase of $^{153}\text{Gd}(\text{DTPA})$ is only slightly, but significantly, different than $^{99\text{m}}\text{Tc}(\text{DTPA})$. $^{153}\text{Gd}(\text{DOTA})$ and $^{153}\text{Gd}(\text{DTPA})$ showed similar results in dogs and rats. HPLC of collected rat urine indicated a single peak at the same retention time found when the chelates were added to urine or to water; TLC confirmed these results. The compounds were excreted to >90 % in urine, and based on the similarity to $^{99\text{m}}\text{Tc}(\text{DTPA})$, were probably eliminated by glomerular filtration.

Table 1. Summary of 2-Compartment Data (N = 6 dogs)

Data:	Tc(DTPA) Mean (+95% CL)	Gd(DTPA) ²⁻ Mean (+95% CL)	Ratio Paired-comparison Gd:Tc	t-	P:
A*	0.0709(0.0078)	0.0719(0.0068)	1.014	0.47	NS
a**	0.3898(0.0330)	0.3773(0.0212)	0.968	0.97	NS
T _{1/2} _(A)	1.79 (0.16)	1.85 (0.11)	1.030	1.030	NS
B*	0.0265(0.0045)	0.0257(0.0044)	0.970	0.87	NS
b**	0.0133(0.0021)	0.0148(0.0013)	1.114	2.72	<0.025
T _{1/2} _(B)	53.61 (8.19)	47.25 (4.12)	0.881	2.77	<0.025

* y-intercept: % ID/g-blood ** -(slope)min⁻¹

Table 2. Summary of Chelate Excretion Data

Chelate	Mean total % ID (+95 % CL)		-Bile: @ 240 min
	Urine: @ 120 min	@ 240 min	
Gd(DTPA) ²⁻	81.07(4.23)	95.64(2.79)	0.0188(0.0057)
Tc(DTPA)	77.38(4.68)	92.48(3.64)	0.1822(0.0365)
Ratio Gd:Tc	1.05	1.03	0.10

¹⁵³Gd(EDTA) and ¹⁵³Gd(TETA) had much longer elimination half-times than ¹⁵³Gd(DOTA) and ¹⁵³Gd(DTPA) (¹⁵³Gd(EDTA) b-slope >10x's ¹⁵³Gd(DTPA) b-slope), probably due to protein binding or instability of the chelates. Stabilities in aqueous solutions of Fe³⁺, Cu²⁺, and PO₄³⁻ showed that ¹⁵³Gd(TETA) reacted in each medium, precipitating ¹⁵³Gd, while ¹⁵³Gd(EDTA) reacted only in the presence of Fe³⁺. To determine serum stability, the relaxivity of the Gd complexes with time was determined in serum.

Comparing the behavior of the stronger chelates of ¹⁵³Gd with DTPA (K_{eq} = 10²²⁻²³) and DOTA (K_{eq} = 10²⁸⁻²⁹) to the weaker chelates, EDTA (K_{eq} = 10¹⁷) and TETA (K_{eq} = 10¹⁶), suggests that stabilities of the order of Gd(EDTA) and Gd(TETA) will not be high enough to allow these complexes to be used as NMR contrast agents.

- Weinmann, H.J., Brasch, R.C., Press, W.R., and Wesby, G.E., AJR, 142:619 (1983).

SOLUTION AND TISSUE RELAXIVITIES OF SOME PARAMAGNETIC COMPLEXES

M.F. Tweedle, H. G. Brittain, A. Krumwiede

Contrast Media Research Department, Squibb Institute for Medical Research, New Brunswick, NJ, 08903

In SPECT and CT the signal intensity in the image is due to absorption of X-rays by (e.g.) iodine or emission of (e.g.) ^{99m}Tc , and signal intensity in the image is linear with the concentration of iodine or ^{99m}Tc in the tissues, regardless of the chemical environment of the agents. In NMR the signal intensity in the image is governed by the concentration and relaxation rate of the water protons in the tissues. Solvated paramagnetic compounds change the NMR signal intensity by increasing the rate of the water-proton relaxation process. Unlike absorption by iodine and gamma emission of ^{99m}Tc , the ability of a paramagnetic compound to increase the water-proton relaxation rate depends on the chemical nature of the compound and on its environment in the tissue.

Relaxation rate enhancement by paramagnetic ions is governed by a second order rate constant which describes each paramagnet ion's ability to relax bulk water protons. The relaxivity of a paramagnet, P , in $\text{M}^{-1}\text{s}^{-1}$ measured at 20 MHz ($^{20}k_1$) is as follows:

$$\frac{1}{T_1} (P) - \frac{1}{T_1} (\text{water}) = {}^{20}k_1 [P] \quad (1)$$

where the term on the left is the difference in measured water-proton relaxation rate due to the presence of P and $[P]$ is the molar concentration of P (or molal for tissues). Relaxation rates are generally linear in paramagnet concentration in the range 10^{-4} to 10^{-3} M in fluids, but nonlinear in some tissues.

Gd(III), a $4f^7$ rare earth, has nearly ideal properties for maximizing its effect on water-proton relaxation. Its half filled f shell gives it a symmetric electronic ground state and the spin only magnetic moment is maximum: $\mu_{\text{eff}}^2 = 63$. The normal water-proton relaxation rate in vivo is on the order 1 to 10 s^{-1} . When water is coordinated to Gd^{3+} its proton relaxation rate is on the order 10^6 s^{-1} , so a rapid water exchange rate in the

TABLE 1. Relaxivities and Water Exchange Rates

Ion	$k_{\text{ex}} \text{ s}^{-1}$	${}^{20}k_1 \text{ M}^{-1} \text{ s}^{-1}$	ref.
$[\text{Gd}(\text{H}_2\text{O})_8]^{3+}$	2×10^9		(1)
$[\text{Mn}(\text{H}_2\text{O})_6]^{2+}$	6×10^8		(1)
$[\text{Fe}(\text{H}_2\text{O})_6]^{3+}$	$1-4 \times 10^2$		(2)
$[\text{Gd}(\text{DTPA})(\text{H}_2\text{O})]^{2-}$	$>10^9$	3.7×10^3	
$[\text{Mn}(\text{EDTA})(\text{H}_2\text{O})]^{2-}$	7×10^8	2.0×10^3	
$[\text{Fe}(\text{EDTA})(\text{H}_2\text{O})]^{-}$		1.6×10^3	
$[\text{Gd}(\text{DOTA})(\text{H}_2\text{O})]^{-}$	$\geq 10^9$	3.4×10^3	
$[\text{Mn}(\text{DOTA})]^{2-}$		1.1×10^3	
$[\text{Fe}(\text{DOTA})]^{-}$		0.4×10^3	
$[\text{Fe}(\text{DTPA})]^{2-}$		0.7×10^3	(3)
$[\text{Mn}(\text{DTPA})]^{3-}$		1.1×10^3	

inner coordination sphere is desired to optimize the number of protons relaxed per second. For Gd^{3+} the exchange rate is nearly diffusion controlled. Table 1 compares the measured relaxivities of free and chelated Fe^{3+} , Mn^{2+} , and Gd^{3+} . The free ion k_{ex} data might lead one to expect low relaxivity for $\text{Fe}(\text{EDTA})(\text{H}_2\text{O})^{-}$, but chelation nearly always increases these rates, and it leads to a relatively high ${}^{20}k_1$ for $\text{Fe}(\text{EDTA})(\text{H}_2\text{O})^{-}$. The new ions, $\text{Fe}(\text{DOTA})^{-}$

and $[\text{Mn}(\text{DOTA})]^{2-}$, probably have no coordinated water, and the observed relaxivity is similar to that of $[\text{Fe}(\text{DTPA})]^{2-}$ and $[\text{Mn}(\text{DTPA})]^{2-}$. Lauffer has found similar relaxivities, $^{20}k_1 = 0.9 \times 10^3 \text{ M}^{-1} \text{ s}^{-1}$, for $\text{Fe}(\text{EHPG})^-$, an $\text{Fe}(\text{III})$ complex with a hexacoordinate ligand and no inner sphere coordinated water. We can view the observed relaxivity as arising from two relaxation processes, one occurring through inner sphere interaction of protons on coordinated water and one occurring through outer sphere interaction (4):

$$^{20}k_1 \text{ observed} = ^{20}k_1 \text{ inner} + ^{20}k_1 \text{ outer} \quad (2)$$

The data in Table 1 allow us to estimate the relative contributions for Mn^{2+} and for Fe^{3+} in $\text{Fe}(\text{EDTA})(\text{H}_2\text{O})^-$. To obtain an estimate for the outer sphere contribution to the relaxivity of the Gd(polyaminecarboxylates), the number of inner sphere waters can sometimes be reduced by making ternary complexes: Gd(EDTA)(citrate) gave a measured $^{20}k_1$ dependent on [citrate] with a lower limit of $\sim 2 \times 10^3 \text{ M}^{-1} \text{ s}^{-1}$ at 50 mM citrate. The number of coordinated water molecules was determined by the Horrocks method (5) for a series of Gd(ligand) complexes where ligand = EDTA, DTPA, DOTA, TETA, and Desferrioxamine, by measuring the emission lifetimes of the corresponding Tb^{3+} and Eu^{3+} chelates in H_2O and D_2O . The outer and inner sphere (per water) contributions were about equal for the Gd^{3+} complexes: $^{20}k_1 \text{ outer}$ was estimated to be $1 - 2 \times 10^3 \text{ M}^{-1} \text{ s}^{-1}$. For Fe^{3+} and Mn^{2+} , the data in Table 1 suggest that the outer sphere contribution for these ions is also equal to that of one coordinated water.

It is well known that correlation phenomena can be used to increase the relaxivity. $^{20}k_1$ values are increased as t_c , the correlation time, increases. For Gd^{3+} , t_c at 20 MHz depends primarily on a rotational component that can be increased by slowing the molecular rotation of the Gd^{3+} ion. This is usually done by binding Gd^{3+} to proteins. Data on $^{20}k_1$ per Gd^{3+} when the Gd^{3+} is bound to proteins could be used to estimate the magnitude of this effect obtainable, but existing data are not normalized by measuring the number of coordinated waters per Gd^{3+} . By directly determining that number for $\text{Gd}^{3+}(\text{aq})$ bound directly to seven proteins and polymers we obtained values for $^{20}k_1$ per coordinated water. This value increases with molecular weight, and can be at least as high as $2.9 \times 10^4 \text{ M}^{-1} \text{ s}^{-1}$ per coordinated water. This compares to about $\sim 2 \times 10^3 \text{ M}^{-1} \text{ s}^{-1}$ per coordinated water for Gd^{3+} chelates. Theory predicts a potential rate increase on the order of 10 - 100, controlled by the water exchange rate, and we saw no leveling of the value at 180,000 daltons.

In vivo the observed relaxivity may be altered by protein binding. Gd concentrations in vivo were determined either by homogenizing tissues of animals injected with Gd and measuring Gd by Ion Coupled Plasma or x-ray fluorescence, or by preparing the Gd(ligand) complexes with ^{153}Gd . Radiolabelling the chelates has proven to be by far the simplest and most accurate technique. Reactions of $^{153}\text{Gd}-\text{Gd}^{3+}$ with ligands were monitored by determining the extent of reaction by ITLC-SG and HPLC. All reactions proceeded smoothly to completion at pH 7 with mild heating as long as acetate was present to keep the Gd^{3+} in solution. Relaxivities were determined for $[\text{Gd}(\text{DOTA})(\text{H}_2\text{O})]^-$ and $[\text{Gd}(\text{DTPA})(\text{H}_2\text{O})]^{2-}$ in serum, kidney and a mouse tumor. No substantial differences were observed between the two chelates, but some concentration dependence of the relaxivity was observed,

particularly in rat kidneys, where relaxivity increased as the $[Gd^{3+}]$ decreased.

Table 2. $^{20}k_1$ Values of Gadolinium Chelates at 20 MHz and 40° C

Chelate	Water ^a	$^{20}k_1$ in $M^{-1}s^{-1}$	
		Dog Serum ^a	Mouse Tumor ^b
$[Gd(DTPA)]^{2-}$	3731±110	4086±417	5599±1921
$[Gd(DOTA)]^{-}$	3376±227	3785±497	4814±1267

^a + 95 % Confidence Limits.

^b 5 min. post intravenous 0.4 mmol/kg in 25 g MRL +/+ mice (n=3) with 8-day old flank implanted mammary adenocanthoma. $[Gd] = 2.2 \pm 0.2$ molal in the tumor in 300 mg tumors. ± Standard Deviation.

1. Burgess, J., Metal Ions in Solution. Chichester, Ellis Horwood, 1978, Chapter 11..
2. Taube, H., Electron Transfer of Complex ions in Solution. New York, Academic Press, 1970, p. 4.
3. Lauffer, R., 4th Society of Magnetic Resonance in Medicine meeting, Abstracts, 1985, p. 881.
4. Oakes, J. and Smith, E., J. Chem. Soc. Faraday, 77, 299, 1981.
5. Horrocks, W.DeW. and Sudnick, D.R., J. Am. Chem. Soc., 101, 334, 1979.